2007-05-15

Pharmacokinetics of Ultrasonically-Released, Micelle-Encapsulated Doxorubicin in the Rat Model and its Effect on Tumor Growth

Bryant J. Staples
Brigham Young University - Provo

PHARMACOKINETICS OF ULTRASONICALLY-RELEASED, MICELLE-

ENCAPSULATED DOXORUBICIN IN THE RAT MODEL

AND ITS EFFECT ON TUMOR GROWTH

by

Bryant J. Staples

A thesis submitted to the faculty of

Brigham Young University

in partial fulfillment of the requirements for the degree of

Master of Science

Department of Chemical Engineering

Brigham Young University

August 2007

BRIGHAM YOUNG UNIVERSITY

GRADUATE COMMITTEE APPROVAL

of a thesis submitted by

Bryant J. Staples

This thesis has been read by each member of the following graduate committee and by majority vote has been found to be satisfactory.

Date	William G. Pitt, Chair

Date	Kenneth A. Solen

Date	Thomas A. Knotts IV

BRIGHAM YOUNG UNIVERSITY

As chair of the candidate's graduate committee, I have read the thesis of Bryant J. Staples in its final form and have found that (1) its format, citations, and bibliographical style are consistent and acceptable and fulfill university and department style requirements; (2) its illustrative materials including figures, tables, and charts are in place; and (3) the final manuscript is satisfactory to the graduate committee and is ready for submission to the university library.

_____
Date

_____
William G. Pitt
Chair, Graduate Committee

Accepted for the Department

_____
Larry L. Baxter
Graduate Coordinator

Accepted for the College

_____
Alan R. Parkinson
Dean, Ira A. Fulton College of Engineering and Technology

ABSTRACT

PHARMACOKINETICS OF ULTRASONICALLY-RELEASED, MICELLE

ENCAPSULATED DOXORUBICIN IN THE RAT MODEL

AND ITS EFFECT ON TUMOR GROWTH

Bryant J. Staples

Department of Chemical Engineering

Master of Science

Chemotherapy is one of the most successful cancer treatments used today. Unfortunately, the amount of chemotherapy a patient can receive is limited by the associated negative side effects, such as cardiotoxicity, immune system suppression, and nephrotoxicity. Encapsulation of these drugs, Doxorubicin (DOX) in particular, in stabilized Pluronic micelles (Plurogel^{TM}) shows success in limiting these harmful side effects. In previous studies, low-frequency ultrasound (US) has been shown, *in vitro*, to locally release DOX from these micelles. In this study, a novel drug delivery system involving the encapsulation of DOX in Plurogel and the release of the drug at the tumor site using ultrasound was studied *in vivo* using rats. These studies determined the effect of ultrasonically released drugs on tumor growth rate and drug delivery to the tumor

tissue. Concurrently, different frequencies (20 kHz, 500 kHz) were tested for the same effects. Treatments consisted of micelle-encapsulated doxorubicin injected intravenously followed by ultrasound application to one of the two bilateral tumors. Also, in different experiments, pharmacokinetic studies of the drug in the heart, liver, leg muscle, and tumors were performed up to a period of one week after treatment.

Results showed that tumors treated with ultrasound displayed, on average, slower growth rates than non-insonated tumors (P = 0.0047). Also, insonated tumors displayed a weak increased concentration of DOX than non-insonated tumors within the first eight hours after treatment (P = 0.064). However, comparison between tumors which received 20 kHz and 500 kHz ultrasound treatment showed no statistical difference (P = 0.9275) in tumor growth rate or DOX concentration. It is noteworthy that the insonated tumor has slower growth even though the amount of DOX was not that much greater in the non-insonated tumor. This suggests that US also affects the uptake and/or processing of the DOX by the tumor cells, and that the therapeutic effect may not be attributed solely to a higher concentration of drug released by insonation.

Pharmacokinetic studies showed significant drug accumulation in the heart but no accumulation in the liver, skeletal leg muscle, or tumors over the course of four weeks of consecutive weekly injections of DOX-encapsulated Plurogel. After 24 hours, DOX concentration remains the greatest in the tumors, regardless of whether they received ultrasound or not.

ACKNOWLEDGMENTS

TABLE OF CONTENTS

x

LIST OF TABLES

LIST OF FIGURES

1 Introduction

Cancer is the second leading cause of death in the United States, just after heart disease. Out of 100,000 people, about 470 people are diagnosed each year with some form of cancer while 200 die from it [1]. Surgery, radiation, and chemotherapy are the three most popular cancer treatments available today. Surgery is a highly invasive treatment used to remove the tumor or in some cases, the entire organ. Radiation uses intense ionizing energy to damage or destroy cancer cells as well as adjacent healthy cells. Chemotherapy uses toxic drugs to kill rapidly dividing cells. Unfortunately, these drugs cannot distinguish between healthy and cancerous cells. Therefore, there is a fine line between administering enough drug to destroy the cancer and giving so much that it kills the patient. Because of the difficulties with conventional chemotherapy, many researchers are looking for novel ways to locally deliver the drugs directly to the tumor, eliminating damaging exposure to healthy tissues.

One such method involves loading chemotherapeutic drugs inside stabilized micelles (drug carriers) and injecting the encapsulated drug into the patient's body. Ultrasound is then used to locally deliver the toxic drug by permeabilizing the cell membranes of cancerous tissue while simultaneously opening up the micelles to release the drugs. This treatment ideally has the potential to not only spare the rest of the body from the toxic effects of the drug, but also locally increase the drug concentration in the

cancerous tissue, thus increasing the drug's effectiveness. However, specific challenges remain and the delivery must be optimized. Important questions to address are: How is the drug distributed within the animal system? Is there an increase in drug concentration in the tumors after ultrasound is applied? Also, since this delivery method is new, there are many unknowns and questions concerning the mechanism of delivery. For example, do different frequencies of ultrasound affect the delivery of the drug? Finally, and most importantly, is this delivery system effective in treating cancer? The purpose of this thesis is to address some of these issues and provide a greater understanding of drug delivery using micelles and ultrasound.

This thesis research uses stabilized polymeric micelles to carry Doxorubicin, a potent chemotherapeutic drug, through the blood system of a rat with solid tumors. Ultrasound is then applied to the tumors. During this research, the distribution of drug in various tissues over time, or its pharmacokinetics, is of special interest.

This report begins with an overview of relevant ultrasound fundamentals and a survey of existing knowledge. The specific objectives are then stated, followed by a detailed explanation of the experimental approach. We conclude with the results and conclusions of the study and a summary of where future work lies.

2 Literature Review

This thesis research studied the pharmacokinetics of Doxorubicin (DOX) that was ultrasonically released from micelles in a rat model and its therapeutic effect on tumor growth. The purpose of this chapter is to review existing knowledge about drug delivery, ultrasound, micelles (particularly Pluronic micelles), Doxorubicin, the pharmacokinetics of Doxorubicin, the tumor model, and drug extraction and quantification using high performance liquid chromatography.

2.1 Targeted Drug Delivery

The subject of targeted drug delivery is large and diversified; however, the general goal is the same: to deliver a specific drug to a specific location at a specific time. Some of the techniques used for targeted delivery include 1) radiation targeting, 2) targeting-ligands on nanoparticles, and 3) passive targeting. In radiation targeting, a mechanism such as ultrasound, heat, or light (using a laser) can be focused on a desired site and selectively activate normally passive particles only at the targeted location.

The second general class of techniques attaches targeting ligands to nanoparticles and sends these particles through the body where the ligands can attach to the specific target (see **N** in Figure 2-1). This technique is beneficial if the target is spread throughout the body in several or unknown locations.

Passive targeting, the third general class, can be used if the target demonstrates enhanced permeability in comparison with other tissues, such as in some capillary beds or some types of tumors [2]. Due to this increased permeability, the drug will more likely enter the targeted area and passively accumulate. Figure 2-1 on page 6 illustrates a few examples of passive particles acting as drug carriers (microbubbles, **J - K**; micelles, **L**; and liposomes, **M**). The technique used in this thesis employs a combination of both radiation and passive targeting.

2.2   What is Ultrasound

Ultrasound is pressure waves with frequencies greater than 20 kHz. It is usually generated by transducers that change a voltage waveform into mechanical movement of the transducer face. Like optical or audio waves, ultrasonic waves can be focused, reflected, refracted, and propagated through a medium. Therefore, ultrasound waves can be directed to and/or focused on a specific tissue area – a useful property that makes ultrasound non-invasive (no surgery required).

In explaining ultrasonic effects, an important topic is that of cavitation, the oscillatory response of a gas bubble in an acoustic field [3]. Ultrasound produces pressure waves that create regions of low and high pressure, and these pressure changes have an effect on gas bubbles in the medium. During moments of low pressure, these bubbles expand, and at moments of high pressure, they contract. If the resulting oscillations in bubble size are fairly stable (repeatable over many cycles), the cavitation is called "stable" (see **B** in Figure 2-1). Such oscillation creates a circulating fluid flow around the

4

bubble – called microstreaming (see **C** in Figure 2-1). Shear forces produced by microstreaming are strong enough to shear open red blood cells [4].

Ultrasound intensity is the amount of energy delivered by the pressure wave per unit area, commonly measured in watts per square centimeter (W/cm^2). As ultrasonic intensity increases, the amplitude of oscillation also increases to a point in which the inward moving wall of fluid has sufficient inertia that it cannot reverse direction when the acoustic pressure reverses. In other words, even though the acoustic pressure decreases, the fluid continues to compress the gas bubble, compressing the gas to a very small volume. At high intensities, this compression creates extremely high pressures and temperatures [5]. This type of cavitation (called transient, inertial or collapse cavitation) can be stressful to cells because of the very high shear stresses in the region of the collapse (see **F - H** in Figure 2-1), the shock wave produced by the collapse (see **D** in Figure 2-1), and the free radicals produced by the high temperatures. Furthermore, if the collapse is near a solid surface (such as a cell), an asymmetrical collapse occurs which ejects a jet of liquid at sufficient speed to pierce nearby cells (see **E** in Figure 2-1) [6]. Figure 2-2 illustrates a bubble experiencing asymmetrical collapse cavitation.

In general, the likelihood and intensity of collapse cavitation increases at higher intensities and lower frequencies [6] and is indicated by the "mechanical index" (*MI*), the ratio of peak negative pressure, *P$^-$*, (in *MPa*) to the square root of frequency, *f*, (in *MHz*):

$$MI = \frac{P^-(MPa)}{\sqrt{f(MHz)}} \qquad\qquad (2.1)$$

5

The threshold for collapse cavitation is about *MI* = 0.3, and tissue damage is likely at

MI > 0.7.
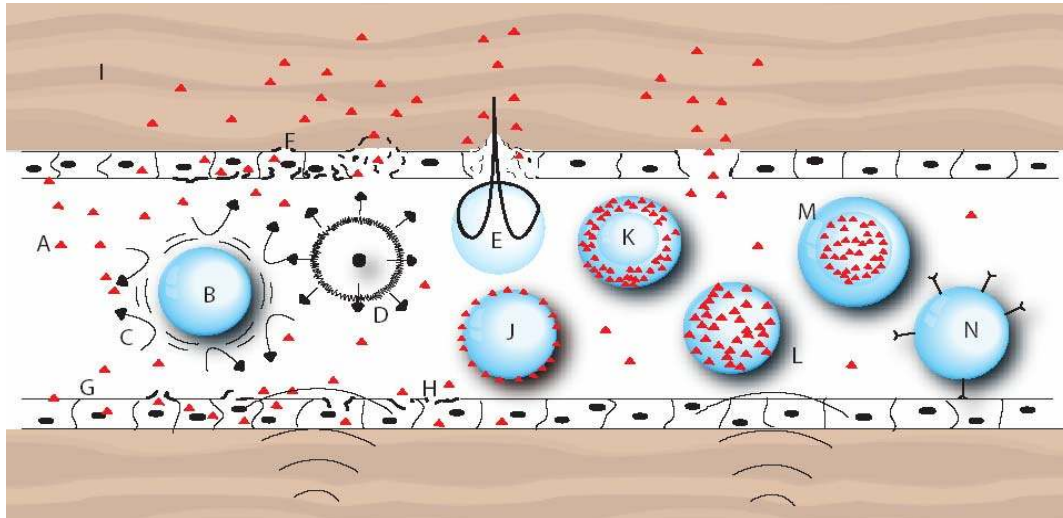
Figure 2-1 Schematic representation of various modes by which drug delivery can be enhanced by ultrasound. **A**) Drug (triangles); **B**) gas bubble undergoing stable cavitation; **C**) microstreaming around a cavitating bubble; **D**) collapse cavitation emitting a shock wave; **E**) asymmetrical bubble collapse producing a liquid jet that pierces the endothelial lining; **F**) completely pierced and ruptured endothelial cell; **G**) non-ruptured cells with increased membrane permeability due to insonation; **H**) cell with damaged membrane from microstreaming or shock wave; **I**) extravascular tissue; **J**) thin-walled microbubble decorated with drug on surface; **K**) thick-walled microbubble with agent in lipophilic phase; **L**) micelle with agent in lipophilic phase; **M**) liposome with agent in aqueous interior; **N**) vesicle decorated with targeting moieties attached to a specific target. [7]
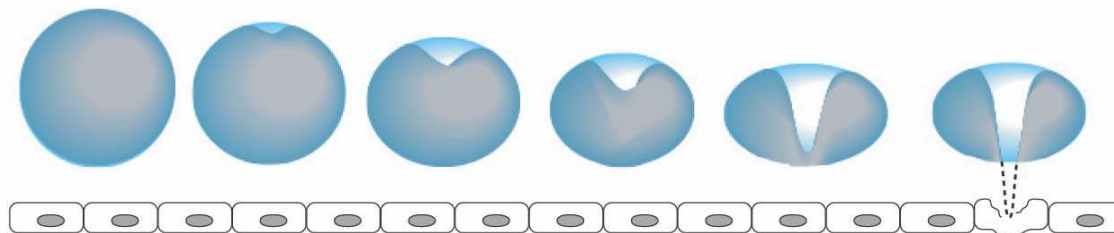
Figure 2-2 Illustration of an asymmetric collapse of a bubble near a surface, producing a jet of liquid toward the surface. [7]

2.3   Micelles in Drug Delivery

In the search for better cancer treatment methods, new innovations in micellar drug delivery have emerged with successful preliminary results. Micelles carry chemotherapeutic drugs within their cores and can deliver these drugs directly to necessary areas. A micelle is an aggregate (collection) of surfactant molecules dispersed in an aqueous solution. These individual surfactant molecules, or unimers, are composed of hydrophilic and hydrophobic ends, which in an aqueous environment, aggregate to form a hydrophobic core and a hydrophilic corona. The formation of micelles is thermodynamically controlled by two competing forces: hydrophobic forces leading towards micelle formation and entropic forces opposing formation because of the micelle's more ordered state. Because of these forces, there is a critical micelle concentration (CMC) and critical micelle temperature (CMT) above which micelles will form. In other words, above the CMC, the entropic penalty of assembling the unimers into micelles is less than the entropic penalty of surrounding the unimer with water molecules. The innate ability of micelles to self assemble is advantageous in drug delivery. Figure 2-3 illustrates the spontaneous combination of unimers to form a micelle, which is then loaded with drug (green dots). The red sections are hydrophobic while the blue sections are hydrophilic.

2.3.1   Pluronic Micelles

Of the many different types of micelles that exist, polymeric micelles have been particularly useful for drug delivery. The field of polymeric micelles as drug carriers was
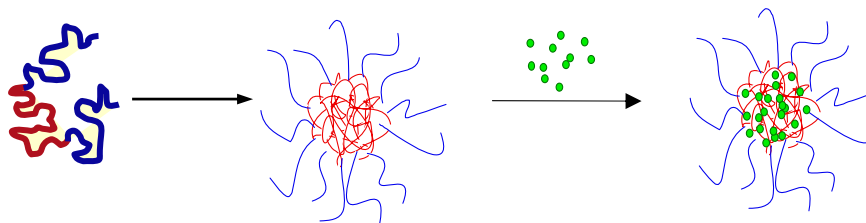
Figure 2-3 Illustration of micelle formation and drug loading. Pluronic P105 forms dense micelles whose hydrophobic core readily sequesters hydrophobic chemotherapeutic drugs (green dots). The red section is hydrophobic, and the blue is hydrophilic.

ignited by three publications. The first publication, by Bader et. al., proposed block copolymer carriers for drug delivery [8]. The second, by Yokoyama et. al., demonstratedthese carriers as feasible conjugates of Doxorubicin as a treatment of cancerous tumors [9]. The third, by Kabanov et. al., proposed the use of Pluronic block copolymer micelles loaded with drug and modified with either brain-specific antibodies or insulin molecules [10]. Pluronic block copolymers consist of polyethylene oxide (PEO) and polypropylene oxide (PPO) blocks arranged in a basic A-B-A structure (Figure 2-4). PEO is hydrophilic and PPO is hydrophobic. Pluronic block copolymer unimers are synthesized by sequential addition of propylene oxide and ethylene oxide monomers in the presence of an alkaline catalyst such as NaOH or KOH. The reaction is initiated by the polymerization of the PPO block followed by the growth of PEO chains at both ends of the PPO block.
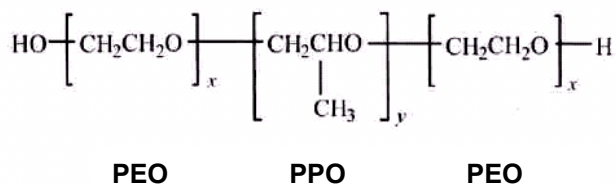
Figure 2-4 Chemical Structure of Pluronic Monomers

Aqueous solutions of block copolymers are characterized by a lower critical solution temperature (LCST). The copolymer solubility decreases with increased temperature, as explained by the dehydration of PPO and PEO blocks. At colder temperatures (X in Figure 2-5), both the PPO and PEO blocks are soluble in water, but as the temperature increases above the CMT (O in Figure 2-5), the PPO block dehydrates (because hydrogen bonding decreases at higher temperature) and micelles are formed. As the temperature continues to rise, it eventually dehydrates the PEO block, destabilizing the micelle. As the block copolymer reaches a concentration just above its CMC, the unimers start to form micelles. As the concentration continues to increase, the number of micelles increases, while the concentration of the fine unimers remains constant. Pluronic P-105, one of the variations of PEO-PPO block copolymers, has a CMC of 0.3 wt% at room temperature and 0.001 wt% at body temperature (37 °C) [11]. Pluronic P-105 is 50% PEO by weight and has a central PPO chain of 3000 daltons.
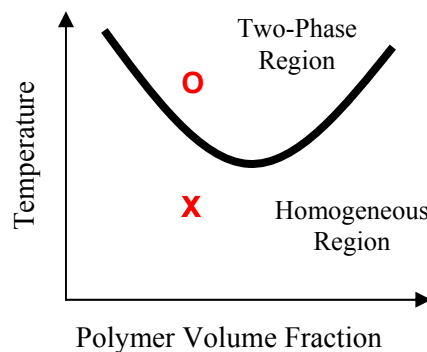
Figure 2-5 LCST Behavior

Pluronic unimers create micelles ideal for intravascular injection. Small particles with diameters of less than 5 to 10 nm are rapidly removed through extravasation and

renal clearance, while particles with diameters larger than 200 nm are usually sequestered by the spleen and phagocytosed. Micelles with diameters between 20 and 80 nm are within the preferred size range for drug delivery systems. Diameters of Pluronic micelles (10 – 80 nm) are larger than most peptides and proteins, close to the size of condensed plasmids, and much smaller than the extended conformation of a 3 kb double-stranded DNA. Thus, many proteins may fit within a micelle whereas many micellar species may bind to a DNA single chain. Pluronic micelles are often termed mild detergents because they do not permanently denature protein but only slightly change its conformation.

Pharmacokinetic studies show that Pluronic is eliminated primarily by renal excretion. For example, one study showed that 94% of the dose of ethylene-^{14}C-labeled block copolymer was excreted in the urine over three days while about 6% appeared in the feces. Only small residues were detected in the kidney, liver, small intestine, and carcass after 24 hours. Biodistribution studies suggest that the retention of the block copolymer in the organs increases as the length of the hydrophobic PPO block increases. The block copolymer concentrations in the plasma remain quite high for several hours after administration. These concentrations are in the same range as the established CMCs for the studied Pluronics, suggesting that micelles might still be present in the circulation [12].

2.3.2   Plurogel: A Modification of Pluronic Micelles

Pluronic P-105 micelles (50 wt% PEO, PPO block-3000 daltons) have shown some promise as drug carriers; however, even though the CMC decreases when heated to body temperature (which makes micelle formation more likely), the diluting effect of the drug entering the circulatory system still tends to dissolve the micelle. To stabilize the

Pluronic micelles, Pruitt et al. formed an interpenetrating network of a thermoresponsive polymer, poly(N,N-diethylacrylamide) (NNDEA), within the hydrophobic micellar core [13]. The network polymer, poly(NNDEA), has a critical solution temperature (LCST) of 28 °C by itself and an LCST of 31 °C when incorporated with Pluronic (Figure 2-6). At temperatures higher than the LCST, the polymer collapses into a hydrophobic state. In other words, the hydrogel networks remain in a swollen state at room temperature and can be loaded with drug. At body temperature above the LCST, the network collapses, locking the drug in the micelle core.
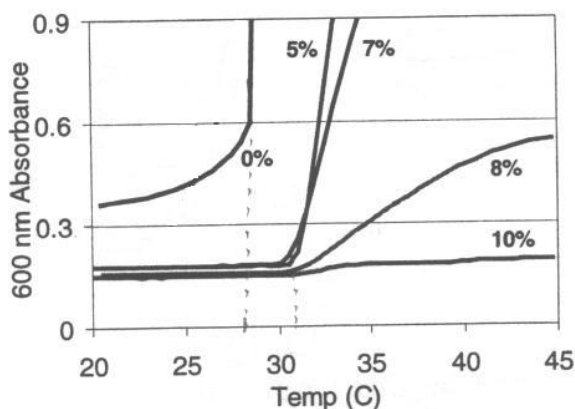
Figure 2-6 Turbidity of 1 wt % poly(NNDEA) samples polymerized in the presence of increasing wt % concentrations of P-105. The change in turbidity represents a change of physical state (i.e. collapsed micelle). [13]

The stabilization of Pluronic micelles enhances its ability to hold a hydrophobic drug in its core. However, over time, this enhanced stability decreases because of the disentanglement of the unimers from the interpenetrating network of poly(NNDEA). This disentanglement happens faster at higher temperatures. A study by Pruitt exposed human leukemia-60 (HL-60) cells to high concentrations of DOX (10 µg/ml) in the presence of

Plurogel micelles or Pluronic P-105 micelles. The Plurogel was better at protecting the HL-60 cells from DOX than Pluronic P-105 for about 12 hours. After this period, the death rate was similar between Pluronic and Plurogel [14].

2.4   Drug Delivery from Pluronic Micelles

Polymeric micelles have the unique ability to deliver pharmaceutical agents into body compartments where drugs cannot normally be transported, such as through the blood-brain barrier [12]. Pluronic block copolymers enhance drug performance by acting as biological response-modifying agents that act directly upon the target cells – enhancing the effectiveness of chemotherapeutic agents in multidrug-resistant tumors. Also, the small size of the micelles allow them to naturally accumulate in highly permeable tissues, such as tumors with hyper-permeable vasculature [15].

The capacity of the "cargo hold" within the micelles core is limited. Therefore, the more drug that can solubilize with the micelle core, the better. The most important factor related to the drug solubilization capacity within the micelle is the compatibility between the drug and the core-forming block. The amount of the incorporated drug increases as the molecular volume of the drug decreases [12]. Pluronic block copolymers have been shown to have much higher drug capacities than lower molecular weight surfactants. Also, they are more selective toward aromatic and heterocyclic compounds – like DOX – than toward aliphatic molecules [16]. Factors such as the micelle core's glass transition temperature, the CMC, the hydrophobic/hydrophilic properties of the drug and Pluronic, and the partition coefficient affect drug retention and release from the micelle [12].

2.5   Ultrasound Release from Pluronic Micelles

Ultrasound has been shown to trigger the release of DOX from Pluronic micelles at certain frequencies [17-21]. Munshi et al. were the first to report that ultrasound enhanced the uptake of Doxorubicin from micelles by human leukemia cell line 60 [22]. *In vitro* studies by Husseini et al. showed that 70 kHz ultrasound released about 10% of the drug from the micelles and that after removing the ultrasound, the drug quickly returned to the micelle [19]. Marin et al. studied the uptake and distribution of doxorubicin released from Pluronic micelles. They concluded that there are two different mechanisms involved. First, ultrasound releases the drug from the micelles, causing a higher concentration than without ultrasound. Second, the ultrasound perturbed the cell membranes, which increased the amount of drug inside the cells [18]. Figure 2-7 is an illustration of ultrasound-induced drug release in a capillary vessel. It shows the micelles releasing their drug load when exposed to the ultrasound waves and then reforming outside of the waves.

Nelson employed an *in vivo* rat model to investigate the effects of ultrasonically controlled release of Plurogel-encapsulated Doxorubicin [23]. During the course of the four-week treatment, the tumor volume was measured. Concentrations of DOX and ultrasound parameters were varied to determine any influence of 1) drug concentration, 2) power density, 3) frequency, 4) power train, and 5) number of ultrasound treatments on the effectiveness of the therapy. The rat hearts were examined using diagnostic ultrasound and the rats themselves were histopathologically examined for evidence of metastatic disease and/or cellular damage. The tumors were exposed to 20 or 70 kHz ultrasound for one hour.

13
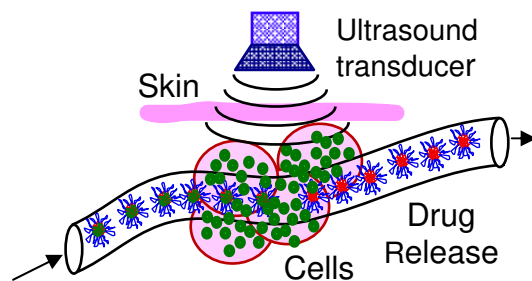
Figure 2-7 Illustration of ultrasound-induced drug release in a capillary vessel. Micelles release the encapsulated drug at the targeted tissue upon application of ultrasound then quickly reform.

Results showed that encapsulated Doxorubicin concentrations of 8 mg/kg-rat were lethal to rats within two weeks of the initial injection. Analysis of other subsets showed that application of low-frequency ultrasound and encapsulated DOX at concentrations equal to or less than 2.67 mg/kg resulted in a significant decrease in tumor size. This result can be seen in Figure 2-8, which shows the growth of an insonated (ultrasonicated) and a non-isonated tumor on the same rat. The arrows depict the days when the rat received ultrasound treatment.

In the same study, evaluation of heart function and physical condition showed that Pluronic micelles protected the heart from the cardiotoxic effects of DOX. However, pulmonary metastases occurred in roughly 75% of insonicated rats, indicating that Pluronic micelles do not prevent the spread of tumors to other tissues. Kidney lesions occurred in all groups receiving more than 1.33 mg/kg of encapsulated DOX, suggesting that these lesions were a side effect of the drug and not the micelle [23].
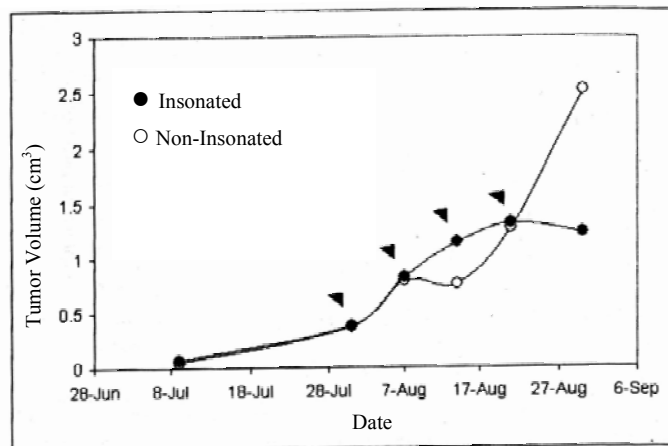
Figure 2-8 Insonated versus non-insonated tumor growth pattern over several weeks. Ultrasound treatment is depicted by arrows. The lines were added only to guide the eye. [23]

2.6   Doxorubicin

Doxorubicin, also known as Adriamycin, is a common chemotherapeutic drug used to treat many forms of cancer. This cytotoxic anthracycline antibiotic, isolated from cultures of *Streptomyces peucetius*, has been used successfully in many neoplastic conditions (about 1/3 of all cases) such as acute lymphoblastic leukemia, acute myeloblastic leukemia, breast and ovarian carcinoma, and Hodgkin's disease. The structure (Figure 2-9) consists of an anthracycline nucleus which presumably binds to phosphate bridges of DNA, inhibiting cell replication by interfering with helicase, DNA topoisomerase, and DNA and RNA polymerase activities. DOX not only stops cell growth, but can also cause cell apoptosis, or self-induced death. Drug decomposition also causes free radical formation and lipid peroxidation, which affects cell membrane stability and, as will be explained later, may be the cause of its cardiotoxicity [24].
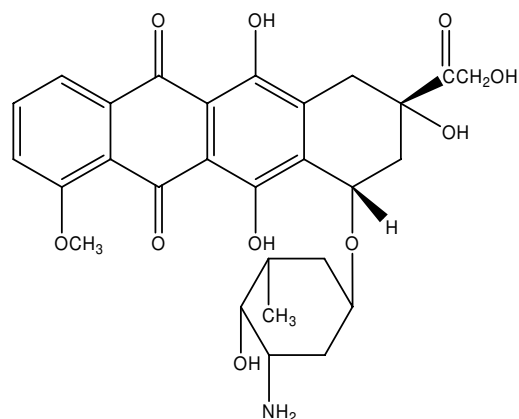
Figure 2-9 Chemical Structure of Doxorubicin (DOX)

While Doxorubicin is successful in fighting cancer, it can, however, cause severe side effects the most frequent being cumulative dose-dependent cardiotoxicity. Cardiac toxicity leads to congestive heart failure, which is usually fatal. Figure 2-10 shows how the probability of acquiring congestive heart failure increases with cumulative doses of DOX [25]. The incidence of Doxorubicin-induced cardiotoxicity becomes critical when the total cumulative dose administered approaches 450 to 500 mg/m^2. (The most common dose is 60-75 mg/m^2 as a single intravenous injection every three weeks.) DOX may also cause testicular atrophy, ulceration and necrosis of the colon, and secondary acute myeloid leukemia. However, in spite of these adverse side effects, Doxorubicin is still one of the more popular chemotherapeutic drugs used today.
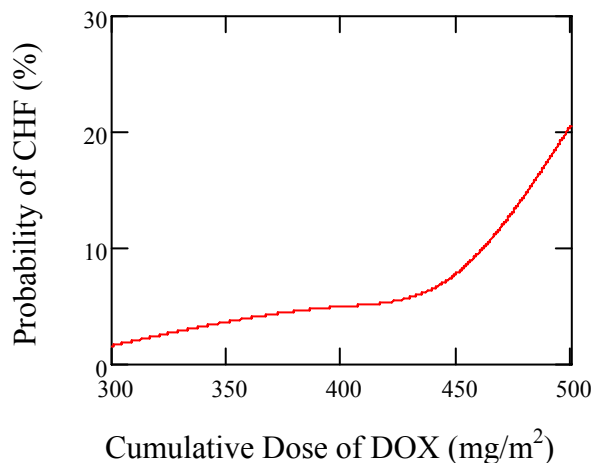
Figure 2-10 Correlation of cumulative dosage of Doxorubicin on the probability of acquiring congestive heart failure. (Created from data contained in Ben Venue Lab. [25])

2.7   Pharmacokinetics of Doxorubicin

Due to the narrow dosage range in which Doxorubicin can effectively and safely be used, it is important to know how the drug moves throughout the body with time. Pharmacokinetic parameters such as the area under the concentration-time curve (AUC), plasma clearance, distributive half-life, and volume of distribution are used to describe drug movement through the body. These parameters can then be correlated to model typical behavior. In a review which described some applications of pharmacokinetic modeling of anticancer drugs, Rousseau and Marquet state that multilinear regression models have been developed for many drugs, including Doxorubicin; and that these models can be used to predict a single exposure variable (such as AUC) from a small number of plasma concentrations obtained at predetermined times after a standard dose administration. However, current models employ the use of databases and population statistics to give more precise predictions. All pharmacokinetic studies of various

17

populations are continually added to databases and analyzed. Results from these studies can be used to aid physicians in adjusting dosages to fit individual needs. Two methods are commonly used: 1) *a priori* formulae that allow the computation of the first dosage based on biological data such as weight, age, gender, creatinine clearance, and glomerular filtration rate; and 2) *a posteriori* methods that use drug plasma levels to adjust the subsequent doses [26]. Both these methods require pharmacokinetic results to establish models that these methods can employ. For the past three decades, researchers have studied the pharmacokinetics of Doxorubicin in various applications. A few of these applications include administration of free DOX (dissolved in saline) [24, 25, 27-29], or loading the drug into carrier molecules such as liposomes [24, 27] or micelles [12]. The pharmacokinetic results are described below.

2.7.1   Pharmacokinetic Studies of Free Doxorubicin

Most pharmacokinetic studies of Doxorubicin focus on its individual dynamics and effects. It is commonly dissolved into saline solution and administered intravenously either as a single injection (bolus) or continuously for a period of time.

Plasma

The most commonly used pharmacokinetic models are either one-compartment or two-compartment models. All drugs initially distribute into a central compartment (circulatory system, major organs) before distributing into the peripheral compartment (adipose, muscle, extremities). In one-compartment models, the drug is assumed to rapidly equilibrate between these two compartments. This assumption allows for a simpler model consisting of just one volume term. However, not all drugs are quickly

18

transported throughout the body. For drug with a slower distribution rate, a two-compartment model is used. Plasma drug concentrations following the two-compartment model, as shown in the left graph of Figure 2-11 on page 21. Such plots, with a log scale on the y-axis, yield a biphasic line. The first part of the line (with a steeper slope) represents the distribution phase, or the time interval where the drug is distributing from the central compartment into the peripheral compartment. During this phase, the time it takes for the drug concentration to decrease to one-half of its original concentration is called the distributive half-life. Once the drug distribution between the compartments reaches an equilibrium state, the line becomes straight. This second part of the line is the elimination phase, or the time interval where the drug is reacting and/or being removed from the system. This is usually a first-order process, thus creating a straight line on a semi-log plot. During this phase, the time it takes for the drug concentration to decrease to one-half of its original concentration is called the terminal half-life.

Doxorubicin displays at least a biphasic deposition after intravenous injection in rats and humans. It has a distributive half-life of about 5 minutes and a terminal half-life of 20 to 48 hours, showing fast drug uptake into but slow elimination from the tissues [25].

Table 1. Free Drug in Plasma [24, 25]	
Distributive Half-Life	~5 minutes
Terminal Half-Life	20-48 Hours
Plasma Clearance	8-20 ml/min/kg
Vol. of Distribution	> 500 L/m2
Protein Binding	50-85%

19

DOX displays wide distribution in the plasma and tissues with a volume of distribution exceeding 500 L/m^2 [24]. The volume of distribution is the theoretical size of the compartment necessary to account for the total drug amount in the body if it were present throughout the body in the same concentration found in the plasma. The volume of distribution (V_d) is calculated by dividing the dose amount by the plasma drug concentration. Factors that may effect the V_d include protein binding, hydration, lean body mass, nutrition, side reactions, etc. Doxorubicin displays plasma protein binding ranging from 50 to 85%. The drug is also metabolized in the liver by aldo-keto reductase to yield Doxorubicinol, a metabolite, which still retains antitumor activity [24].

Studies by Danesi et al. using maximum-effect modeling showed significant relationships between the area under the concentration-time curve (AUC) of DOX and the leukocyte and platelet counts, as well as between the AUC of Doxorubicinal, another metabolite, and the decrease in neutrophils and platelets [24]. These relationships can then be applied to predict the AUC given a few blood samples; which then, in turn, is used to determine the most efficient drug dosage for that patient.

The same study showed that the maximum concentration, rather than the AUC, is related to the cardiotoxic effects of the drug [24]. Therefore, Doxorubicin-induced cardiotoxicity may be reduced by prolongation of intravenous infusion, instead of bolus injections, without affecting the tumor response.

Renal and Biliary Excretion

Tavoloni and Guarino studied the biliary and urinary excretion of Doxorubicin in rats by evaluating the role of the liver or the liver and kidneys together [28]. Half of the rats had their kidneys ligated, or tied off. Then, they intravenously injected a

20

radioactively labeled drug in concentrations of 5, 20, or 40 mg/kg. Plasma drug levels were measured for three hours and biliary and urine excretions over ten hours (Figure 2-11) using radioassay and fluorescence detection.
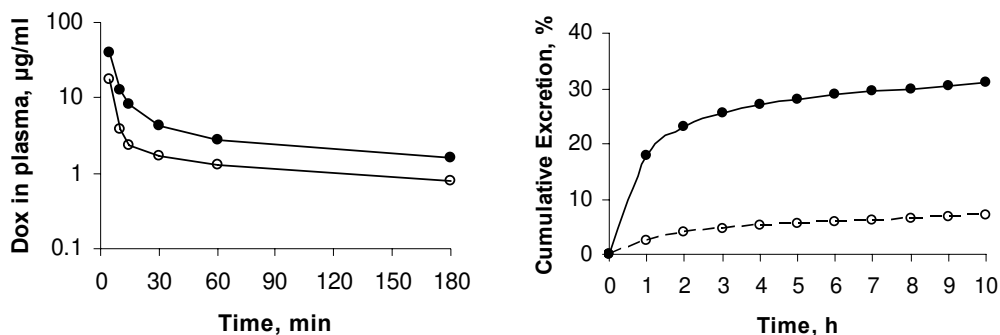
Figure 2-11 Concentration of Doxorubicin in blood plasma in rats over time for intravenous injections of 20 (○) and 40 (●) mg/kg (left). Average biliary (●) and urinary (○) excretion of total DOX equivalents in rats for injections of 5-40 mg/kg (right). [28]

When data of drug excretions in bile and urine were analyzed, according to a two-compartment pharmacokinetic model, both biliary and urinary excretion followed the biphasic pattern in all but one instance – the urinary excretion after 40 mg/kg did not fit either one- or two-compartment analysis. At this high dose, renal function temporarily shut down for 30-45 minutes, possibly due to the toxicity of the drug. The time courses of DOX excretion following 20 and 40 mg/kg injections are comparable. After both injections, the labeled drug appeared in the bile within 3-5 minutes and reached peak excretion and concentration levels after 30 minutes, with the peak concentration (c_{max}) strictly proportional to the administered dose. After peaking, the excretion of the drug declined with time in a monophasic pattern.

Within 60 minutes of the injection, 18-20% of the dosage had left the body. The overall excretion of DOX was found to be linearly related to the dose administered. However, there were distinct differences between biliary and urinary excretion of the drug. Biliary excretion was linearly related to the administered dose, while urinary excretion greatly varied from linearity. However, due to the small role that urinary excretion plays in the overall drug removal, it is not surprising that the overall excretion is still linearly related to dosage.

The researchers came to the following conclusions: First, when DOX is injected intravenously into rats, it is rapidly cleared from the plasma and extensively excreted through the biliary route but was only moderately eliminated in urine. Second, the urinary pathways of DOX elimination are of minor importance to the overall excretion of the drug. The results demonstrated that blocking the renal route, by ligation of the kidneys, increases the biliary excretion of the drug, which compensates for amounts otherwise eliminated in the urine. Third, the biliary excretion of DOX within the tested doses (5-40 mg/kg) is proportional to the dosage administered because no saturation has occurred, but the urinary excretion of the drug appears to be a dose-limited process, as evidenced by the severe impediment of urine flow at 40 mg/kg [28].

Danesi et al. published similar findings, concluding that the liver cleared more Doxorubicin than the kidneys. After 6 days, about 12% of the total dose is recovered in the urine, while 50% is excreted in the bile within 7 days of treatment (50% unchanged DOX, 23% Doxorubicinol, 27% other metabolites). Since hepatic clearance plays a major role in the pharmacokinetics, patients with liver disorders will handle the drug differently than normal patients [24].

Table 2. Renal and Biliary Excretion of Free DOX [24]	
Time for drug to appear in bile	3-5 minutes
Peak Bile Excretion	30 minutes
Renal clearance in 6 days	12% of total
Biliary clearance in 7 days	50% of total 50% DOX 23% Doxorubicinol 27% other metabolites

Solid Prostate Tumors

Understanding how Doxorubicin distributes through and departs from the blood is important; however, it is far more important to understand the pharmacokinetics of the drug in tumors. Afterall, its ultimate purpose is to fight cancer and combat neoplastic tissue. Following a systemic intravenous injection, drug delivery to the tumor core involves three processes: 1) Distribution through vascular space, 2) transport across microvessel walls, and 3) diffusion through interstitial space in tumor tissue.

Studies performed by Zheng et al. examined whether Doxorubicin penetration into prostate tumors is time and/or concentration dependent [29]. They examined the kinetics of drug penetration and the effects of tumor cell density on drug penetration. Prostate tumors were obtained from patients and human xenograft tumors maintained in immunodeficient mice. Histocultures of the tumors were treated with 0.02 to 20 μM Doxorubicin for up to 96 hours. The drug concentration in the tumor was analyzed by high performance liquid chromatography and quantitative fluorescence microscopy. Figure 2-12 shows the kinetics of uptake, accumulation, and retention of DOX in the

xenograft tumors at various initial extracellular concentrations. The drug-containing medium was replaced with drug-free medium at 96 hours.
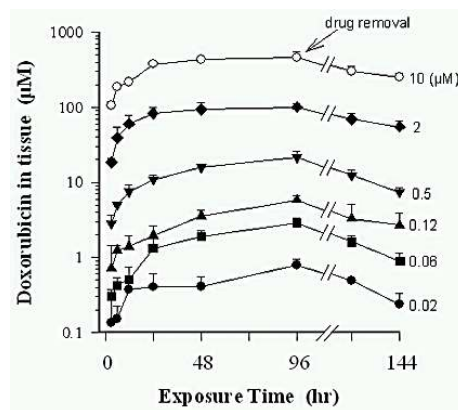
Figure 2-12 Kinetics of uptake, accumulation, and retention of Doxorubicin in xenograft tumors at different initial extracellular concentrations. [29]

The drug concentrations in tumors reached plateau levels between 48 and 96 hours, even though DOX in the blood was cleared much more rapidly. The maximum drug concentration in tumors increased with the initial drug concentration in the culture medium. The ratio of the maximal tumor concentration to the final concentration in the culture medium was approximately 100%, with 60% and 40% remaining after 24 and 48 hours, respectively. The high drug accumulation and slow drug release are likely the result of the hydrophobic drug binding to intracellular macromolecules.

Spatial distribution of Doxorubicin in tumor tissue was visualized using fluorescence microscopy. Figure 2-13 shows how the drug penetrated the tumor over time. Drug concentrations were measured at different distances from the periphery. The results at the lower concentration (1 μM) showed Doxorubicin remaining in the periphery of both patient and xenograft tumors at 72 hours. However, at higher concentrations (5

24

μM or 20 μM), the drug was initially confined to the periphery for 12-24 hours (depending on the tissue), and was then followed by an abruptly enhanced drug penetration such that an equal distribution was attained shortly thereafter (24-36 hours). For both patient and xenograft tumors, the concentration gradient from the periphery to the center of a tumor decreased with increasing treatment time and drug concentration; however, the xenograft tumors showed greater periphery-to-center concentration gradients.
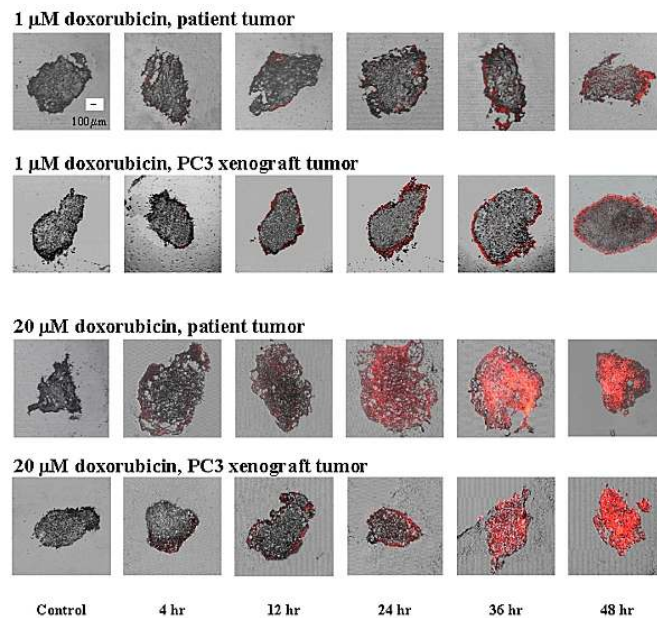
Figure 2-13 Doxorubicin penetration in patient and xenograft tumors at different time intervals. Drug distribution is show in bright orange. Tumor histocultures were treated with 1 μM and 20 μM Doxorubicin. Magnification X 40. [29]

The delay in Doxorubicin penetration to the center of the tumors was attributed to high tumor-cell density. The differences in cell density between the xenograft and the patient tumors (23%) was similar to the differences in drug accumulation between these tumors. This explains the greater periphery-to-center concentration gradients in the more

25

dense xenograft tumors. Also, the abrupt change in penetration rates exhibited by those tumors treated with higher concentrations is thought to be caused by drug-induced cell death and the subsequent reduction of cell density [29].

In summary, this study suggests cellularity as a major determinant of the rate and extent of Doxorubicin penetration and accumulation in solid tumors. The results demonstrate an interesting new concept in the relationship between drug delivery and drug effect in that the pharmacological effect of a drug can modify its own delivery. The penetration dynamics are greatly affected by the tissue density and composition, drug concentration, and the treatment duration.

Table 3. Prostate Tumor Histocultures in DOX solution [29]	
Drug plateau time	48-96 hours
Max [tumor]/[medium] ratio	100
% remaining after 24 hours	60%
% remaining after 48 hours	40%
Major factors influencing DOX penetration dynamics in tumors:	Tumor density Drug Conc. Treatment Time

2.7.2 Pharmacokinetic Studies of Doxorubicin in Drug Carriers

Using polymer drug carriers for delivery is a subject of growing research and popularity. The desire to eliminate the side effects of chemotherapy and to more efficiently deliver higher concentrations of Doxorubicin to cancerous tissue has led to many designs of drug carriers. These carriers shield the effects of the drug and also

lengthen the drug's half-life. Many methods are being explored to disrupt these carriers and locally unload its drug contents.

Liposomes

Liposomes are spherical vesicles in an aqueous medium formed by a lipid bilayer enclosing an aqueous compartment. The bilayer of the liposome is designed to protect and confine the enclosed drug until the liposome binds with the outer membrane of target cells. By delivering treatments directly to the cells needing them, drug efficacy may be increased while overall toxicity is reduced. They are composed mainly of fully hydrogenated phospholipids and are easily metabolized with only mild toxicity [27]. DOX in polyethyleneglycol (PEG)-coated liposomes, or "stealth" liposomes, allow for increased drug concentration while decreasing its side effects. The PEG coating prevents liposomal detection by plasma proteins and phagocytosis, or uptake, by the reticuloendothelial system. Cardiac toxicity is uncommon using this method. The pharmacokinetics of DOX released from PEG-liposomes are described by a monoexponential elimination curve with a long half-life (79 hours), low total body clearance (0.04 L/h), and a small volume of distribution (3.9 L/m^2) when compared to free drug. The maximum concentration and AUC increase linearly with the dosage [24]. In a study performed by Linkesch et al. [27], nine human patients with aggressive Non-Hodgkin's lymphoma were infused with Doxorubicin-loaded, PEG-coated liposomes (Caelyx®) at a rate of 0.79 mg Caelyx® per minute for one hour. Blood samples were drawn at 0, 15, 30, 45 and 60 minutes after the start of infusion and thereafter on each day from the first day to day 21. DOX concentration was quantified by solid phase

extraction followed by reversed-phase high performance liquid chromatography using fluorescence detection.

Table 4. DOX loaded Liposomes [24, 27]	
Half-life	79 Hours
Body Clearance	0.04 L/h
Vol. of Distribution	3.9 L/m^2
DOX serum concentrations: log([DOX]) = -0.160*days + 3.902.	

After infusion (= 1 hour), the drug concentration in the blood increased until reaching an average c_{max} of 4.595 ± 2.849 mg/ml with a mean t_{max} of 1.79 ± 1.55 days. About 27% of the administered dose was present at t_{max}, after which the DOX concentrations decreased slowly. The majority of the liposomes had completely released their load of DOX by one week after infusion.

Regression analysis of the mean logarithmic DOX serum concentrations versus days showed a strong linear correlation (R=0.988):

$$\log[DOX] = -0.160 \text{ days} + 3.902. \qquad \textbf{(2.1)}$$

The linear decay gives evidence of an open one-compartment model. DOX metabolites could not be detected in any blood sample; evidence that the author uses to claim that the liposomes prevent first-pass metabolism of DOX in the liver. The small volume of distribution for the central compartment gave evidence that liposomes circulated in the

blood over many days and distributed into the tissue continuously but to a small extent. The total body clearance of liposome-DOX was about 20% of the total body clearance of free drug [27].

Micelles

Like liposomes, micelles can also act as drug carriers. Micelles currently being tested in drug delivery are made of block copolymer chains consisting of a hydrophobic part (e.g. PPO) and a hydrophilic part (e.g. PEO), which can spontaneously assemble in aqueous solutions to form spherical micelles with a hydrophobic core. Hydrophobic drugs, such as Doxorubicin, will partition strongly into these cores and remain there in aqueous solutions as long as the micelle remains stable.

Alakhov et al. studied the pharmacokinetics and tissue distribution of DOX formulated with SP1049C, a modified Pluronic compound, in normal and tumor bearing mice [30]. Comparing free Doxorubicin and the DOX/SP1049C formulation, the block copolymers showed little effect on the pharmacokinetic profiles of the drug in liver, kidney, heart, or lung in either normal or tumor-bearing mice. However, the area under the concentration-time curve in the brain was increased 2.9 and 1.7 times in normal and tumor-bearing mice, respectively. The authors suggest that the increase in brain accumulation of Doxorubicin may be related to inhibition by Pluronic of the drug efflux systems expressed in the blood brain barrier, which is designed to keep harmful substances out of the very sensitive brain tissue. Also, a substantial 1.7-fold increase in drug accumulation in solid tumor was also observed with the drug/micelle formulation compared with free drug. Other pharmacokinetic studies show that Pluronic block

copolymers are eliminated primarily by renal excretion [12]. Also, Pluronic concentrations in the plasma remain quite high for several hours after administration [31].

2.8   Tumor Model

Cancerous cells, in basic terms, are normal cells that replicate faster than usual, usually because of genetic mutations. These mutations "activate" growth and replication genes or "deactivate" genes that inhibit these processes. These fast-growing cells require many nutrients and thus require a large blood supply. In order to satisfy this requirement, tumors have leaky capillaries which allow the plasma and nutrients in the blood stream to easily leak out and "bathe" the rapidly growing cells. This becomes advantageous when attempting to deliver drugs because the drugs have an easy access to the tumor. Also, particle drug carriers, such as micelles, can easily leave the blood system through these leaky capillaries and possibly become trapped in the cancerous tissue.

As strange as it may sound, growing tumors in rats is a difficult task. Normally, the rat must be immune-compromised to prevent its immune system from attacking the tumor. Then, because of the lack of immune system, the rat must be contained in a sterile chamber to prevent other infections. However, the BDIX rat has been specially bred to accept the DHD/K12/TRb colorectal epithelial cancer cell line. Studies show that this cancer line can be injected anywhere in the BDIX and it will successfully produce tumors [32]. This cell line is susceptible to the Doxorubicin [33].

2.9   Drug Extraction/Quantification

In this thesis, Doxorubicin must be extracted from various tissues and analyzed to determine it concentration in those tissues. Thus, extraction and quantification methods are required. These methods must be versatile, for there are many types of tissues containing different compounds. Also, they be consistent and reproducible. Finally, the methods must be quick and simple because Doxorubicin stability cannot be guaranteed over a long period of time due to its heat- and light-sensitivity.

Álvarez-Cedrón et al. have developed a quick and simple extraction and high performance liquid chromatography (HPLC) method that can be used for a variety of tissues including kidney, liver, heart, lung, and muscle. Their extraction method only requires a single solvent deproteinising step. Results showed that their method successfully recovered 95.6 to 97.3% from the tissues. The limit of accuracy is 5 ng/ml. A linear fit proves satisfactory ($r^2 > 0.991$) over the 5-5000 ng/ml range when comparing drug concentration with the height or area peak given from the HPLC detector [34].

3 Objectives

The objective of this research is to investigate the effect of ultrasound on micellar drug delivery *in vivo*; more specifically, 1) to study the pharmacokinetics of Doxorubicin in the rat model using this delivery method, and 2) to study the effects of different ultrasound frequencies. These two main objectives can be divided into several sub-objectives:

1) Determine the pharmacokinetics of Doxorubicin in the rat model using delivery from Plurogel^{TM} and ultrasound at 20 kHz and 500 kHz.

 A) Use chemical extraction and high performance liquid chromatography to determine the concentration of Doxorubicin in ultrasonicated and non-ultrasonicated tumors over a time period of one week, with special attention to the first twelve hours after drug/micelle injection, and determine whether application of ultrasound makes a difference on concentration.

 B) Determine the Doxorubicin concentration in the heart, liver, and skeletal muscle over the one week period after drug/Plurogel^{TM} injection

C) Discover if there is drug accumulation in any of the above-mentioned tissues over the course of several weekly treatments. The heart is of special interest because of the cardiotoxic effect of Doxorubicin.

2) Determine the effects of different ultrasound frequencies.

A) Determine if there is any difference in drug concentration in the tumor when using two different ultrasound frequencies while using the same mechanical index and time-averaged power density.

B) Determine if there is any difference in tumor growth *in vivo* when using two different ultrasound frequencies but the same mechanical index and time-averaged power density.

While Nelson's method for drug injection, ultrasound application, and tumor measurement will be used for this project, there are some important distinctions and improvements worth emphasizing. This project will measure the *drug concentration* in the tumors and also in other important tissues such as the liver, heart, and muscle tissue adjacent to the tumor. Nelson's objectives were to develop a cancer model and treatment method. He also observed the effects caused by changing power density, frequency, power train, and number of treatments per week. However, because of the large number of variables used in his experiments and the large inherent variability between rats, he could not reach any statistically supported conclusions about these variables; he could only conclude that the treatment reduced tumor growth rate. This proposed project looks specifically into the possible mechanisms (i.e. drug concentration and ultrasound

frequency) that could cause reduced tumor growth rate. While Nelson varied mechanical index with the frequency, this project will hold mechanical index constant in order to look solely at the effect of frequency. The effect will be a more rigorously determined understanding of the distribution of DOX, the effect of ultrasound frequency, and the possible mechanisms of drug delivery than previously found in the literature.

4   Experimental Approach

4.1   Drug/Plurogel® Preparation

The drug carrying micelles were formed from Pluronic™ P105, a tri-block copolymer consisting of a central block of poly(propylene oxide) flanked by blocks of poly(ethylene oxide). These micelles were stabilized by polymerizing an interpenetrating network of a thermally responsive N,N-dimethylacrylamide within the core of the micelle [13]. A solution of 10 wt% stabilized Pluronic micelles (Plurogel™) was analyzed for size using light scattering and turbidity using a spectrophotometer. Acceptable micelle diameters were between 75-150 nm. Acceptable turbidity measurements were between 0.1-0.3 using a wavelength of $\lambda = 600$ nm.

Doxorubicin was loaded into the micelles by introducing 3.75 ml of Plurogel into a 10 mg vial of DOX via a 0.22 μm membrane filter. The mixture was shaken until visually homogenous. If the DOX-encapsulated micelles were not immediately injected, the vial was stored at -20 °C.

4.2   Tumor Implantation

The DHD/K12/TRb rat colonic cancer cell line was used in this study. The cells were cultured *in vitro* in RPMI containing 2 mM Nystatin, 0.2 mM Gentamicin, 2mM L-Glutamine, and 20% Fetal Bovine Serum (FBS). The cells were incubated at 37 °C and

5% CO_2 in 7 mL polystyrene cell culture flasks (Nalge Nunc International, Rochester, NY) and were split 1:3 using 0.25% trypsin/EDTA when the cells reached confluency. Prior to injection in the rat, the cells were washed in phosphate buffered saline (PBS) and then suspended by incubation with 0.25% trypsin for five minutes at 37 °C. Following suspension, aliquots of cells were tested for viability using a trypan blue assay. The cells were then washed in RPMI plus 20% FBS to inactivate the trypsin, and resuspended at 2.5×10^6 cells/ml PBS for injection.

Rats were partially anesthetized with an interperitoneal injection of ketamine (0.5 ml/kg-rat). The rats' legs were shaved and depilated with Nair[®], a hair removal cream, which was applied for 1 minute and then immediately washed off with water. A volume of 0.025 ml of tumor cell suspension was injected subcutaneously, using an insulin syringe, over the gastrionemius in each lower leg of a female BDIX rat, the original host for this cancer cell line. Tumors were allowed to grow for at least three weeks before any treatments. Only rats with bilateral tumors were used in tumor growth studies that measured the effect of ultrasound because one tumor had to be used as an internal control (i.e. did not receive ultrasound). Rats that did not grow bilateral tumors were used only for pharmacokinetic studies, including those that grew no tumors. If a rat only grew one tumor, that tumor received ultrasound treatment. If a rat did not grow a tumor, the leg muscle received ultrasound treatment in the pharmacokinetic study.

4.3   Ultrasound Frequency / Tumor Growth Experiment

In this experiment, rats were treated for six consecutive weeks. Once a week, each rat received systemic drug injection and ultrasound treatment on one of the two tumors

using either a 20 or 500 kHz transducer; half of the rats were ultrasonicated using the 20 kHz probe (continuous wave, intensity of 1.0 W/cm^2, pressure amplitude of .173 MPa) and the other half were treated using a 500 kHz transducer with pulsed ultrasound at 23.61 W/cm^2. The mechanical index needed to be constant between the two different frequencies. The mechanical index of 20 kHz frequency at 1.0 W/cm^2 was 1.22. In order to match that mechanical index at the 500 kHz frequency, an intensity of 23.61 W/cm^2 (pressure amplitude of 0.842 MPa) was required. However, transmitting this amount of energy would most likely cook the tumor and burn the rat. Therefore, the 500 kHz transducer was pulsed with a pulse repetition frequency (PRF) of 20.161 Hz (1000 cycles on; 22,610 cycles off) to create an average intensity of 1.0 W/cm^2. Thus both ultrasonic applications had the same mechanical index of 1.22 and temporal average power density of 1.0 W/cm^2. The non-insonated tumor served as a control. Tumor sizes were measured weekly. After the sixth treatment, the rats were euthanized, the tumors were removed, and the drug was extracted and quantified. The goals of this experiment were to:

1) Determine if there is any difference in drug concentration in the tumor when using different ultrasound frequencies while using the same mechanical index.

2) Determine if there is any difference in tumor growth *in vivo* when using different ultrasound frequencies but the same mechanical index.

The details of the drug administration and ultrasound application are given below.

4.3.1 DOX-encapsulated Plurogel Injection

DOX-encapsulated Plurogel was prepared as previously described. Twenty-three rats were anesthetized initially with only ketamine (0.5 ml/kg) and then pretreated with dexamethasone (4.0 mg/kg sq, neck) and diphenydramine (5.0 mg/kg sq, neck)

subcutaneous injections to prevent anaphylactic shock. The hind legs and tail were shaved, and the hair at the tumor site receiving ultrasound was completely removed through application of Nair® for sixty seconds. Ophthalmic ointment was also administered to prevent the rats' eyes from drying and becoming irritated during the anesthetic period. Then the encapsulated DOX was administered intravenously as follows.

Administration of the encapsulated DOX at 2.67 mg-drug / kg-rat was given via infusion set in the lateral tail vein. The infusion set consisted of a Surflo® winged butterfly infusion, 27-gauge with 8" tubing (#0197, Termo® Medical Corp., Somerset, NJ), connected to a microbore extension set (#4612, Abbot Laboratories, North Chicago, IL) fitted with a 3 ml syringe filled with sterile saline flush. The appropriate volume of encapsulated DOX was drawn into a 1 ml syringe and then administered through the septum of the microbore extension, followed by 3 ml of the saline to completely flush the drug from the catheter.

4.3.2 Ultrasound Application

Following the injection of DOX, the rats were given medetomidine (0.3 mg/kg, ip), a muscle relaxer, which when combined with the previously administered ketamine, produced adequate anesthesia. Medetomidine prevented the rats from moving their legs after the ultrasound transducer had been carefully positioned over the tumor.

Only one tumor on the animal was exposed to ultrasound and the same tumor was exposed each week immediately (about five minutes) after the DOX injection. Ultrasound was applied for fifteen minutes. For insonation at 20 kHz, ultrasound-conducting gel was applied on the skin of the leg above the tumor, and the probe was placed in this gel using

caution to not directly touch the skin. For insonation at 500 kHz, ultrasound-conducting gel was applied on the transducer casing, over the focal point. Then the tumor to be treated was placed in the gel, and the leg was taped down to prevent any possible movement. After the fifteen minute ultrasound treatment, the tumor sizes were measured, and the rats were injected subcutaneously with atipamezole (84.0 μl/kg), the reversal for medetomidine.

4.3.3   Tumor Growth Measurement

For these experiments, the rats were treated weekly for six consecutive weeks. Every week following insonation, each tumor was measured by making two perpendicular measurements (a and b, with $a \geq b$) using calipers. Tumor volume (TV) was then determined using the formula

$$TV = \frac{a \cdot b^2}{2}\qquad\text{(4.1)}$$

The formula approximately represents the volume of a prolate spheroid with a major axis, a, and minor axis, b. In some cases, multiple measurements were taken of the same tumor for statistical analysis.

4.4   Fluorescent Microscopy Study

Five different rats' tumors (ten total tumors) were examined under a fluorescent microscope. Instead of homogenizing the tissue for drug extraction, these tumors were cut into 300 micron slices and viewed under blue fluorescence ($\lambda = 470$ nm).

Doxorubicin fluoresces red while the tumor tissue itself appears green. Each rat received a different drug/ultrasound treatment as described in Table 5. All were euthanized and the tumor recovered one hour after treatment. The goal of this procedure was to qualitatively observe any differences in DOX distribution in the tumors.

Table 5. Experimental Design for the Fluorescent Microscopy Study

Rat	Anesthetic Drugs	DOX / Plurogel	Ultrasound
1	No	No	No
2	Yes	No	20 kHz
3	Yes	Yes	20 kHz
4	Yes	Yes	500 kHz
5	Yes	DOX ONLY	No

4.5 Pharmacokinetics Experiments

These experiments determined the amount of Doxorubicin in different tissues post insonation, thirty minutes to one week after ultrasound treatment. Since, the rat had to be euthanized in order to extract the drug from its organs, multiple rats were required – at least two for each "snapshot" of time after treatment. The goals of these experiments were:

1) to use chemical extraction and high performance liquid chromatography to determine the concentration of Doxorubicin in ultrasonicated and non-ultrasonicated

tumors over a time period of one week, with special attention to the first twelve hours after drug/micelle injection, and to determine whether application of ultrasound makes a difference on concentration.

2) to determine the Doxorubicin concentration in the heart, liver, and skeletal muscle over the one week period after drug/micelle injection

3) to discover if there is drug accumulation in any of the above-mentioned tissues. The heart is of special interest because of the cardiotoxic effect of Doxorubicin.

4.5.1   DOX-encapsulated Plurogel Injection

All the rats used in this study were prepared and injected with DOX-encapsulated Plurogel as described in section 4.3.1.

4.5.2   Ultrasound Application

Thirty-nine rats, used only in the pharmacokinetic study, were ultrasonicated using the 20 kHz probe (continuous wave, average intensity of 1.0 W/cm^2, pressure amplitude of 0.173 MPa) for fifteen minutes as described in section 4.3.2. These rats were treated only once before euthanization. The tumors from sixteen of the twenty-three rats in the Ultrasound Frequency / Tumor Growth experiments described above (Section 4.3) were also used in the pharmacokinetic study. This latter group of rats had received six consecutive weeks of treatment as opposed to a single treatment for the former group.

4.5.3   Euthanasia and Tissue Removal

The 16 rats from the Ultrasound Frequency / Tumor Growth experiments were euthanized after their sixth week of treatment at either 0.5, 3, 6, or 12 hours (four rats per group) after the last ultrasound application, and both the ultrasonically-treated and non-treated tumors were removed.

Twelve of the 39 rats used for the pharmacokinetic study were euthanized at either 1, 6, 12, 24, or 48 hours after ultrasound application and the heart, liver, leg muscle, and tumor (if any) were removed.

The other 15 of the 39 rats were used in more extended pharmacokinetic study. They were euthanized at either 0.5, 8, 12, 48, 96, or 168 hours after ultrasound application and only the heart and tumors (if any) were removed.

The rats were euthanized by placing each rat in a CO_2 chamber for one minute because injection of lethal medication, the more common procedure, contaminates the chemical analysis performed later. After asphyxiation, the desired tissues were immediately removed, placed in vials, and set inside a box of crushed dry ice. Only the tumors were removed from the rats included in the Ultrasound Frequency / Tumor Growth experiment. The tumors, adjacent leg muscles, hearts, and livers were removed from all other rats in the pharmacokinetic study. The tissues remained frozen at -80°C until the drug was extracted, as described later in section 4.6, "Doxorubicin Extraction and HPLC Analysis".

4.5.4   Drug Accumulation Experiment

Three rats were given the drug/ultrasound treatment for four consecutive weeks before being euthanized six hours after the last treatment in order to examine any

accumulation effects. After euthanasia, the heart, liver, leg muscle, and tumor tissue (both ultrasonically treated and untreated) were cut out and stored at -40°C until drug extraction.

4.6 Doxorubicin Extraction and HPLC Analysis

The chemical extraction method was adapted from the Doxorubicin extraction method described by Álvarez-Cedrón et al. [34]. The entire tissue (heart, tumor, etc.) was weighed and then homogenized with 0.067 M potassium phosphate solution in an Ultra-Turrax® T 25 Basic dispersion tool (IKA Works, Inc; Wilmington, NC) according to the following concentrations:

Liver – 50 mg-tissue/ml phosphate solution

Heart, Muscle, and Tumor – 15 mg-tissue/ml phosphate solution

For every collected tissue, two extractions and high performance liquid chromatography (HPLC) runs were performed. First, 0.15 ml of tissue homogenate was added to a 3 ml microfuge vial containing 0.20 ml of 50/50 v/v methanol / 40% $ZnSO_4$ solution. The mixture was vortex mixed for 30 seconds, after which it was centrifuged at 13,000 rev/min for 10 minutes. After being centrifuged, 50 µl of the supernatant was injected into the HPLC system. This system used 65/35 v/v methanol / 0.01 M phosphate buffer mobile phase (1.2 ml/min, 3000 psi), a Waters Novapak C18 column, a Waters fluorescence detector ($\lambda_{excitation}$ = 480nm, $\lambda_{emission}$ = 550 nm), and Millennium[32] data analysis software (Waters Corp., Milford, MA). The HPLC system quantified the amount of DOX in each injection, which was used to calculate the drug concentration in the collected tissues.

4.6.1 HPLC Calibration

A calibration curve was created to correlate the area of the DOX peak in the fluorescence-time graph (Figure 4-1) to the amount of DOX present in a given 50 μl sample injected into the HPLC system. To do this, six vials where created with varying Doxorubicin concentrations of 5000, 1000, 500, 100, 50, and 10 ng DOX per ml of HPLC-grade buffered water (pH 4). Buffered acidic water was used to prevent the degradation of DOX, which is most stable in acidic solutions. These concentrations correspond with 50 μl injections of 250, 50, 25, 5, 2.5, and 0.5 ng DOX, respectively. The calibration curve displayed a linear fit. The calculations used to create the calibration solutions and the resulting calibration curve can be found in the Appendix.

4.7 Statistical Procedure

The tumor volume data were fitted to both linear growth and an exponential growth models, and the data fit best with the following exponential model:

$$V = A_0 e^{kt} \tag{4.2}$$

where t is the time after the first drug injection, V is the tumor volume at time t, A_0 is the tumor volume at $t = 0$, and the exponential factor, k, is the tumor growth rate constant.

Tumor volumes were transformed to the natural logarithmic scale:

$$\ln(V) = \ln(A_0) + kt \tag{2.3}$$

Log-transformed volumes were then analyzed using a linear mixed model with ultrasound treatment, frequency, days after initiation of treatment, and all possible interaction of these factors as fixed effects using SAS software (SAS Institute Inc.; Cary, NC). Initial tumor volumes, rat-specific tumor growth rates, and repeated volume
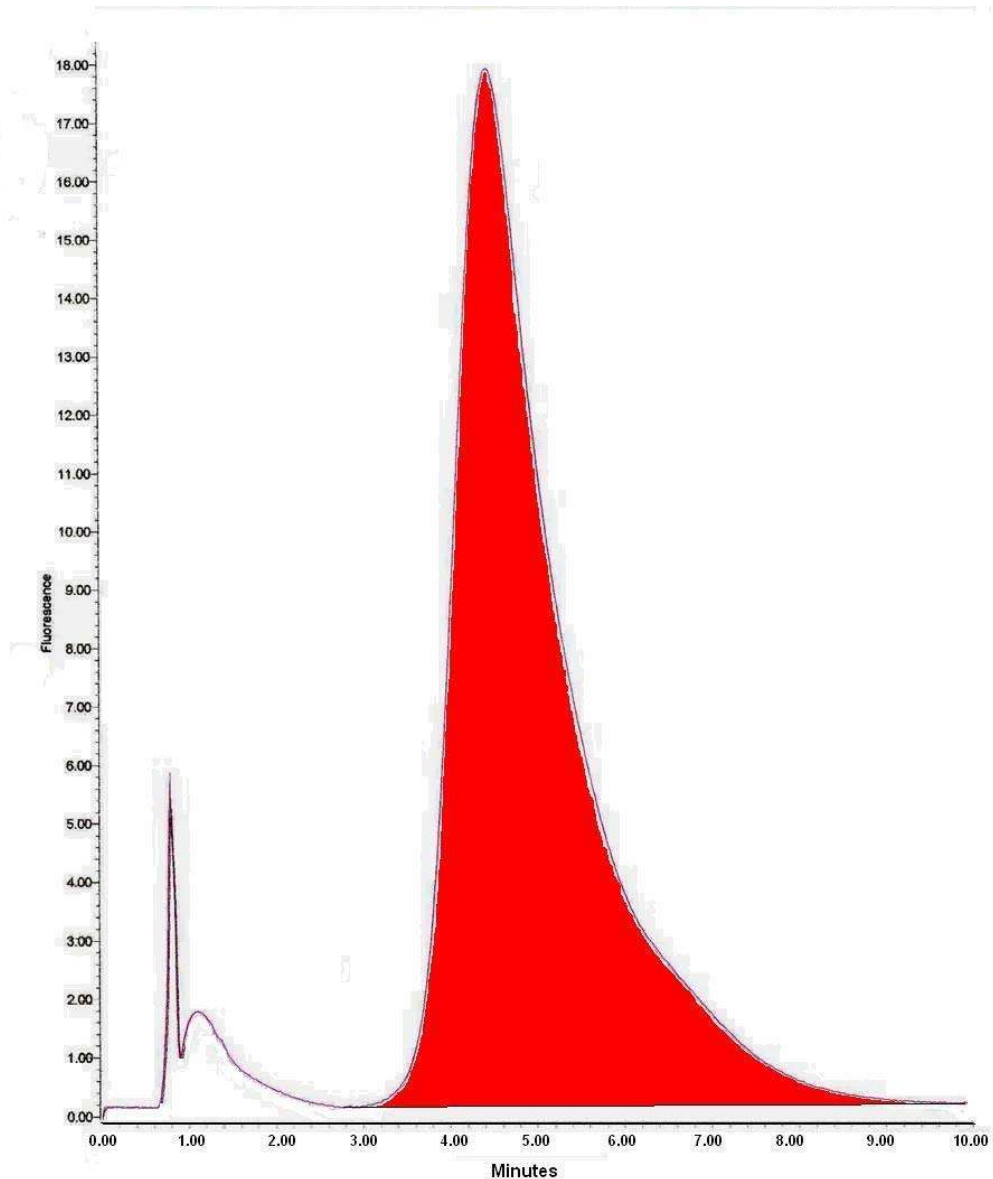
Figure 4-1 A Fluorescence-Time Graph from a HPLC injection. The shaded area represents the area of a peak. The area can be correlated to the amount of a substance injected, where that peak was created the presence of that substance in the fluorescence detector.

47

determinations were considered to be random effects. The model was fitted using residual maximum likelihood for the variance components and estimated generalized least squares for the fixed effects. Residuals were computed and plotted versus predicted values to assess goodness-of-fit of the model. Main effects and interactions of the fixed effects were tested using approximate F-tests based on the Kenward-Roger adjustment for small-sample inferences. Dr. Bruce Schaalje of the Brigham Young University Statistics Department guided the statistical analysis.

5 Results

5.1 Ultrasound Frequency / Tumor Growth Experiment

Of the 24 rats initially used in the experiment, 23 survived all six weeks. One died prematurely because of hypothermia, not because of the treatment or cancer. However, most of the rats did become lethargic and started to loose substantial weight (greater than 10% over a week) after the fifth week of treatments (Figure 5-1). It is suspected that this was due to the combination of the chemotherapy and the growing tumors, some of which had metastasized to the lungs.

Rat Mass Data
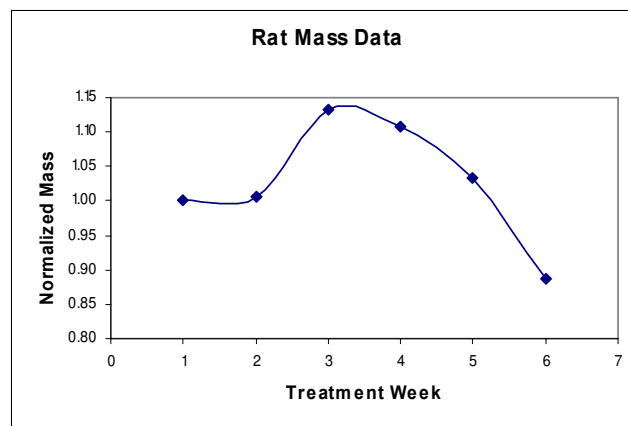
Figure 5-1 Mass of one of the rats in the study over the six week period. The loss of mass during the last two weeks was typical of most of the rats in the study. The mass in this graph was normalized to the measurement from the first week.

The tumor growth rate was adequately modeled by an exponential growth rate. The exponential growth rate constant for the untreated tumors was 0.0465 day^{-1} (standard error = 0.0066), while that for treated tumors – both 20 kHz and 500 kHz frequencies – was 0.0402 day^{-1} (standard error = 0.0066). The difference was 0.0063 day^{-1} (standard error = 0.0022). Comparison between the growth rates of the ultrasonicated tumors and non-ultrasonicated tumors showed that the ultrasonicated tumors displayed significantly slower growth (p = 0.0047). However, comparison between tumors that received 20 kHz and those that received 500 kHz ultrasound treatment showed no statistical difference (p = 0.9275) in tumor growth rate. Figure 5-2 shows an example of tumor growth data that was collected from one of the rats in the study. While the tumors on each individual rat grew (or shrank) differently, this graph is representative of the overall results of the study. The appendix shows the tumor growth rate data from all 24 rats.
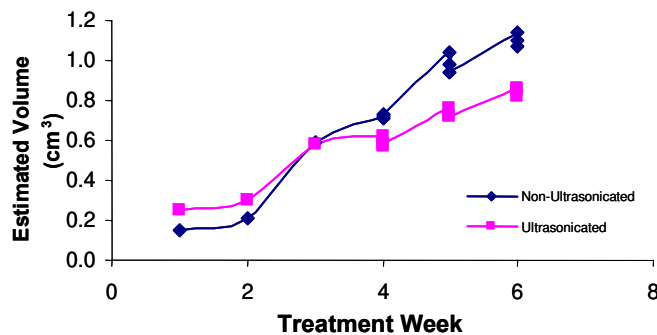
Figure 5-2 Tumor growth measurement data collected from one of the rats (K60) in the study. This graph is representative of the overall results of the study. The blue diamonds (◆) represent the measured volumes of the tumor that did not receive ultrasound. The pink squares (■) represent the measured volumes of the tumor that received ultrasound.

5.2   Pharmacokinetics Experiments

The DOX in various tissues was extracted and quantified using high performance liquid chromatography (HPLC). Figure 5-3 shows the average doxorubicin concentration in the studied tissues (heart, liver, leg muscle, non-ultrasonicated tumor, and ultrasonicated tumor) over the course of one week (168 hours) following drug administration. Over the period of one week, DOX was completely cleared from the liver and muscle tissue but still remained in the tumors. One rat contained a very small amount of DOX (0.04 µg/g) in its heart after one week.

It is necessary to explain that these data were collected from individual rats over the period of two years. Each point represents anywhere between 1 to 20 measurements from 1 to 9 tissue samples. A total of 44 rats and 263 measurements were used to construct these plots. Drug concentrations at short times after ultrasound application were of particular interest, as were the drug concentrations in the treated and untreated tumors. The number of different rats and the number of drug extractions and concentration analysis measurements used per time period after ultrasound treatment, for each of the tissues, is shown on Table 6. The different n-values between tissue types was caused by premature deaths of some of the rats, unsuccessful/unreliable drug extractions, the combination of three pharmacokinetic studies over two years, or errors in drug quantification which required the data to be discarded.
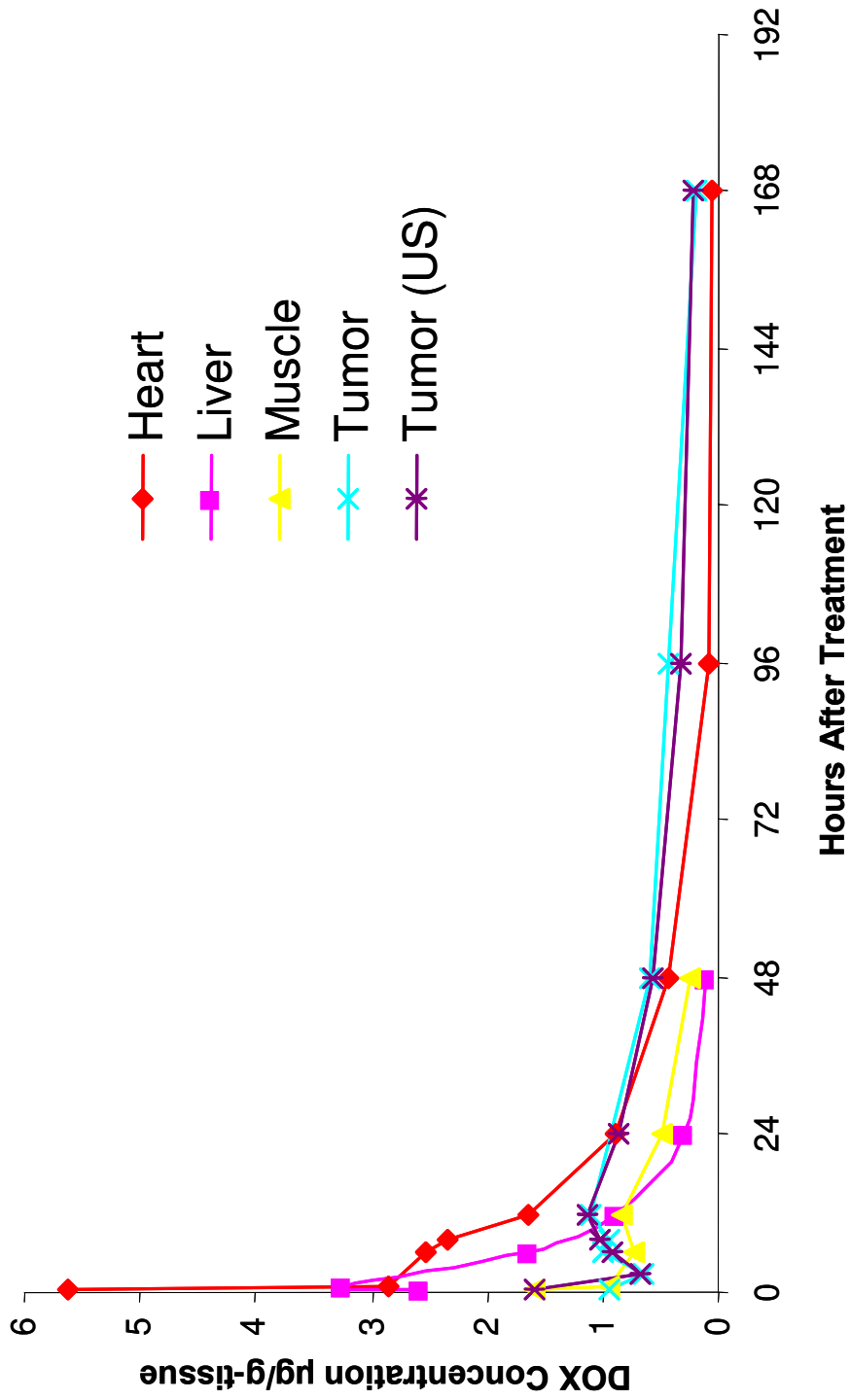
Figure 5-3 Average DOX concentration (µg/gram-tissue) in the heart (◆), liver (■), muscle (▲), non-ultrasonicated tumor (✕), and ultrasonicated tumor (✲) over the course of one week (168 hours).

Table 6. Number of Rats and Drug Concentration Measurements per Tissue Type at each Time Interval after Ultrasound Treatment

Time (hours)	Heart Rats #	Heart Measurements #	Tumor (untreated) Rats #	Tumor (untreated) Measurements #	Tumor (sonicated) Rats #	Tumor (sonicated) Measurements #
0.5	4	7	6	11	6	14
1	2	4	-	-	-	-
3	-	-	4	8	3	6
6	4	8	4	8	8	15
8	3	6	3	10	4	16
12	5	10	7	16	8	18
24	2	4	-	-	2	3
48	4	8	2	5	4	9
96	2	3	2	6	2	5
168	1	1	2	4	2	4

Time	Liver Rats #	Liver Measurements #	Leg Muscle Rats #	Leg Muscle Measurements #
1	2	3	2	5
6	4	7	4	8
12	2	4	2	4
24	2	4	2	4
48	2	4	2	4

The Doxorubicin concentrations in each of the studied tissues are shown below. The heart initially contained the highest DOX concentration but decreased to levels lower than in the tissues by two days after treatments (Figure 5-4). Similarly, the liver initially contained elevated DOX concentrations but, within 24 hours after treatment, decreased to less than one-fourth the levels seen in the tumors (Figure 5-5). The leg muscle (adjacent to the tumors) initially contained DOX concentrations comparable to those in the tumors, but after about 12 hours, the levels in the leg decreased faster than in the tumors (Figure 5-6). The DOX concentrations in the non-ultrasonicated (Figure 5-7) and ultrasonicated (Figure 5-8) tumors were initially much less than in the more vascularized tissues (i.e. heart, liver) but decreases less (even increased slightly up to 12 hours after ultrasound treatment) compared with other tissues, resulting in higher average drug concentrations in the tumors than in the other tissues after as little as 24 hours.
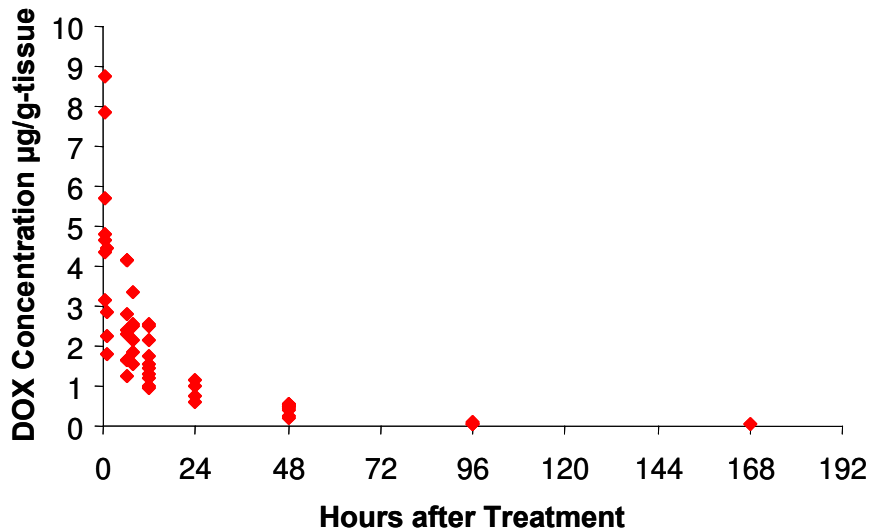
Figure 5-4 Concentration of DOX (µg/g-heart) in the heart over the course of one week (168 hours) after ultrasound treatment.

54
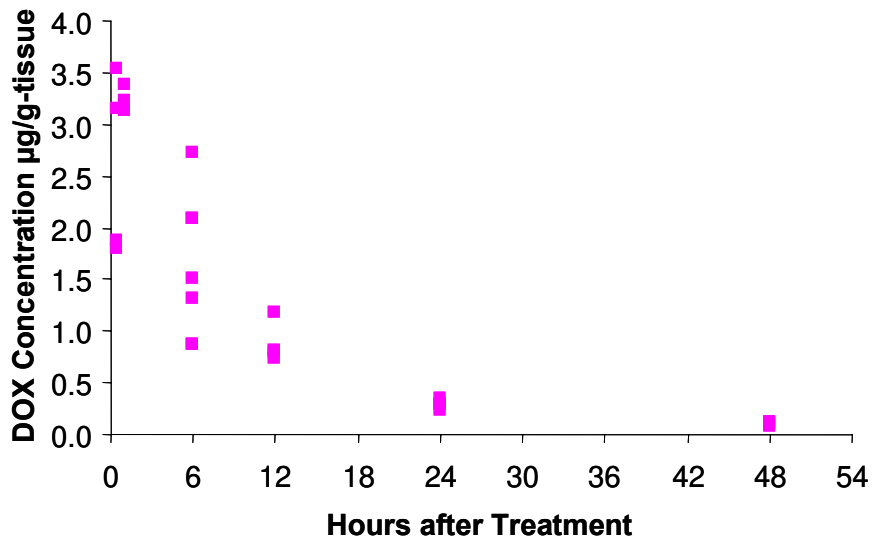
Figure 5-5 Concentration of DOX (µg/g-liver) in the liver over the course of two days (48 hours) after ultrasound treatment.
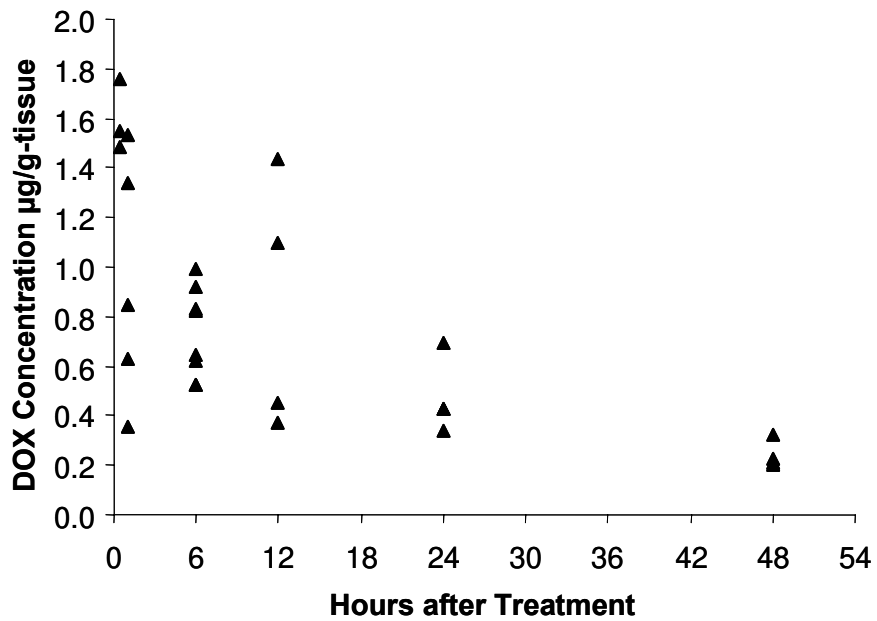
Figure 5-6 Concentration of DOX (µg/g-muscle) in the muscle tissue in the leg over the course of two days (48 hours) after ultrasound treatment.
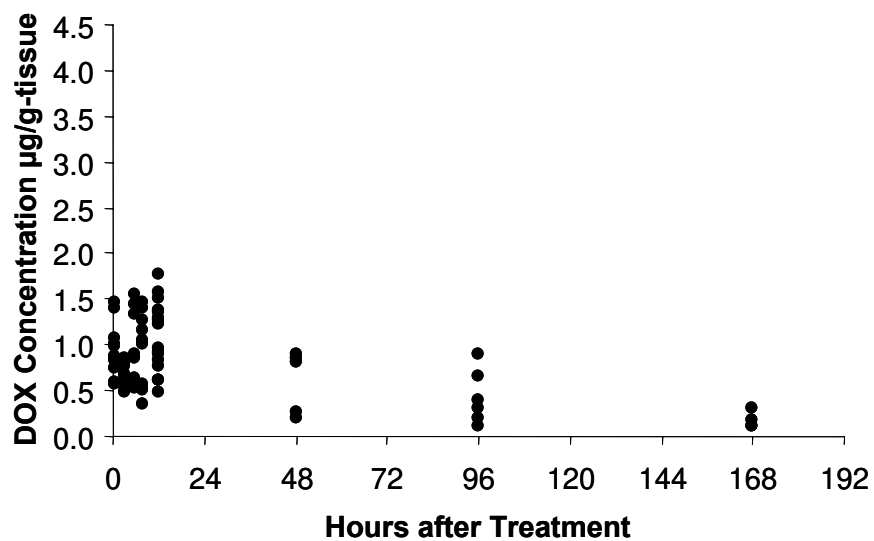
Figure 5-7 Concentration of DOX (µg/g-tumor) in the non-ultrasonicated tumor over the course of one week (168 hours) after ultrasound treatment (to the other tumor).
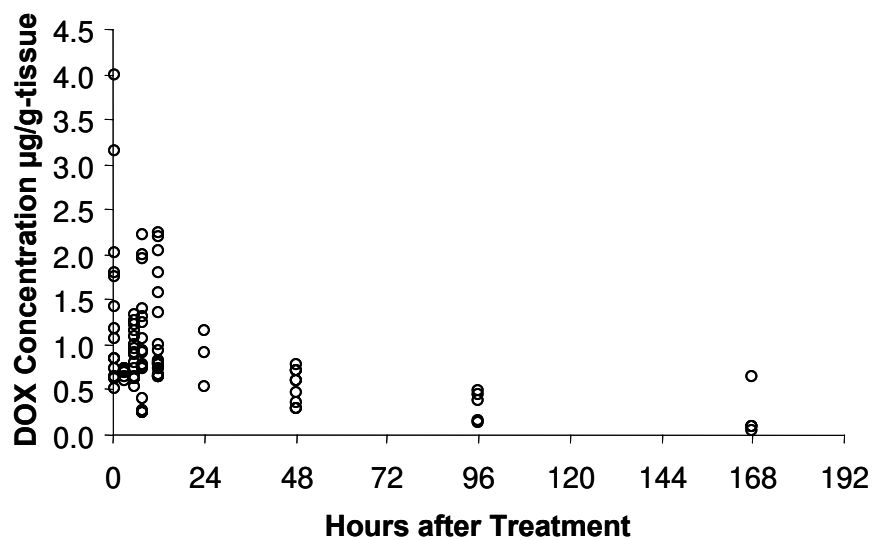
Figure 5-8 Concentration of DOX (µg/g-tumor) in the ultrasonicated tumor over the course of one week (168 hours) after ultrasound treatment.

Using the drug concentrations in each tissue, the total weight of each organ or tumor, and the total amount of Doxorubicin injected for each rat, the percent of the total initial amount of DOX injection found in each organ or tumor was calculated. For example, although the concentration of DOX in the heart 30 minutes after treatment was higher than in the liver, the fraction of the initial dose was higher in the liver (because of its larger size compared to the heart). About 5% of the amount of DOX injected in the rat was in the liver during the first hour after treatment whereas only about 0.5% was in the heart during the same time. Table 7 displays the average percentage of the injected DOX in the liver, heart, and tumors – insonated (US) and non-insonated – at different times after treatment.

Table 7. The Percent of Initial Injection of Doxorubicin Dose Found in Various Tissues after Different Times After Treatment

Tissue	Hours After Treatment									
	0.5	1	3	6	8	12	24	48	96	168
Liver	4.871%	5.432%		2.744%		1.476%	0.484%	0.172%		
Heart	0.668%	0.379%		0.297%	0.261%	0.206%	0.126%	0.056%	0.011%	0.007%
Tumor	0.086%		0.077%	0.060%	0.050%	0.108%		0.009%	0.024%	0.006%
Tumor (US)	0.057%		0.117%	0.050%	0.063%	0.106%	0.011%	0.009%	0.026%	0.007%

5.2.1 Drug Concentrations in Treated (Ultrasonicated) versus Non-treated Tumors

Figure 5-9 shows the average drug concentration (μg/gram-tumor) of DOX in rat tumors (insonated and non-insonated) over the course of two days after ultrasound treatment. Comparison (Table 8) between ultrasonicated tumors (US) versus non-ultrasonicated tumors (no-US) showed no statistical difference in DOX concentrations for any single time period after treatment (i.e. 3 hours, 6 hours). When

comparing the insonated and non-insonated tumors 30 minutes after treatment, the mean

DOX concentration was 1.47 µg/g-tumor and 0.94 µg/g-tumor, respectively (P = 0.055).

Thus, the data suggest that the application of ultrasound to the tumor weakly increases

the average amount of DOX in that tumor for about 30 minutes to one hour after

treatment. After one hour, there was no observed difference between the two groups of

tumors.
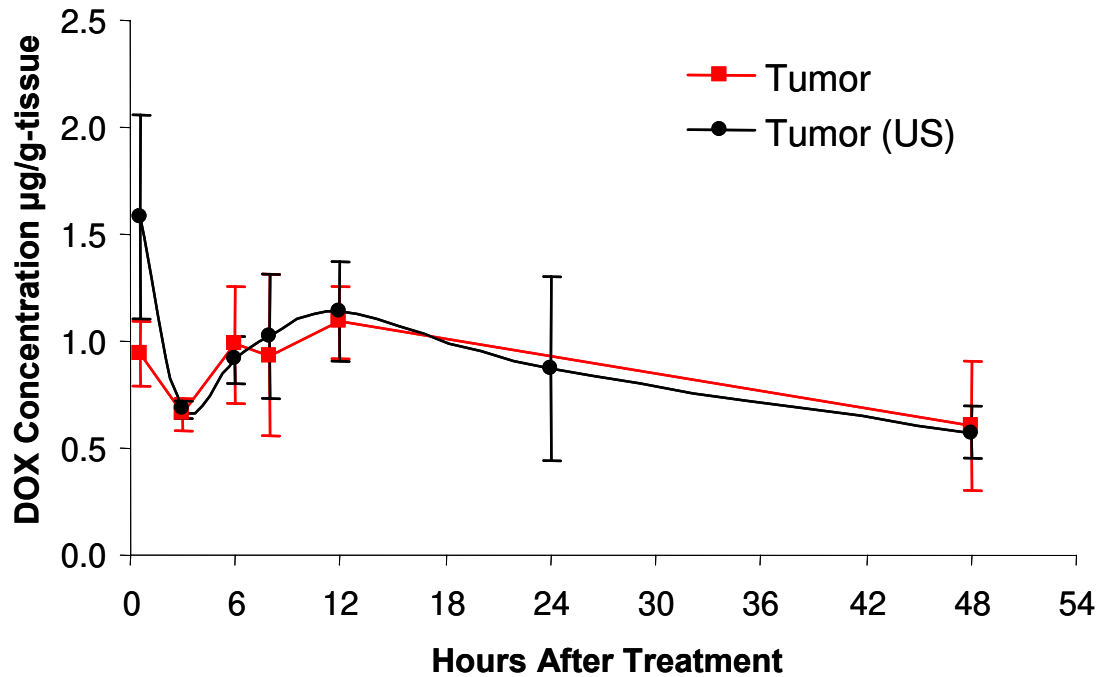
Figure 5-9 Average drug concentration (µg/gram-tumor) of DOX in rat tumors over the course of two days after ultrasound treatment. The graph compares tumors which received ultrasound (US) (●) and those that did not (■). The bars represent the 95% confidence intervals.

Table 8. Statistical Summary: DOX Concentrations in Insonated Tumors (US) Versus Non-Insonated Tumors (no-US)

Time after treatment (hours)		0.5	3	6	8	12	24	48	96	168
Mean DOX conc. (mg-DOX/g-tumor)	(US)	1.47	0.69	0.92	1	1.14	0.874	0.532	0.32	0.22
Mean DOX conc. (mg-DOX/g-tumor)	(no-US)	0.94	0.66	0.98	0.652	1.09	-	0.604	0.43	0.18
Standard Deviation (mg-DOX/g-tumor)	(US)	1.018	0.056	0.258	0.672	0.574	0.315	0.188	0.164	0.282
Standard Deviation (mg-DOX/g-tumor)	(no-US)	0.287	0.13	0.402	0.657	0.384	-	0.343	0.302	0.092
Sample size - n	(US)	14	6	15	16	18	3	9	5	4
Sample size - n	(no-US)	11	8	8	10	16	0	5	6	4
P-value (one-tail)		0.055	0.326	0.317	0.105	0.395	N/A	0.340	0.246	0.399
95% conf. interval	(US)	0.99 - 1.95	0.64 - 0.73	0.80 - 1.03	0.70 - 1.29	0.90 - 1.37	0.45 - 1.30	0.42 - 0.65	0.17 - 0.47	0.00 - 0.52
95% conf. interval	(no-US)	0.78 - 1.09	0.57 - 0.74	0.72 - 1.25	0.28 - 1.03	0.92 - 1.26	-	0.30 - 0.91	0.19 - 0.67	0.08 - 0.27

Referring to the experiments monitoring tumor growth with 20 or 500 kHz insonation (Section 4.3), 16 of those rats were euthanized either 0.5, 3, 6, or 12 hours after receiving their last ultrasound treatment on the sixth week, four rats at each time point– two of which received treatment from the 20 kHz transducer and two from the 500 kHz transducer. Each drug concentration measurement was performed twice for each of the two tumors (insonated and control tumors). Paired-sample comparison of insonated and control tumor on the same rat was evaluated using a student t-test and showed no statistical difference between the drug concentrations in the ultrasonicated tumors and non-ultrasonicated tumors ($P = 0.988$), regardless of frequency used. Comparing the tumors in the group that received 20 kHz and doing similarly in the group that received 500 kHz ultrasound showed no difference in drug concentration between the ultrasonicated and non-ultrasonicated tumors in either group ($P = 0.957$ and $P = 0.934$, respectively).

5.2.2   Doxorubicin Accumulation Study

In the accumulation study, the DOX concentrations in the heart, liver, leg muscle, and tumor (which was exposed to 20 kHz insonation) were compared between rats that had received four consecutive weeks of drug injection and ultrasound treatment and rats that received only a single treatment. The accumulation study results are displayed in Figure 5-10, which displayed all the measurements, and Figure 5-11, which compares the averages. Statistical analysis using a student's t-test showed an increase in the amount of DOX in the heart tissue at the end of four weeks ($P = 0.044$), but no significant difference in concentrations between the single and multiple treatment groups in the liver, leg muscle, and tumor tissues ($P = 0.262$, $P = 0.397$, and $P = 0.327$, respectively).
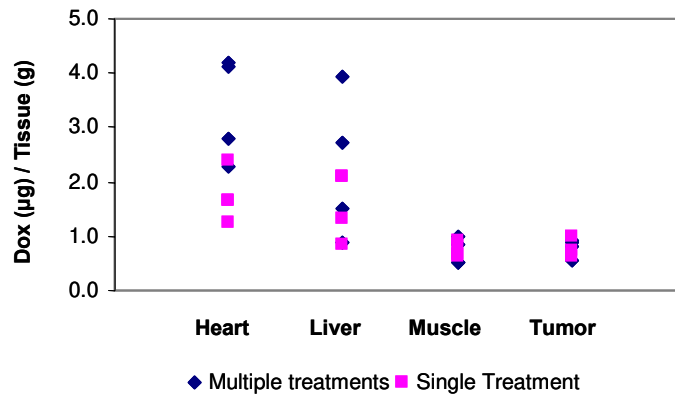
Figure 5-10 Data collected from the accumulation study which compared the drug concentration in different rat tissues (heart, liver, leg muscle, and tumor). Two rats were euthanized after four consecutive weeks of treatment (◆) and two rats were euthanized after only one treatment (■). All four were euthanized six hours after ultrasound treatment (20 kHz for fifteen minutes). The measurements were duplicated.
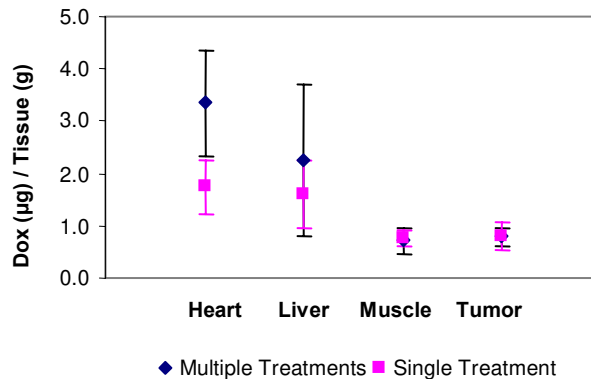
Figure 5-11 Averages of the data contained in Figure 5-10. Compares the concentration of doxorubicin in different rat tissues (heart, liver, leg muscle, and tumor). The groups compared were rats euthanized after four consecutive weeks of treatment (◆) and rats euthanized after only one treatment (■). All rats were euthanized six hours after ultrasound treatment (20 kHz for fifteen minutes). The bars represent 95% confidence intervals.

5.3 Fluorescent Microscopy Study

Thin slices of tumors were examined under a fluorescent microscope to look for

the distribution of DOX within the tumors. Figure 5-12 shows views of a slice of a tumor

from a rat which received no injection of DOX, but still received ultrasound treatment at 20 kHz frequency for fifteen minutes. The photograph on the left is the tumor slice as viewed with normal light and the photograph on the right is that same slice viewed under blue lighting (λ = 470nm). Doxorubicin absorbs light at this wavelength and then fluoresces red (as shown in the small insert at the bottom-right corner). There was no DOX observed in this tumor sample, as would be expected.
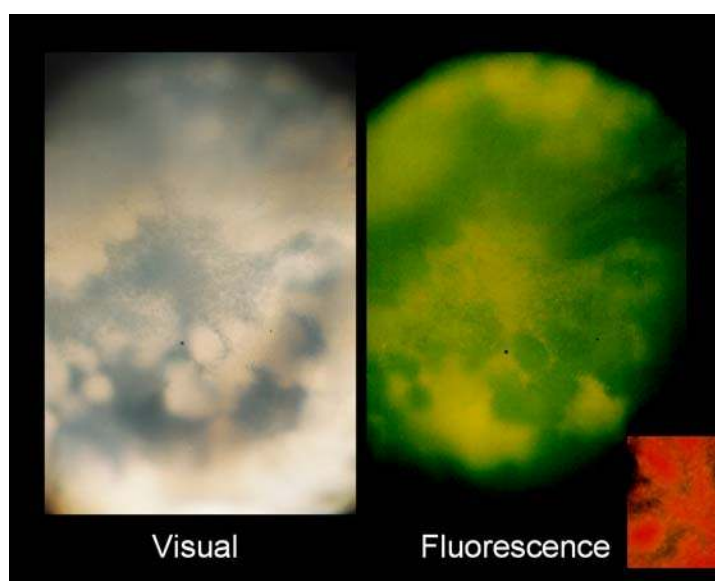
Figure 5-12 Microscopic views (5x) of a 300 µm slice of tumor from a rat which received no DOX, but did receive 20 kHz ultrasound. The left picture is the slice viewed with normal visual lighting. The right picture shows the same view under blue fluorescent lighting (λ=470nm). The inset on the bottom right corner shows how DOX looks under the same fluorescent lighting.

The photographs in Figure 5-13 show a tumor slice from a rat injected with DOX-encapsulated micelles and exposed to 20 kHz ultrasound for fifteen minutes. This tumor had received six consecutive weeks of ultrasound treatment. The graph on the right shows the growth of the tumor over the six weeks of treatment. The rat carrying this tumor was euthanized one hour after ultrasound application after the sixth treatment. In the photo on

the right, a small concentrated area of red fluorescence is seen, indicating that DOX is

present, and implying the localized delivery of Doxorubicin in the insonated tumor tissue.
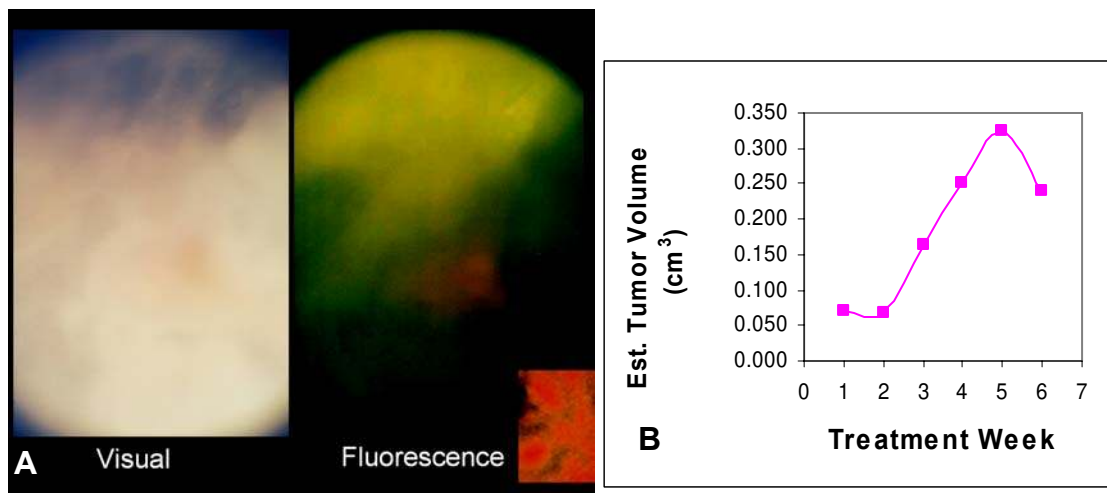
Figure 5-13   (A) Microscopic views (5x) of a 300 µm slice of tumor from a rat treated with DOX-encapsulated micelles and 20 kHz ultrasound. The left picture is the slice viewed with normal visual lighting. The right picture shows the same view under blue fluorescent lighting (λ=470nm). The inset on the bottom right corner shows how a known DOX sample looks under the same fluorescent lighting. (B) A graph showing the growth of the tumor over the six weeks of treatment.

Figure 5-14 shows nine different slices (300 microns thick), starting from the

surface directly facing the ultrasound transducer, from a tumor treated with DOX-

encapsulated micelles and 500 kHz ultrasound (fifteen minutes). (These photographs are

magnified 1.25 times normal.) There was a large amount of drug present towards the

largely necrotic middle of the tumor (see photograph 9 in Figure 5-14). The observable

amount of drug dramatically decreased as one looks further toward the tumor surface

(toward the transducer). Figure 5-15 shows the growth of the tumor over these six weeks.
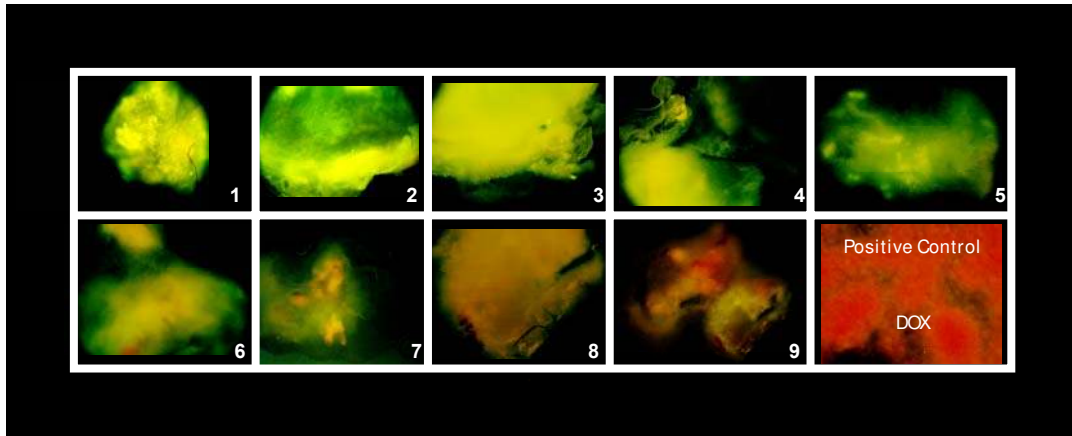
Figure 5-14 Microscopic views (1.25x) of a tumor sliced into nine different 300 µm slices from a rat treated with DOX-encapsulated micelles and 500 kHz ultrasound. The photographs are ordered from the top of the tumor (which faced the ultrasound probe) down towards the center of the tumor. Each photo was taken under blue fluorescent lighting (λ=470nm). The photo in the bottom right corner shows how a known DOX sample looks under the same fluorescent lighting.
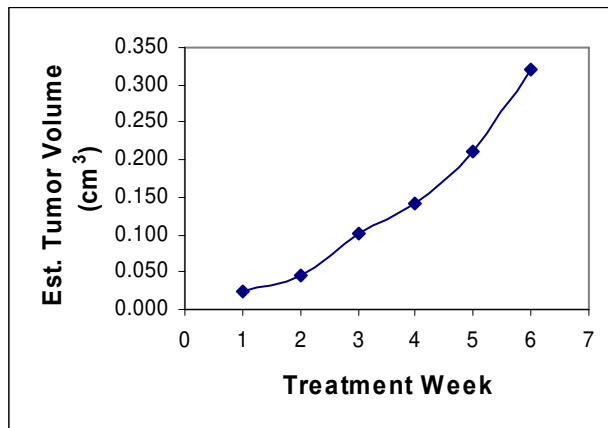
Figure 5-15 Volume of the tumor in Figure 5-14 over the six weeks of ultrasound treatment with 500 kHz ultrasound.

6 Discussion

A new cancer treatment method was tested *in vivo* using the rat model. This treatment involves the localized delivery of a chemotherapeutic drug (Doxorubicin) using stabilized Pluronic micelles (Plurogel^{TM}) as the drug carrier and low frequency ultrasound as the mechanism to release the drug directly into cancerous tissue. As part of this research, the pharmacokinetics of Doxorubicin and the effects of different ultrasound frequencies on tumor growth and drug delivery were successfully studied.

There was a great deal of scatter in tumor volumes and drug concentrations measured during the course of this experiment, but the small number of variables and the large number of samples allowed for greater statistical confidence in the obtained results. These results show that localized drug delivery using micelle carriers and ultrasound presents promise as a method to fight cancerous tumors. The study comparing the growth rate between tumors which had received insonation versus tumors that had not been exposed to ultrasound, after injection of DOX-encapsulated Plurogel, showed that insonated tumors statistically grew slower than non-insonated tumors. This is consistent with other similar studies in mice [35-37].

There could be many possible reasons for this result. Although blood with the same concentration of drug perfused both bilateral tumors, the ultrasound may have released more drug from the micelles, depositing more DOX in the ultrasonicated tumor

tissue. Although such a hypothesis is consistent with many *in vitro* studies [17, 18, 20-22], it had never been demonstrated *in vivo*. The pharmacokinetic study, which demonstrated a slightly, though not statistically, increased concentration of drug in insonated tumors ($P = 0.055$ within the first thirty minutes after treatment), supports this hypothesis. Since DOX must enter the cell's nucleus to be effective as a DNA replication inhibitor, one of the biggest obstacles for the hydrophobic drug is passing through the hydrophobic cell membrane. Therefore, another proposed explanation for decreased tumor growth could be that the ultrasound increased the permeability of the capillaries and cell membranes, allowing the drug – and possibly the whole micelle – to leave the circulatory system and enter individual cells at higher and more therapeutic concentrations. Schlicher et al. demonstrated that ultrasound facilitates uptake and retention of molecules present during sonication and introduced shortly after sonication ends. Also, they show that cells exposed to ultrasound show membrane wounds or pores that are eventually repaired [38]. The capillaries in many tumors are already very permeable due to the enhanced permeation and retention (EPR) effect, in which tumor capillaries have hyperpermeable (extra leaky) capillary walls to allow a large volume of plasma to wash the tumor cells with nutrients they desperately need to quickly grow and replicate. Since the capillaries are already porous, an increase in the drug concentration inside insonated tumors is more likely because of cell membrane permeabilization. However, the drug extraction method used in this study cannot distinguish between drug in the intercellular and extracellular fluids. Also, it cannot distinguish between released drug and drug still inside the micelles.

It is also possible that, along with lethal effect of DOX, the ultrasound itself lysed the cells or killed them indirectly via necrosis or stress-induced apoptosis. Low-frequency ultrasound at high enough intensities has alone been demonstrated to trigger cell-mediated death [39], but the intensities reported for cell death are much higher than those used in the experiments herein.

Surprisingly, this study found that the ultrasonic frequency has no measurable effect on either tumor growth rate or on DOX concentration in tumor tissues. From this observation one could imply that an increase in drug concentration is necessary for tumor growth rate reduction. The implication is that future studies can use the most convenient setup to apply ultrasound to the tumors as long as the *MI* and amplitude are appropriate. The experiments herein were carefully crafted to vary ultrasound frequency while keeping the mechanical index and time-average density constant. The effect of mechanical index and power density on tumor growth are still unknown. Thus, in order to obtain similar results, any chosen frequency must be accompanied with the pressure amplitude to produce a mechanical index of 1.22 as well as a pulse length and pulse repetition frequency needed to create a time average density of 1.0 W/cm^2. A larger mechanical index or power density could produce a stronger therapeutic effect, but that remains to be tested.

Though this study showed that frequency has no effect on the treatment, other factors such as exposure time, mechanical index, number of treatments per week, and drug concentration in the micelles could be changed to improve the effectiveness. Mechanical index (*MI*) is thought to be especially important in permeating cell membranes and releasing drugs from the micelles. Once again, the mechanical index is a

measure of the likelihood and intensity of collapse cavitation. In general, the mechanical index increases at higher intensities and lower frequencies [6]. These studies used a mechanical index of 1.22, which is above the threshold for tissue damage (0.7). All ultrasound treatments were performed at this *MI* level. The results showing no difference between the tumor growth rates of the ultrasonicated tumors supports the idea that the mechanical index is the factor determining how much drug is delivered to the cells. Using the same logic, time-average intensity could also be a determining factor in tumor growth rate since that parameter was also held constant in these experiments (1.0 W/cm^2). Future studies should look at the effect of different mechanical indexes and time-averaged power intensities on tumor growth rates as well as drug concentrations in the tumors.

In a similar study, Nelson et al. used a similar *in vivo* rat model to investigate the effects of ultrasonically controlled release of Plurogel-encapsulated Doxorubicin [23]. During the course of his four-week treatments, the tumor volumes were also measured. The tumors were exposed to 20 or 70 kHz ultrasound for one hour. The comparison of the final tumor volumes showed that the ultrasonicated tumors had grown less at the four week endpoint than tumors that were not exposed to ultrasound. His previous results support the results reported herein. The current project, however, is more thorough because it compared all measured tumor sizes throughout the six weeks of treatment and determined exponential growth rate constants for both insonated and non-insonated tumors. Another difference is that these studies used ultrasound treatments lasting 15 minutes whereas Nelson's treatments lasted one hour.

The pharmacokinetic results of DOX in the studied tissues are worth discussion. Because Doxorubicin is known to be cardiotoxic, it is important that there is a small

amount of this drug in the heart. These studies showed that while there was initially a high concentration of drug in the heart (compared to other tissues), the concentration quickly decreased within the first twelve hours to low levels. Since there were no control studies performed using non-encapsulated (or free) DOX, no conclusion can be stated as to the effect of the Plurogel, if any, in protecting the heart by decreasing the amount of drug in the heart.

The initial higher concentration of DOX in the liver was not unexpected considering that Doxorubicin is primarily cleared through the biliary route. After two days, the amount of DOX in the liver was negligible; indicating that, after two days, the drug had left the circulatory system and had settled in its final locations such as the tumors, which unfortunately still included the heart.

It was encouraging to see that in the long term (> 2 days), there was a higher concentration of DOX in the tumors than in the liver, muscle, and especially heart. Though there was no difference in drug concentration between insonated and non-insonated tumors after one week, a detectable amount of active drug persisted in the tumors. It remains unknown if this drug had been present in the tumor for the whole week or even if it had been released from the micelle during ultrasound application. It is possible that sustained concentration of the drug in the tumors occurred because the micelles protected the drug from being metabolized or excreted by the liver or kidneys. It is also possible that the drug remained in the stabilized micelle after the micelle had left the circulatory system through the leaky tumor capillaries. However, it is likely that after one week the stabilized micelle would have disassociated, thus releasing its drug load. The studies by Pruitt showed that after 12 hours, the Plurogel micelles (crosslinked

Pluronic micelles) lost their stability [14]; and since Pluronic micelles dissolve in dilute concentrations, it would be expected that the Plurogel micelles would also dissolve and would release their cargo.

Kabanov et al. reported that in one experiment, a substantial 1.7-fold increase in drug accumulation in solid tumor was observed with the DOX/SP1049C micelle formulation when compared to free drug [12]. The current study did not test the pharmacokinetics of free drug. However, something can be learned by comparing this result with the increase in drug concentration caused by the ultrasound application. There was only a 1.2-fold increase in drug concentration in solid tumor with ultrasound when compared to a non-insonated tumor (averaged over the first eight hours after treatment). This increase is smaller than the 1.7-fold increase reported by Kabanov in using only the drug-encapsulated Pluronic micelle. Thus, the use of the drug/micelle formulation may contribute a greater effect on drug delivery than ultrasound.

While the statistical results showed that ultrasound improves the effectiveness of DOX delivery using micelles, the combined treatment failed to completely treat and cause regression of the cancerous tumors. Only two of the 24 tumors that received ultrasound completely regressed, and at least one of them is thought to have regressed mainly because of the rat's immune system because the contralateral tumor in this rat did not grow as fast as the control tumors in other rats. The other 22 insonated tumors continued growing in size, albeit at a slower rate than their contralateral control, on average. It is often heard from health care providers that early detection is key to a successful treatment of cancer. The studied tumors had been allowed to grow for at least three weeks prior to any treatment. It is likely that the treatment would have been more

successful in removing the tumor if it had been initiated earlier. The increased effectiveness when using ultrasound could widen the critical window for detection leading to a positive outcome, allowing a few extra days before the tumor grows beyond "the point of no return".

7 Conclusions / Recommendations

7.1 Conclusions

The combination of DOX-encapsulated Plurogel followed by the exposure to low-frequency ultrasound (at an intensity large enough to promote inertial cavitation) was effective in decreasing the tumor growth rate compared with non-ultrasonicated tumors. The tumor volumes were satisfactorily fitted to an exponential growth model where the growth rate constant for insonated tumors was $0.0402 \ \text{day}^{-1}$, while the rate constant for non-insonated tumors was $0.0465 \ \text{day}^{-1}$. The application of ultrasound to the tumors also weakly increased the average drug concentration in the tumor for the first thirty minutes after treatment. This supports the hypothesis that ultrasound increases drug delivery to targeted tumors. However, the exact mechanism is still unknown. The ultrasound could have 1) released more drug from the micelle carriers; 2) increased the permeability of the capillaries, allowing more plasma and its contents to enter into adjacent tissue; and/or 3) increased the permeability of the cancer cells, allowing the drug to enter in higher concentrations into the intercellular fluid. Any single one, or combination, of these mechanisms could cause an increased amount of DOX in the tumor tissue. The effect of ultrasound on average drug concentration is, however, short lived. After twelve hours, there is no difference in DOX concentration between insonated and non-insonated tumors. Furthermore, different ultrasound frequencies (at the same mechanical index and

73

time-averaged power density) showed no effect on tumor growth rate and also produced no measurable effect on DOX concentration in the tumors.

Pharmacokinetic studies showed significant drug accumulation in the heart but no accumulation in the liver, skeletal leg muscle, or tumors over the course of four weeks of consecutive weekly injections of DOX-encapsulated Plurogel. Concentration-versus-time studies showed that initially, DOX concentrations are highest in the heart and then the liver, but they quickly decrease to at least one-fifth the initial concentration within the first 24 hours. After 24 hours, DOX concentration remains the greatest in the tumors, regardless of whether they received ultrasound or not.

7.2 Recommendations

The studies performed in this research project only focused on a few aspects of ultrasonic drug delivery. This is a large topic and much of it is not fully understood. This section describes areas where this project could have been improved and gives suggestions for further studies.

It is recommended that future studies repeat the tumor growth studies described herein using different time-averaged power densities and different mechanical indices. These studies would help determine the effects, if any, of these two important parameters on tumor growth rate and drug delivery to the tumors. The mechanical index used in this thesis's studies was 1.22, already above the threshold for tissue damage (0.7). The use of a higher mechanical index, at least at a level high enough to create a statistical difference in tumor growth rate (if any difference), might cause major tissue damage. While tumor damage may seem to be a favorable outcome, this damage would cause unnatural

necrosis instead of the healthier cell-mediated apoptosis. Therefore, a study using a different *MI* would have to use a lower level than 1.22. While using a lower *MI* may demonstrate the effect of *MI* on tumor growth and drug delivery, the change may not improve the effectiveness of the treatment. Changes in the time-average power density could be performed by increasing the pulse length (to 2000 or 4000 cycles from 1000 cycles) or the pulse repetition frequency (to 40 or 80 Hz from 20 Hz). An increase in power density will increase the temperature of the tumor during treatment. A preliminary run will have to be performed to ensure this temperature increase does not cause thermal damage to the tissue.

The tumor growth experiments performed for this thesis followed the method created by Nelson and incorporated a few of his recommendations [23]. For example, these experiments were carried out for six weeks instead of four. Also, atipamezole was administered to the rats as a reversing agent for the anesthetic. This shortened the recovery time from six to seven hours to less than one hour. Another recommendation that was implemented was beginning the treatments earlier at three weeks following tumor inoculation. The reason for this recommendation was to reduce the effects of metastasis. By starting the treatment earlier, this gave more time to treat the rat before the cancer's effects were critically apparent – particularly metastasis to the lungs. As mentioned before, the rats' health began to deteriorate after the fifth week of treatments. For that reason, it is suspected that the tumors still metastasized (addition tumor growths were also found in various locations, including the lungs). It is recommended, therefore, that future studies do not last longer than nine weeks after tumor inoculation.

As previously mentioned, early tumor detection is important for an individual to have a high probability for successful treatment. Each cancer has a "point of no return" where detection after this time is too late and treatment has a limited chance for success. The treatment studied herein may be even more effective if started earlier than three weeks after tumor inoculation. The latest possible detection time, or "point of no return", could be determined for which the success of this treatment could be insured. Another interesting study could measure the extra amount of time gained for tumor detection if ultrasound were used with DOX-loaded micelles, compared with traditional free drug injection. Put another way, how many days can this treatment add before the "point of no return"?

An important control study must be performed which measures the tumor growth rate and pharmacokinetics of DOX when used independently, that is to say free DOX without micelle encapsulation. Treatments with and without ultrasound should be performed. From these control studies, conclusions could be made as to the effects of the Plurogel micelle carriers in drug delivery to the tumor and other tissues. Experimental data still have not ruled out the possibility that, *in vivo*, ultrasound alone is responsible for the increased drug concentration in ultrasonicated tumors. Also, pharmacokinetic studies could compare the drug concentration in the heart when using free drug versus encapsulated drug. Though Nelson's experiments showed that the micelles protected the heart from the toxic effects of the drug by using stress tests [23], finding a decreased amount of drug in the heart by using micelles would be more convincing evidence of the micelle's protective nature.

In measuring the amount of drug in a given tissue sample, the extraction methods used did not discriminate between intercellular or extracellular compartments. Also, there was no way to determine how much of the DOX, if any, was still encapsulated inside the micelles. Therefore, the concentrations measured and reported represent all the drug present in the tissue, whether it was therapeutically available or not. Most likely only a fraction of the measured drug was able to disrupt cell replication. It is therefore desirable to determine the amount of drug present inside the cell's nucleus or intercellular matrix, or at the very least, to determine the amount released from the micelles. It is thus recommended that a method be found (or developed) that can distinguish between the amount of drug inside and outside the micelles and inside and outside the cells. This method would not only be useful in these studies, but could be employed in numerous other biological studies.

In the production of Plurogel, a small amount of fluorescent monomer could be incorporated so that the amount of carrier can be measured in a given tissue sample. This could be used to determine if the amount of DOX delivered to an area is correctly proportional to the amount of Plurogel in that same area. These kinds of studies could help determine where the micelles accumulate (i.e. tumor, adipose tissue, liver, kidney) and also determine if the drug arrived at a tissue by means of the micelle carrier or separate from the carrier.

For future experiments using a similar treatment method as described in this thesis, there are a few recommendations to note. Because of the natural variability between each rat and their inoculated tumors, tumor growth studies should use no less than twelve rats in each study group. A smaller sample size would not allow statistics to

77

separate enough "signal" from the noise of the data. Next, with experiments using the 20 kHz ultrasound probe, ultrasound gel was placed between the probe and the tumor. Gas bubbles within the gel vibrated in the ultrasound field and pounded against the skin next to the tumor. Over time, these vibrations broke this sensitive skin, causing the tumor to bleed. It is therefore recommended that the gel be degassed or that special care is taken to not use the applied gel if air bubbles exist. Finally, the use of depilatory cream (Nair[®]) to remove the hair from this skin above the tumor causes skin irritation and sometimes causes the tumor to bleed. After a couple times, a scab forms over the tumor which may reduce the effectiveness of ultrasound treatment. A couple of changes may help with this problem. An ointment can be applied to the skin after treatment or a vinegar wash can be used to neutralize the effects of the depilatory cream. Another possible solution is to start removing the hair weeks before treatments begin. It was noticed that after three or four weeks of hair removal, the hair discontinued growing. If the skin could be treated such that the hair stopped growing before the cancer treatments started, then the skin would not have to endure the stress of both the ultrasound and the depilatory cream.

8 References

[1]   N.I.H. National Cancer Institute, Cancer Statistics Home Page - National Cancer Institute. Vol. 2007, 2006.

[2]   T. Tanaka, S. Shiramoto, M. Miyashita, Y. Fujishima, Y. Kaneo, Tumor targeting based on the effect of enhanced permeability and retention (EPR) and the mechanism of receptor-mediated endocytosis (RME). International Journal of Pharmaceutics 277(1-2) (2004) 39-61.

[3]   S.B. Barnett, G.R. Terhaar, M.C. Ziskin, W.L. Nyborg, K. Maeda, J. Bang, Current Status of Research on Biophysical Effects of Ultrasound. Ultrasound in Medicine and Biology 20(3) (1994) 205-218.

[4]   J.A. Rooney, Hemolysis Near an Ultrasonically Pulsating Gas Bubble. Science (1970) 869-871.

[5]   D.J. May, J.S. Allen, K.W. Ferrara, Dynamics and fragmentation of thick-shelled microbubbles. Ieee Transactions on Ultrasonics Ferroelectrics and Frequency Control 49(10) (2002) 1400-1410.

[6]   R.J. Urick, Principles of Underwater Sound, McGraw-Hill Book Company, San Fransisco, 1983.

[7]   W.G. Pitt, G. Husseini, B.J. Staples, Ultrasonic Drug Delivery - a General Review. Expert Opinion on Drug Delivery 1(1) (2004) 37-56.

[8]   H. Bader, H. Ringsdorf, B. Schmidt, Watersoluble Polymers in Medicine. Angewandte Makromolekulare Chemie 123(Aug) (1984) 457-485.

[9]   M. Yokoyama, M. Miyauchi, N. Yamada, T. Okano, Y. Sakurai, K. Kataoka, S. Inoue, Characterization and Anticancer Activity of the Micelle-Forming Polymeric Anticancer Drug Adriamycin-Conjugated Poly(Ethylene Glycol)-Poly(Aspartic Acid) Block Copolymer. Cancer Research 50(6) (1990) 1693-1700.

[10]   A.V. Kabanov, V.P. Chekhonin, V.Y. Alakhov, E.V. Batrakova, A.S. Lebedev, N.S. Meliknubarov, S.A. Arzhakov, A.V. Levashov, G.V. Morozov, E.S. Severin, V.A. Kabanov, The Neuroleptic Activity of Haloperidol Increases after Its Solubilization in

Surfactant Micelles - Micelles as Microcontainers for Drug Targeting. Febs Letters 258(2) (1989) 343-345.

[11]   P. Alexandridis, T. Nivaggioli, T.A. Hatton, Temperature Effects on Structural-Properties of Pluronic P104 and F108 Peo-Ppo-Peo Block-Copolymer Solutions (Vol 11, Pg 1468, 1995). Langmuir 11(7) (1995) 2847-2847.

[12]   A.V. Kabanov, V.Y. Alakhov, Pluronic (R) block copolymers in drug delivery: From micellar nanocontainers to biological response modifiers. Critical Reviews in Therapeutic Drug Carrier Systems 19(1) (2002) 1-72.

[13]   J.D. Pruitt, G. Husseini, N. Rapoport, M.G. Pitt, Stabilization of pluronic P-105 micelles with an interpenetrating network of N,N-diethylacrylamide. Macromolecules 33(25) (2000) 9306-9309.

[14]   J. Pruitt, Stabilization of Pluronic P-105 Micelles for Targeted Nanoparticle Drug Delivery. Chemical Engineering, Vol. Doctor of Philosophy, Brigham Young University, Provo, Utah, 2001, p. 118.

[15]   M. Cegnar, J. Kristl, J. Kos, Nanoscale polymer carriers to deliver chemotherapeutic agents to tumours. Expert Opinion on Biological Therapy 5(12) (2005) 1557-1569.

[16]   R. Nagarajan, Solubilization of hydrocarbons and resulting aggregate shape transitions in aqueous solutions of Pluronic (PEO-PPO-PEO) block copolymers. Coll Surfaces B Biointerfaces 16(55) (1999).

[17]   G.A. Husseini, N.Y. Rapoport, D.A. Christensen, J.D. Pruitt, W.G. Pitt, Kinetics of ultrasonic release of doxorubicin from pluronic P105 micelles. Colloids and Surfaces B-Biointerfaces 24(3-4) (2002) 253-264.

[18]   A. Marin, M. Muniruzzaman, N. Rapoport, Acoustic activation of drug delivery from polymeric micelles: effect of pulsed ultrasound. J Control Release 71(3) (2001) 239-249.

[19]   G.A. Husseini, G.D. Myrup, W.G. Pitt, D.A. Christensen, N.A.Y. Rapoport, Factors affecting acoustically triggered release of drugs from polymeric micelles. J Control Release 69(1) (2000) 43-52.

[20]   G.A. Husseini, C.M. Runyan, W.G. Pitt, Investigating the mechanism of acoustically activated uptake of drugs from Pluronic micelles. Bmc Cancer 2 (2002) -.

[21]   J.D. Pruitt, W.G. Pitt, Sequestration and ultrasound-induced release of doxorubicin from stabilized pluronic P105 micelles. Drug Deliv 9(4) (2002) 253-258.

[22]   N. Munshi, N. Rapoport, W.G. Pitt, Ultrasonic activated drug delivery from pluronic P-105 micelles. Cancer Lett 118(1) (1997) 13-19.

[23]   J.L. Nelson, Ultrasonically enhanced drug delivery of Doxorubicin in vivo from stabilized pluronic micelle carriers. Brigham Young University. Dept. of Chemical Engineering, 2002., 2002, pp. ix, 80 p.

[24]   R. Danesi, S. Fogli, A. Gennari, P. Conte, M. Del Tacca, Pharmacokinetic-pharmacodynamic relationships of the anthracycline anticancer drugs. Clinical Pharmacokinetics 41(6) (2002) 431-444.

[25]   Adriamycin (DOXOrubicin HCL) for Injection, USP. Ben Venue Laboratories, 2002.

[26]   A. Rousseau, P. Marquet, Application of pharmacokinetic modelling to the routine therapeutic drug monitoring of anticancer drugs. Fundamental & Clinical Pharmacology 16(4) (2002) 253-262.

[27]   W. Linkesch, M. Weger, I. Eder, H.W. Auner, C. Pernegg, C. Kraule, M.J. Czejka, Long-term pharmacokinetics of doxorubicin HCl stealth liposomes in patients after polychemotherapy with vinorelbine, cyclophosphamide and prednisone (CCVP). European Journal of Drug Metabolism and Pharmacokinetics 26(3) (2001) 179-184.

[28]   N.G. Tavoloni, Anthony M, Biliary and Urinary Excretion of Adriamycin in Anesthetized Rates. Pharmacology 20 (1980) 256-267.

[29]   J.H. Zheng, C.T. Chen, J.L.S. Au, M.G. Wientjes, Time- and concentration-dependent penetration of doxorubicin in prostate tumors. Aaps Pharmsci 3(2) (2001) -.

[30]   V. Alakhov, E. Klinski, S.M. Li, G. Pietrzynski, A. Venne, E. Batrakova, T. Bronitch, A. Kabanov, Block copolymer-based formulation of doxorubicin. From cell screen to clinical trials. Colloids and Surfaces B-Biointerfaces 16(1-4) (1999) 113-134.

[31]   R.C. Jewell, S.P. Khor, D.F. Kisor, K.A.K. LaCroix, W.A. Wargin, Pharmacokinetics of RheothRx injection in healthy male volunteers. J Pharm Sci 86(7) (1997) 808-812.

[32]   F. Martin, Caignard, A., Jeannin, J.F., Leclerc, A. and Martin, M., Selection by Trypson of Two Sublines of Rat Colon Cancer Celles Forming Progressive or Regressive Tumors. International Journal of Cancer 32 (1983) 623-627.

[33]   P. Jacquet, O.A. Stuart, R. Dalton, D. Chang, P.H. Sugarbaker, Effect of intraperitoneal chemotherapy and fibrinolytic therapy on tumor implantation in wound sites. Journal of Surgical Oncology 62(2) (1996) 128-134.

[34]   L. Alvarez-Cedron, M.L. Sayalero, J.M. Lanao, High-performance liquid chromatographic validated assay of doxorubicin in rat plasma and tissues. Journal of Chromatography B 721(2) (1999) 271-278.

[35]   J.L. Nelson, B.L. Roeder, J.C. Carmen, F. Roloff, W.G. Pitt, Ultrasonically activated chemotherapeutic drug delivery in a rat model. Cancer Research 62(24) (2002) 7280-7283.

[36]   G. Myhr, J. Moan, Synergistic and tumour selective effects of chemotherapy and ultrasound treatment. Cancer Lett 232(2) (2006) 206-213.

[37]   N. Rapoport, W.G. Pitt, H. Sun, J.L. Nelson, Drug delivery in polymeric micelles: from in vitro to in vivo. J Control Release 91(1-2) (2003) 85-95.

[38]   R.K. Schlicher, H. Radhakrishna, T.P. Tolentino, R.P. Apkarian, V. Zarnitsyn, M.R. Prausnitz, Mechanism of intracellular delivery by acoustic cavitation. Ultrasound in Medicine and Biology 32(6) (2006) 915-924.

[39]   W.L. Nyborg, Biological effects of ultrasound: Development of safety guidelines. Part II: General review. Ultrasound in Medicine and Biology 27(3) (2001) 301-333.

Appendix A

This appendix contains data and important procedures used in the experiments performed for this thesis.

1. **Procedure to Create the Doxorubicin Calibration Solutions**

   These two pages describe how different concentrations of Doxorubicin were created to create the Doxorubicin/fluorescence calibration curve.

2. **High Performance Liquid Chromatography Solutions**

   A summary of the different solutions used to extract DOX from the tissue and analyze it in the HPLC system. For the given volume of solution, the amount of reagents to add is given.

3. **Tumor Volumes from the rats in the Ultrasound Frequency / Tumor Growth Experiment**

   All of the tumor volumes measured from each rat through the experiment. The ultrasound frequency used for treatment and the rats' masses at that given day are also displayed.

4. **Statistical Results from the Ultrasound Frequency / Tumor Growth Experiment**

   The results from the SAS software analysis of the data from the ultrasound frequency / tumor growth experiment.

5. **HPLC Results for the Pharmacokinetic Studies**

   All of the HPLC runs performed in the pharmacokinetic studies. The chart shows the

   names of each rat, the tissue analyzed, the time after drug injection that the rat was

   euthanized, the area under the DOX fluorescent peak, the mass of tissue extracted

   from the rat, the volume of 1/15 M Phosphate solution used to homogenize the

   tissues, the measured amount of Doxorubicin detected in the sample injected into the

   HPLC system, and the calculated concentration of Doxorubicin in the extracted

   tissue.

6. **Results of a Study on the Effects of Temperature and pH on DOX Fluorescence**

   This experiment showed that the amount of DOX detected in the HPLC system is

   strongly dependent on the temperature and pH of the sample and system.

7. **Tumor Growth Results from the Tumor Growth / Frequency Study**

   Charts for each rat in the study which show the volume of the sonicated and non-

   sonicated tumors over the six weeks of treatments.

CALIBRATION SOLUTIONS FOR DOX ANALYSIS

Density of Dox solution is assumed to be that of water. (The drug was dissolved in an acidic (pH 4) aqueous solution.) :

$$\rho_w := 1000 \frac{kg}{m^3}$$

In the vial of solid Dox, the mass fraction of DOX in that solid is: $\quad x_{Dox} := \frac{10mg}{60mg}$

The volume of an injection into the HPLC apparatus is: $\quad V_{inj} := 50\mu L$

To perform the calibration, we will make vials with different concentrations of DOX:

5000ng/mL   1000ng/mL   500ng/mL   100ng/mL   50ng/mL   10ng/mL

For 5000ng/mL solution:

We created a volume of:	$Vol_1 := 50mL$
Amount of solid Dox that was added:	$m_{Dox1} := 1.5mg$
Amount of water that was added:	$m_{w1} := 50gm$
Mass fraction of Dox in solution:	$x_{Dox1} := \frac{x_{Dox} \cdot m_{Dox1}}{m_{Dox1} + m_{w1}}$
Amount of Dox in Solution:	$m_{Dox.sol} := Vol_1 \cdot \rho_w \cdot x_{Dox1}$
Amount of Dox per injection:	$m_{Dox.inj} := \frac{V_{inj}}{Vol_1} \cdot m_{Dox.sol}$ $\quad \boxed{m_{Dox.inj} = 250ng}$

For 1000ng/mL solution:

We created a volume of:	$Vol_2 := 10mL$
Amount of 5000ng/mL soln. that was added:	$m_{Doxvial} := 2.03gm$
Amount of fresh solution that was added:	$m_{sol} := 7.9965gm$
Mass fraction of Dox in solution:	$x_{Dox2} := \frac{x_{Dox1} \cdot m_{Doxvial}}{m_{Doxvial} + m_{sol}}$
Amount of Dox in Solution:	$m_{Dox.sol} := Vol_2 \cdot \rho_w \cdot x_{Dox2}$
Amount of Dox per injection:	$m_{Dox.inj} := \frac{V_{inj}}{Vol_2} \cdot m_{Dox.sol}$ $\quad \boxed{m_{Dox.inj} = 50.6ng}$

For 500ng/mL solution:

We created a volume of:	$Vol_3 := 10mL$
Amount of 1000ng/mL soln. that was added:	$m_{Doxvial2} := 4.9285gm$
Amount of fresh solution that was added:	$m_{sol3} := 5.0615gm$
Mass fraction of Dox in solution:	$x_{Dox3} := \frac{x_{Dox2} \cdot m_{Doxvial2}}{m_{Doxvial2} + m_{sol3}}$
Amount of Dox in Solution:	$m_{Dox.sol} := Vol_3 \cdot \rho_w \cdot x_{Dox3}$
Amount of Dox per injection:	$m_{Dox.inj} := \frac{V_{inj}}{Vol_3} \cdot m_{Dox.sol}$ $\quad \boxed{m_{Dox.inj} = 25ng}$

For 100ng/mL:

We created a volume of:

$Vol_4 := 10 mL$

Amount of 500ng/mL soln. that was added:

$m_{Doxvial3} := 2.0088 gm$

Amount of fresh solution that was added:

$m_{sol4} := 7.9984 gm$

Mass fraction of Dox in solution:

$$x_{Dox4} := \frac{x_{Dox3} \cdot m_{Doxvial3}}{m_{Doxvial3} + m_{sol4}}$$

Amount of Dox in Solution:

$m_{Dox.sol} := Vol_4 \cdot \rho_w \cdot x_{Dox4}$

Amount of Dox per injection:

$$m_{Dox.inj} := \frac{V_{inj}}{Vol_4} \cdot m_{Dox.sol}$$

$m_{Dox.inj} = 5 ng$

For 50 ng/mL:

We created a volume of:

$Vol_5 := 10 mL$

Amount of 100ng/mL soln. that was added:

$m_{Doxvial4} := 4.9813 gm$

Amount of fresh solution that was added:

$m_{sol5} := 5.0027 gm$

Mass fraction of Dox in solution:

$$x_{Dox5} := \frac{x_{Dox4} \cdot m_{Doxvial4}}{m_{Doxvial4} + m_{sol5}}$$

Amount of Dox in Solution:

$m_{Dox.sol} := Vol_5 \cdot \rho_w \cdot x_{Dox5}$

Amount of Dox per injection:

$$m_{Dox.inj} := \frac{V_{inj}}{Vol_5} \cdot m_{Dox.sol}$$

$m_{Dox.inj} = 2.5 ng$

For 10ng/mL:

We created a volume of:

$Vol_6 := 10 mL$

Amount of 100ng/mL soln. that was added:

$m_{Doxvial5} := 1.9976 gm$

Amount of fresh solution that was added:

$m_{sol6} := 8.0095 gm$

Mass fraction of Dox in solution:

$$x_{Dox6} := \frac{x_{Dox5} \cdot m_{Doxvial5}}{m_{Doxvial5} + m_{sol6}}$$

Amount of Dox in Solution:

$m_{Dox.sol} := Vol_6 \cdot \rho_w \cdot x_{Dox6}$

Amount of Dox per injection:

$$m_{Dox.inj} := \frac{V_{inj}}{Vol_6} \cdot m_{Dox.sol}$$

$m_{Dox.inj} = 0.5 ng$

HPLC SOLUTIONS

65:35 v/v Methanol/.01M Phosphate buffer, adjusted to pH 2.96 with 19M KOH

$Vol := .5L$ Input Value Wanted (add that)

$V_{meth} = 325mL$ What you should add to get it.

$V_{PO4} = 175mL$

To Make 1/15M Phosphate Buffer (pH 7.4)

$Vol_{water} := 500mL$

$mass_{H2PO4} = 1.039gm$

$mass_{HPO4} = 6.916gm$

To Make 19M KOH

$Vol_{Water} := 100mL$

$m_{KOH} = 106.601gm$

To Make .01M Phosphate Buffer

$Vol_{H2O} := .5L$

$V_{acid} = 0.576mL$

To Make 40% ZnSO$_4$

$Vol_{sol} := 100mL$

$m_{ZnSO4} = 40gm$

Tumor Volumes from the rats in the Ultrasound Frequency / Tumor Growth Experiment

Rat Name	Week	Day	Frequency (kHz)	Rat Mass (g)	Treated Volume (cm³)	Untreated Volume (cm³)
K60	0	0	500	177	0.25	0.15
K60	1	8	500	182	0.30	0.21
K60	2	14	500	193	0.58	0.59
K60	3	20	500	180	0.62	0.72
K60	3	20	500	180	0.57	0.71
K60	3	20	500	180	0.58	0.73
K60	4	28	500	181	0.76	1.04
K60	4	28	500	181	0.72	0.98
K60	4	28	500	181	0.72	0.94
K60	5	35	500	174	0.86	1.14
K60	5	35	500	174	0.82	1.10
K60	5	35	500	174	0.85	1.07
K61	0	0	20	150	0.20	0.21
K61	1	8	20	160	0.28	0.28
K61	2	14	20	168	0.51	0.40
K61	3	20	20	170	0.62	0.54
K61	3	20	20	170	0.61	0.52
K61	3	20	20	170	0.57	0.49
K61	4	28	20	168	0.93	0.59
K61	4	28	20	168	0.93	0.65
K61	4	28	20	168	0.89	0.65
K61	5	35	20	156	1.16	1.01
K61	5	35	20	156	1.07	0.87
K61	5	35	20	156	1.04	0.96
K62	0	0	500	137	0.36	0.12
K62	1	8	500	146	0.35	0.13
K62	2	14	500	156	0.66	0.38
K62	3	20	500	151	0.78	0.38
K62	3	20	500	151	0.76	0.32
K62	3	20	500	151	0.77	0.37
K62	4	28	500	145	1.41	0.72
K62	4	28	500	145	1.52	0.79
K62	4	28	500	145	1.36	0.68
K62	5	35	500	147	1.40	0.76
K62	5	35	500	147	1.51	0.73
K62	5	35	500	147	1.27	0.73
K63	0	0	20	140	0.08	0.02
K63	1	8	20	145	0.03	0.02
K63	2	14	20	150	0.13	0.02
K63	3	20	20	150	0.15	0.07
K63	3	20	20	150	0.15	0.08
K63	3	20	20	150	0.16	0.07
K63	4	28	20	151	0.25	0.11
K63	4	28	20	151	0.33	0.13
K63	4	28	20	151	0.26	0.12

Rat Name	Week	Day	Frequency (kHz)	Rat Mass (g)	Treated Volume (cm³)	Untreated Volume (cm³)
K63	5	35	20	140	0.26	0.12
K64	0	0	20	148	0.06	0.08
K64	1	8	20	153	0.12	0.13
K64	2	14	20	159	0.18	0.28
K64	3	20	20	165	0.24	0.45
K64	3	20	20	165	0.23	0.40
K64	3	20	20	165	0.22	0.45
K64	4	28	20	151	0.36	0.48
K64	4	28	20	151	0.36	0.51
K64	4	28	20	151	0.37	0.47
K64	5	35	20	149	0.40	0.62
K64	5	35	20	149	0.37	0.57
K64	5	35	20	149	0.38	0.65
K65	0	0	500	166	0.00	0.01
K65	1	6	500	156	0.00	0.00
Both tumors disappeared after 2 weeks (possibly due to a strong immune system)						
K66	1	8	500	155	0.07	0.06
K66	2	14	500	157	0.09	0.08
K66	3	20	500	150	0.09	0.09
K66	3	20	500	150	0.09	0.12
K66	3	20	500	150	0.07	0.10
K66	4	28	500	140	0.11	0.10
K66	4	28	500	140	0.11	0.13
K66	4	28	500	140	0.11	0.13
K66	5	35	500	147	0.14	0.16
K66	5	35	500	147	0.14	0.16
K66	5	35	500	147	0.13	0.16
K67	0	0	20	146	0.17	0.04
K67	1	8	20	149	0.21	0.12
K67	2	14	20	157	0.37	0.16
K67	3	20	20	157	0.65	0.33
K67	3	20	20	157	0.62	0.36
K67	3	20	20	157	0.57	0.28
K67	4	28	20	152	0.65	0.45
K67	4	28	20	152	0.71	0.47
K67	4	28	20	152	0.69	0.48
K67	5	35	20	154	1.02	0.69
K67	5	35	20	154	0.92	0.70
K67	5	35	20	154	0.88	0.73
K69	0	0	500	147	0.06	0.02
K69	1	8	500	150	0.08	0.04
K69	2	14	500	158	0.06	0.04
K69	3	20	500	147	0.03	0.05
K69	3	20	500	147	0.03	0.05
K69	3	20	500	147	0.03	0.05
K69	4	28	500	145	0.05	0.08
K69	4	28	500	145	0.05	0.08

Rat Name	Week	Day	Frequency (kHz)	Rat Mass (g)	Treated Volume (cm^3)	Untreated Volume (cm^3)
K70	0	0	500	184	0.03	0.03
K70	2	14	500	192	0.03	0.03
K70	3	21	500	186	0.01	0.07
K70	3	21	500	186	0.01	0.05
K70	3	21	500	186	0.01	0.05
K70	4	28	500	181	0.01	0.08
K70	4	28	500	181	0.01	0.09
K70	4	28	500	181	0.01	0.09
K70	5	35	500	145	0.00	0.17
K70	5	35	500	145	0.00	0.19
K70	5	35	500	145	0.00	0.17
The treated tumor completely disappeared						
K71	0	0	20	160	0.02	0.04
K71	2	14	20	168	0.02	0.16
K71	3	21	20	159	0.21	0.35
K71	3	21	20	159	0.20	0.34
K71	3	21	20	159	0.20	0.34
K71	4	28	20	163	0.56	0.41
K71	4	28	20	163	0.48	0.43
K71	4	28	20	163	0.41	0.39
K71	5	35	20	104	0.63	0.80
K71	5	35	20	104	0.59	0.82
K71	5	35	20	104	0.53	0.75
K72	0	0	20	153	0.14	0.05
K72	1	8	20	155	0.09	0.09
K72	2	14	20	158	0.12	0.11
K72	3	20	20	159	0.33	0.18
K72	3	20	20	159	0.31	0.16
K72	3	20	20	159	0.31	0.15
K72	4	28	20	155	0.37	0.23
K72	4	28	20	155	0.33	0.21
K72	4	28	20	155	0.37	0.19
Died during anesthesia						
K73	0	0	500	141	0.02	0.03
K73	2	14	500	151	0.10	0.04
K73	3	20	500	153	0.15	0.03
K73	3	20	500	153	0.15	0.03
K73	3	20	500	153	0.13	0.02
K73	4	28	500	158	0.23	0.03
K73	4	28	500	158	0.21	0.03
K73	4	28	500	158	0.20	0.02
K73	5	35	500	147	0.31	0.04
K73	5	35	500	147	0.32	0.05
K73	5	35	500	147	0.32	0.05
K74	0	0	20	100	0.08	0.06
K74	1	6	20	105	0.13	0.09
K74	2	14	20	122	0.13	0.20

Rat Name	Week	Day	Frequency (kHz)	Rat Mass (g)	Treated Volume (cm³)	Untreated Volume (cm³)
K74	3	21	20	130	0.00	0.25
K74	3	21	20	130	0.00	0.25
K74	4	28	20	134	0.00	0.39
K74	4	28	20	134	0.00	0.39
K74	4	28	20	134	0.00	0.40
K74	5	35	20	135	0.00	0.57
K74	5	35	20	135	0.00	0.56
K74	5	35	20	135	0.00	0.52
The treated tumor completely disappeared						
K75	0	0	500	110	0.05	0.13
K75	2	14	500	127	0.16	0.17
K75	3	21	500	134	0.26	0.26
K75	3	21	500	134	0.24	0.29
K75	3	21	500	134	0.23	0.26
K75	4	28	500	139	0.42	0.45
K75	4	28	500	139	0.37	0.40
K75	4	28	500	139	0.38	0.39
K75	5	35	500	110	0.44	0.51
K75	5	35	500	110	0.44	0.53
K75	5	35	500	110	0.41	0.53
K77	0	0	20	145	0.03	0.04
K77	1	6	20	150	0.06	0.09
K77	2	14	20	175	0.09	0.07
K77	3	21	20	177	0.11	0.07
K77	3	21	20	177	0.10	0.07
K77	3	21	20	177	0.11	0.07
K77	4	28	20	171	0.15	0.15
K77	4	28	20	171	0.15	0.17
K77	4	28	20	171	0.15	0.17
K77	5	35	20	138	0.20	0.14
K77	5	35	20	138	0.17	0.12
K77	5	35	20	138	0.19	0.14
K79	0	0	500	155	0.02	0.04
K79	1	6	500	156	0.04	0.07
K79	2	14	500	181	0.08	0.15
K79	3	21	500	181	0.16	0.25
K79	3	21	500	181	0.16	0.23
K79	3	21	500	181	0.16	0.23
K79	4	28	500	169	0.21	0.31
K79	4	28	500	169	0.19	0.30
K79	4	28	500	169	0.17	0.31
K79	5	35	500	130	0.18	0.33
K79	5	35	500	130	0.20	0.36
K79	5	35	500	130	0.18	0.31
K80	0	0	20	146	0.05	0.10
K80	1	6	20	165	0.08	0.10
K80	2	14	20	197	0.18	0.42

Rat Name	Week	Day	Frequency (kHz)	Rat Mass (g)	Treated Volume (cm³)	Untreated Volume (cm³)
K80	3	21	20	193	0.48	1.14
K80	3	21	20	193	0.44	1.25
K80	4	28	20	188	0.56	1.38
K80	4	28	20	188	0.50	1.40
K80	4	28	20	188	0.52	1.50
K80	5	35	20	154	0.32	2.60
K80	5	35	20	154	0.34	2.83
K80	5	35	20	154	0.30	2.53
K81	0	0	500	175	0.02	0.03
K81	1	6	500	176	0.04	0.06
K81	2	14	500	198	0.07	0.08
K81	3	21	500	194	0.12	0.18
K81	3	21	500	194	0.16	0.16
K81	3	21	500	194	0.15	0.17
K81	4	28	500	181	0.19	0.22
K81	4	28	500	181	0.20	0.23
K81	4	28	500	181	0.18	0.22
K81	5	35	500	155	0.18	0.34
K81	5	35	500	155	0.16	0.33
K81	5	35	500	155	0.17	0.31
K82	0	0	20	160	0.05	0.07
K82	1	8	20	179	0.15	0.14
K82	2	15	20	173	0.20	0.23
K82	2	15	20	173	0.18	0.22
K82	2	15	20	173	0.16	0.23
K82	3	22	20	191	0.10	0.24
K82	3	22	20	191	0.11	0.22
K82	3	22	20	191	0.09	0.23
K82	4	29	20	153	0.17	0.35
K82	4	29	20	153	0.18	0.31
K82	4	29	20	153	0.19	0.34
K82	5	32	20	167	0.14	0.33
K82	5	32	20	167	0.13	0.39
K82	5	32	20	167	0.12	0.37
K83	0	0	20	184	0.07	0.07
K83	1	8	20	202	0.07	0.16
K83	2	15	20	199	0.16	0.20
K83	2	15	20	199	0.16	0.19
K83	2	15	20	199	0.16	0.17
K83	3	22	20	168	0.23	0.72
K83	3	22	20	168	0.27	0.75
K83	3	22	20	168	0.25	0.69
K83	4	29	20	138	0.34	0.93
K83	4	29	20	138	0.33	0.87
K83	4	29	20	138	0.31	0.88
K83	5	32	20	151	0.24	1.18
K83	5	32	20	151	0.24	1.16

Rat Name	Week	Day	Frequency (kHz)	Rat Mass (g)	Treated Volume (cm³)	Untreated Volume (cm³)
K84	0	0	20	162	0.08	0.04
K84	1	3	20	167	0.07	0.04
K84	2	9	20	172	0.07	0.05
K84	2	9	20	172	0.09	0.06
K84	2	9	20	172	0.09	0.06
K84	3	17	20	142	0.26	0.07
K84	3	17	20	142	0.27	0.08
K84	3	17	20	142	0.22	0.05
K84	4	24	20	160	0.30	0.11
K84	4	24	20	160	0.25	0.12
K84	4	24	20	160	0.26	0.11
K84	5	32	20	163	0.55	0.22
K84	5	32	20	163	0.54	0.20
K84	5	32	20	163	0.51	0.18
K85	0	0	500	161	0.15	0.18
K85	1	7	500	156	0.20	0.33
K85	1	7	500	156	0.23	0.32
K85	1	7	500	156	0.22	0.30
K85	2	14	500	151	0.22	0.19
K85	2	14	500	151	0.21	0.16
K85	2	14	500	151	0.23	0.19
K85	3	21	500	119	0.53	1.19
K85	3	21	500	119	0.46	1.30
K85	3	21	500	119	0.49	1.12
K85	4	24	500	133	0.56	0.73
K85	4	24	500	133	0.53	0.65
K85	4	24	500	133	0.54	0.75

Treatment cut short due to time constraints (vacation) - The rat started treatment later than the rest

Statistical Results from the Ultrasound Frequency / Tumor Growth Experiment

Model Information

Data Set	WORK.D1
Dependent Variable	logvol
Covariance Structure	Variance Components
Subject Effects	Rat*treat, Rat
Estimation Method	REML
Residual Variance Method	Profile
Fixed Effects SE Method	Prasad-Rao-Jeske-Kackar-Harville
Degrees of Freedom Method	Kenward-Roger

Class Level Information

Class	Levels	Values
Rat	22	K60 K61 K62 K63 K64 K66 K67 K69 K70 K71 K72 K73 K74 K75 K77 K79 K80 K81 K82 K83 K84 K85
treat	2	n y
Frequency	2	20 500
daycat	17	0 3 6 7 8 9 14 15 17 20 21 22 24 28 29 32 35

Dimensions

Covariance Parameters	4
Columns in X	8
Columns in Z Per Subject	195
Subjects	1
Max Obs Per Subject	530

Number of Observations

Number of Observations Read	530
Number of Observations Used	518
Number of Observations Not Used	12

Iteration History

Iteration	Evaluations	-2 Res Log Like	Criterion
0	1	1403.74010540	
1	2	595.09376713	0.27188789
2	1	532.89972729	0.14095213
3	1	495.03205630	0.07415386
4	1	473.48578893	0.03526624
5	1	462.96306180	0.01325774
6	1	459.05677635	0.00315702
7	1	458.17268192	0.00029606
8	1	458.09634859	0.00000369
9	1	458.09545093	0.00000000

Convergence criteria met.

94

Covariance Parameter Estimates

Cov Parm	Subject	Estimate	Standard Error	Z Value	Pr Z
Intercept	Rat*treat	0.5407	0.1317	4.11	<.0001
Day	Rat	0.000328	0.000131	2.50	0.0062
Rat*daycat		0.04763	0.01014	4.69	<.0001
Residual		0.06579	0.004825	13.64	<.0001

Fit Statistics

-2 Res Log Likelihood	458.1
AIC (smaller is better)	466.1
AICC (smaller is better)	466.2
BIC (smaller is better)	458.1

Solution for Fixed Effects

Effect	treat	Frequency	Estimate	Standard Error	DF	t Value	Pr > |t|
treat	n		-2.7949	0.2102	42.7	-13.30	<.0001
treat	y		-2.7321	0.2102	42.7	-13.00	<.0001
Frequency		20	0.02187	0.2391	45	0.09	0.9275
Frequency		500	0	.	.	.	.
Day*treat	n		0.04647	0.0066	21.8	7.05	<.0001
Day*treat	y		0.04016	0.0066	22	6.08	<.0001
Day*Frequency		20	0.01623	0.0088	20.5	1.85	0.0791
Day*Frequency		500	0	.	.	.	.

Type 3 Tests of Fixed Effects

Effect	Num DF	Den DF	F Value	Pr > F
treat	1	37.5	0.08	0.7843
Frequency	1	45	0.01	0.9275
Day*treat	1	377	8.10	0.0047
Day*Frequency	1	20.5	3.42	0.0791

Estimates

Label	Estimate	Standard Error	DF	t Value	Pr > |t|
growth diff	0.006304	0.002215	377	2.85	0.0047

HPLC Results for the Pharmacokinetic Studies

Rat	Hours	Tissue	Run	Area	Mass Ext	Vol PO4	Dox in Inj (ng)	Dox(mg)/ Tissue(g)
K56	0.5	Heart	1	45970	0.5053	33.68	1.84	5.72
K57	0.5	Heart	1	63365	0.4370	29.00	2.53	7.85
K57	0.5	Heart	2	70938	0.4370	29.00	2.84	8.79
K52	0.5	Heart	1	84887	0.5680	11.40	3.40	3.18
K52	0.5	Heart	2	116780	0.5680	11.40	4.67	4.38
K35	0.5	Heart	2	124647	0.5812	11.60	4.99	4.64
K35	0.5	Heart	1	128910	0.5812	11.60	5.16	4.80
K10	1	Heart	1	14365	0.0412	2.75	0.57	1.79
K2	1	Heart	1	35970	0.0510	3.40	1.44	4.48
K10	1	Heart	2	18160	0.0375	2.50	0.73	2.26
K2	1	Heart	2	23010	0.0360	2.40	0.92	2.86
K1	6	Heart	1	33560	0.0648	4.32	1.34	4.18
K8	6	Heart	1	22510	0.0681	4.54	0.90	2.80
K11	6	Heart	1	13440	0.0500	3.33	0.54	1.67
K4	6	Heart	1	13390	0.0473	3.15	0.54	1.67
K1	6	Heart	2	18345	0.0498	3.32	0.73	2.28
K8	6	Heart	2	33225	0.0563	3.75	1.33	4.13
K11	6	Heart	2	9920	0.0400	2.67	0.40	1.24
K4	6	Heart	2	19245	0.0510	3.40	0.77	2.39
K36	8	Heart	1	12565	0.4297	28.65	0.03	0.09
K36	8	Heart	2	15040	0.4297	28.65	0.04	0.11
K50	8	Heart	2	58028	0.5250	10.40	2.32	2.15
K50	8	Heart	1	67730	0.5250	10.40	2.71	2.50
K38	8	Heart	2	69630	0.6060	12.00	2.79	2.57
K38	8	Heart	1	91255	0.6060	12.00	3.65	3.37
K39	12	Heart	1	68979	0.5375	10.70	2.76	2.56
K39	12	Heart	2	67420	0.5375	10.70	2.70	2.51
K39	12	Heart	1	57760	0.5375	10.70	2.31	2.15
K53	12	Heart	1	41039	0.5812	11.60	1.64	1.53
K53	12	Heart	2	39050	0.5812	11.60	1.56	1.45
K53	12	Heart	1	32910	0.5812	11.60	1.32	1.23
K7	12	Heart	2	14170	0.0449	2.99	0.57	1.76
K13	12	Heart	2	10310	0.0367	2.45	0.41	1.28
K13	12	Heart	1	7990	0.0520	3.47	0.32	0.99
K7	12	Heart	1	7610	0.0443	2.95	0.30	0.95
K6	24	Heart	1	9275	0.0470	3.13	0.37	1.15
K9	24	Heart	1	4990	0.0500	3.33	0.20	0.62
K6	24	Heart	2	8010	0.0438	2.92	0.32	1.00
K9	24	Heart	2	6185	0.0402	2.68	0.25	0.77
K5	48	Heart	2	1630	0.0383	2.55	0.07	0.20
K12	48	Heart	1	3495	0.0481	3.21	0.14	0.44
K12	48	Heart	2	3980	0.0344	2.29	0.16	0.49
K5	48	Heart	1	4245	0.0489	3.26	0.17	0.53
K30	48	Heart	1	7320	0.4950	9.90	0.29	0.27
K33	48	Heart	1	10710	0.4826	9.65	0.43	0.40

Rat	Hours	Tissue	Run	Area	Mass Ext	Vol PO4	Dox in Inj (ng)	Dox(mg)/ Tissue(g)
K37	96	Heart	1	2705	0.5140	10.30	0.11	0.10
K47	96	Heart	2	1560	0.6060	12.00	0.06	0.06
K47	96	Heart	1	1250	0.6060	12.00	0.05	0.05
K28	168	Heart	1	1160	0.5130	10.30	0.05	0.04
K57	0.5	Liver	1	48170	3.8843	77.65	1.93	1.80
K56	0.5	Liver	1	94950	4.4664	89.33	3.80	3.54
K57	0.5	Liver	2	50557	3.8843	77.65	2.02	1.89
K56	0.5	Liver	3	84540	4.1558	83.10	3.38	3.16
K10	1	Liver	1	83860	0.1421	2.84	3.35	3.13
K10	1	Liver	2	86315	0.1443	2.89	3.45	3.23
K2	1	Liver	1	91020	0.1569	3.14	3.64	3.40
K1	6	Liver	1	40610	0.1612	3.22	1.62	1.52
K8	6	Liver	1	23210	0.2040	4.08	0.93	0.87
K11	6	Liver	1	35360	0.1052	2.10	1.41	1.32
K4	6	Liver	1	23140	0.1774	3.55	0.93	0.86
K8	6	Liver	2	73320	0.1528	3.06	2.93	2.74
K11	6	Liver	2	56140	0.1600	3.20	2.25	2.10
K4	6	Liver	2	56190	0.1505	3.01	2.25	2.10
K13	12	Liver	1	19515	0.1740	3.48	0.78	0.73
K7	12	Liver	1	21520	0.1970	3.94	0.86	0.80
K13	12	Liver	2	21750	0.1610	3.22	0.87	0.81
K7	12	Liver	2	31865	0.1606	3.21	1.27	1.19
K6	24	Liver	1	6060	0.1336	2.67	0.24	0.23
K9	24	Liver	1	7940	0.1211	2.42	0.32	0.30
K6	24	Liver	2	7710	0.1300	2.60	0.31	0.29
K9	24	Liver	2	9360	0.1667	3.33	0.37	0.35
K12	48	Liver	1	3280	0.0960	1.92	0.13	0.12
K5	48	Liver	1	2935	0.1539	3.08	0.12	0.11
K12	48	Liver	2	2730	0.1150	2.30	0.11	0.10
K5	48	Liver	2	2110	0.1819	3.64	0.08	0.08
K57	0.5	Muscle	1	11970	0.1790	11.90	0.48	1.49
K56	0.5	Muscle	1	12575	0.3025	20.00	0.50	1.55
K57	0.5	Muscle	2	14205	0.1790	11.90	0.57	1.76
K10	1	Muscle	1	5040	0.0398	2.65	0.20	0.63
K2	1	Muscle	1	10750	0.0508	3.39	0.43	1.34
K10	1	Muscle	2	2850	0.0431	2.87	0.11	0.35
K2	1	Muscle	2	12330	0.0468	3.12	0.49	1.53
K2	1	Muscle	2	6830	0.0400	2.67	0.27	0.85
K1	6	Muscle	1	6650	0.0580	3.87	0.27	0.83
K8	6	Muscle	1	4250	0.0524	3.49	0.17	0.53
K11	6	Muscle	1	7400	0.0342	2.28	0.30	0.92
K4	6	Muscle	1	6710	0.0467	3.11	0.27	0.83
K1	6	Muscle	2	4250	0.0580	3.87	0.17	0.53
K8	6	Muscle	2	7960	0.0545	3.63	0.32	0.99
K11	6	Muscle	2	5220	0.0422	2.81	0.21	0.65
K4	6	Muscle	2	5000	0.0527	3.51	0.20	0.62
K13	12	Muscle	1	3610	0.0383	2.55	0.14	0.45
K7	12	Muscle	1	11560	0.0472	3.15	0.46	1.44
K13	12	Muscle	2	8820	0.0417	2.78	0.35	1.10

Rat	Hours	Tissue	Run	Area	Mass Ext	Vol PO4	Dox in Inj (ng)	Dox(mg)/ Tissue(g)
K7	12	Muscle	2	2980	0.0461	3.07	0.12	0.37
K6	24	Muscle	1	5580	0.0463	3.09	0.22	0.70
K9	24	Muscle	1	2740	0.0396	2.64	0.11	0.34
K6	24	Muscle	2	3445	0.0326	2.17	0.14	0.43
K9	24	Muscle	2	3415	0.0492	3.28	0.14	0.42
K12	48	Muscle	1	2600	0.0453	3.02	0.10	0.32
K5	48	Muscle	1	1790	0.0462	3.08	0.07	0.22
K12	48	Muscle	2	1695	0.0445	2.97	0.07	0.21
K5	48	Muscle	2	1500	0.0297	2.10	0.06	0.20
K35	0.5	Tumor	1	7785	0.0745	5.00	0.31	0.98
K52	0.5	Tumor	1	6700	0.1894	12.60	0.27	0.83
K73	0.5	Tumor	1	17810	0.0347	2.30	0.27	0.84
K81	0.5	Tumor	1	29430	0.3150	21.00	0.45	1.40
K80	0.5	Tumor	1	12514	1.6470	110.00	0.19	0.60
K52	0.5	Tumor	2	8030	0.1894	12.60	0.32	1.00
K73	0.5	Tumor	2	18300	0.0347	2.30	0.28	0.87
K81	0.5	Tumor	2	30535	0.3150	21.00	0.47	1.46
K80	0.5	Tumor	2	15476	1.6470	110.00	0.24	0.74
K10	1	Tumor	1	6615	0.0490	3.27	0.26	0.82
K10	1	Tumor	2	4030	0.0416	2.77	0.16	0.50
K74	3	Tumor	2	11240	0.2425	16.20	0.17	0.54
K75	3	Tumor	2	13247	0.4800	32.00	0.20	0.63
K74	3	Tumor	1	14000	0.2425	16.20	0.21	0.67
K60	3	Tumor	2	15471	0.7818	34.65	0.24	0.49
K64	3	Tumor	1	16710	0.3120	20.00	0.26	0.77
K60	3	Tumor	1	17150	0.7818	34.65	0.26	0.54
K64	3	Tumor	2	17205	0.3120	20.00	0.26	0.79
K75	3	Tumor	1	17661	0.4800	32.00	0.27	0.84
K8	6	Tumor	1	4330	0.0399	2.66	0.17	0.54
K11	6	Tumor	2	5110	0.0370	2.47	0.20	0.64
K11	6	Tumor	1	5960	0.0253	1.69	0.24	0.74
K8	6	Tumor	2	6480	0.0606	4.04	0.26	0.81
K1	6	Tumor	1	7160	0.0481	3.21	0.29	0.89
K1	6	Tumor	2	7240	0.0606	4.04	0.29	0.90
K4	6	Tumor	2	8070	0.0147	0.98	0.32	1.00
K77	6	Tumor	2	11276	0.1785	11.80	0.17	0.53
K77	6	Tumor	1	12900	0.1785	11.80	0.20	0.61
K67	6	Tumor	1	13370	0.6380	43.00	0.20	0.64
K67	6	Tumor	2	17890	0.6380	43.00	0.27	0.86
K66	6	Tumor	2	18600	0.0888	6.00	0.28	0.90
K79	6	Tumor	2	27764	0.1722	11.50	0.43	1.33
K79	6	Tumor	1	30048	0.1722	11.50	0.46	1.43
K66	6	Tumor	1	32320	0.0888	6.00	0.50	1.56
K36	8	Tumor	2	2760	0.5122	34.50	0.01	0.02
K36	8	Tumor	5	3940	0.5122	34.50	0.01	0.03
K36	8	Tumor	1	4415	0.5122	34.50	0.01	0.04
K36	8	Tumor	4	4520	0.5122	34.50	0.01	0.03
K38	8	Tumor	1	8186	0.1757	11.70	0.33	1.02
K36	8	Tumor	3	8270	0.5122	34.50	0.02	0.06

Rat	Hours	Tissue	Run	Area	Mass Ext	Vol PO4	Dox in Inj (ng)	Dox(mg)/ Tissue(g)
K50	8	Tumor	2	9410	0.1310	8.70	0.38	1.17
K50	8	Tumor	1	10275	0.1310	8.70	0.41	1.27
K38	8	Tumor	2	11305	0.1757	11.70	0.45	1.41
K38	8	Tumor	1	11770	0.1757	11.70	0.47	1.46
K32	12	Tumor	1	3870	0.1400	9.30	0.15	0.48
K13	12	Tumor	1	4900	0.0520	3.68	0.20	0.65
K13	12	Tumor	2	6235	0.0366	2.44	0.25	0.78
K7	12	Tumor	1	6360	0.0450	3.00	0.25	0.79
K7	12	Tumor	2	7540	0.0342	2.28	0.30	0.94
K53	12	Tumor	1	9874	0.1971	13.10	0.39	1.23
K53	12	Tumor	2	10289	0.1971	13.10	0.41	1.28
K39	12	Tumor	2	10420	0.1014	6.70	0.42	1.29
K53	12	Tumor	2	11001	0.1971	13.10	0.44	1.36
K53	12	Tumor	1	12184	0.1971	13.10	0.49	1.51
K39	12	Tumor	1	12820	0.1014	6.70	0.51	1.58
K71	12	Tumor	2	12876	0.9216	61.40	0.20	0.61
K71	12	Tumor	1	13029	0.9216	61.40	0.20	0.62
K39	12	Tumor	1	14360	0.1014	6.70	0.57	1.77
K62	12	Tumor	1	15825	0.8838	59.00	0.24	0.76
K62	12	Tumor	2	17310	0.8838	59.00	0.27	0.82
K61	12	Tumor	2	18760	1.2450	83.00	0.29	0.89
K61	12	Tumor	1	19415	1.2450	83.00	0.30	0.93
K70	12	Tumor	1	20414	0.0860	5.70	0.31	0.97
K70	12	Tumor	2	29130	0.0860	5.70	0.45	1.38
K6	24	Tumor	1	9300	0.0112	0.75	0.37	1.16
K9	24	Tumor	1	7400	0.0459	3.06	0.30	0.92
K9	24	Tumor	2	4330	0.0338	2.25	0.17	0.54
K30	48	Tumor	2	1640	0.0346	2.30	0.07	0.20
K30	48	Tumor	1	2095	0.0346	2.30	0.08	0.26
K12	48	Tumor	1	2310	0.0368	2.45	0.09	0.29
K12	48	Tumor	2	2890	0.0308	2.05	0.12	0.36
K5	48	Tumor	2	3790	0.0306	2.04	0.15	0.47
K5	48	Tumor	1	6320	0.0272	1.81	0.25	0.79
K33	48	Tumor	1	6416	0.0808	5.40	0.26	0.80
K30	48	Tumor	1	6836	0.0346	2.30	0.27	0.85
K33	48	Tumor	2	7280	0.0808	5.40	0.29	0.91
K37	96	Tumor	1	825	0.2458	16.40	0.03	0.10
K37	96	Tumor	1	1555	0.2458	16.40	0.06	0.19
K47	96	Tumor	1	2498	0.1560	10.40	0.10	0.31
K37	96	Tumor	2	5338	0.2458	16.40	0.21	0.66
K47	96	Tumor	2	3103	0.1560	10.40	0.12	0.39
K47	96	Tumor	2	7250	0.1560	10.40	0.29	0.90
K28	168	Tumor	1	871	0.1430	9.60	0.03	0.11
K27	168	Tumor	1	1450	0.1430	9.60	0.06	0.18
K28	168	Tumor	2	2431	0.1430	9.60	0.10	0.30
K27	168	Tumor	2	890	0.1430	9.60	0.04	0.11
K52	0.5	T-(US)	1	8050	0.0981	11.40	0.32	1.75
K52	0.5	T-(US)	1	9320	0.0981	11.40	0.37	2.02
K35	0.5	T-(US)	1	11439	0.1630	10.90	0.46	1.43

Rat	Hours	Tissue	Run	Area	Mass Ext	Vol PO4	Dox in Inj (ng)	Dox(mg)/ Tissue(g)
K73	0.5	T-(US)	2	11950	0.2000	12.00	0.18	0.51
K80	0.5	T-(US)	2	13491	0.4540	30.00	0.21	0.64
K73	0.5	T-(US)	1	14320	0.2000	12.00	0.22	0.61
K35	0.5	T-(US)	2	14350	0.1630	10.90	0.57	1.79
K80	0.5	T-(US)	1	18023	0.4540	30.00	0.28	0.85
K81	0.5	T-(US)	1	22499	0.1282	8.50	0.34	1.07
K81	0.5	T-(US)	2	24694	0.1282	8.50	0.38	1.17
K60	3	T-(US)	1	16125	0.9320	60.00	0.25	0.74
K75	3	T-(US)	1	13970	0.7773	50.00	0.21	0.64
K64	3	T-(US)	1	15530	0.2275	15.00	0.24	0.73
K60	3	T-(US)	2	12995	0.9320	60.00	0.20	0.60
K75	3	T-(US)	2	14770	0.7773	50.00	0.23	0.68
K64	3	T-(US)	2	15160	0.2275	15.00	0.23	0.71
K77	6	T-(US)	2	12770	0.1910	12.80	0.20	0.61
K77	6	T-(US)	1	12865	0.1910	12.80	0.20	0.62
K67	6	T-(US)	2	20475	0.2980	19.50	0.31	0.96
K67	6	T-(US)	1	23185	0.2980	19.50	0.36	1.08
K79	6	T-(US)	2	24211	0.1030	6.90	0.37	1.16
K66	6	T-(US)	1	25530	0.0717	4.80	0.39	1.22
K66	6	T-(US)	2	26450	0.0717	4.80	0.41	1.27
K79	6	T-(US)	1	27812	0.1030	6.90	0.43	1.33
K36	8	T-(US)	2	1875	0.5906	39.50	0.01	0.02
K44	8	T-(US)	1	1890	1.0692	71.50	0.08	0.24
K36	8	T-(US)	1	2200	0.5906	39.50	0.01	0.02
K44	8	T-(US)	4	3150	1.0692	71.50	0.13	0.39
K38	8	T-(US)	1	5830	0.2610	17.50	0.23	0.73
K38	8	T-(US)	2	5960	0.2466	16.50	0.24	0.74
K50	8	T-(US)	1	6295	0.1504	10.00	0.25	0.78
K50	8	T-(US)	1	7400	0.1504	10.00	0.30	0.92
K38	8	T-(US)	1	7410	0.2610	17.50	0.30	0.93
K38	8	T-(US)	1	8620	0.2466	16.50	0.34	1.08
K50	8	T-(US)	2	10070	0.1504	10.00	0.40	1.25
K50	8	T-(US)	1	10545	0.1504	10.00	0.42	1.31
K50	8	T-(US)	2	11320	0.1504	10.00	0.45	1.40
K38	8	T-(US)	2	15572	0.2466	16.50	0.62	1.94
K50	8	T-(US)	2	16133	0.1504	10.00	0.65	2.00
K50	8	T-(US)	2	17860	0.1504	10.00	0.71	2.22
K32	12	T-(US)	1	2020	0.0505	3.37	0.08	0.25
K39	12	T-(US)	1	5200	0.0508	3.40	0.21	0.65
K39	12	T-(US)	1	7990	0.5080	3.40	0.32	0.10
K53	12	T-(US)	1	8150	0.2636	17.50	0.33	1.01
K39	12	T-(US)	2	8270	0.5080	3.40	0.33	0.10
K39	12	T-(US)	2	8350	0.5080	3.40	0.33	0.10
K39	12	T-(US)	1	10840	0.0508	3.40	0.43	1.35
K32	12	T-(US)	2	12795	0.0560	3.70	0.51	1.58
K71	12	T-(US)	1	13706	0.8136	54.20	0.21	0.65
K71	12	T-(US)	2	14132	0.8136	54.20	0.22	0.67
K39	12	T-(US)	2	14370	0.0508	3.40	0.57	1.80
K62	12	T-(US)	2	15380	1.2525	83.00	0.24	0.73

Rat	Hours	Tissue	Run	Area	Mass Ext	Vol PO4	Dox in Inj (ng)	Dox(mg)/ Tissue(g)
K53	12	T-(US)	1	16430	0.2636	17.50	0.66	2.04
K61	12	T-(US)	2	16490	1.1398	76.00	0.25	0.79
K62	12	T-(US)	1	16760	1.2525	83.00	0.26	0.79
K61	12	T-(US)	1	17010	1.1398	76.00	0.26	0.81
K53	12	T-(US)	2	17810	0.2636	17.50	0.71	2.21
K53	12	T-(US)	2	18191	0.2636	17.50	0.73	2.25
K30	48	T-(US)	1	2330	0.0388	2.60	0.09	0.29
K33	48	T-(US)	1	4769	0.1037	6.90	0.19	0.59
K30	48	T-(US)	1	5625	0.0388	2.60	0.23	0.70
K30	48	T-(US)	2	5615	0.0388	2.60	0.22	0.70
K33	48	T-(US)	2	4780	0.1037	6.90	0.19	0.59
K37	96	T-(US)	1	3070	0.2029	13.40	0.12	0.38
K47	96	T-(US)	1	1260	0.3800	25.30	0.05	0.16
K47	96	T-(US)	1	3590	0.3800	25.30	0.14	0.45
K37	96	T-(US)	2	3890	0.2029	13.40	0.16	0.48
K47	96	T-(US)	2	1035	0.3800	25.30	0.04	0.13
K27	168	T-(US)	1	5130	0.1411	9.40	0.21	0.64
K28	168	T-(US)	1	330	0.1069	7.10	0.01	0.04
K27	168	T-(US)	2	750	0.1411	9.40	0.03	0.09
K28	168	T-(US)	2	760	0.1069	7.10	0.03	0.09

HPLC Results: DOX Concentration in the Sonicated and Non-Sonicated Tumors

Freq	Tissue	mg/ml ratio	grams mass$_{tone}$	ml V$_{calculated}$	V$_{Used}$	Date	Run 1 Retention	Height	Area	Dox in Injection (ng)	Dox(mg)/Tissue(g)	Run 2 Retention	Height	Area	Dox in Injection (ng)	Dox(mg)/Tissue(g)
500 kHz	**KT3 (30 min)** Tumor	15	0.0347	2.3133	2.30	7/31/2006	5.446	418	17810	0.27	0.84	5.494	441	18300	0.28	0.87
500 kHz	Tumor (US)	15	0.2000	13.3333	12.00	7/31/2006	5.510	332	14320	0.22	0.61	5.533	290	11950	0.18	0.51
500 kHz	**K81 (30 min)** Tumor	15	0.3150	21.0000	21.00	8/1/2006	6.084	563	29430	0.45	1.40	6.033	595	30535	0.47	1.46
500 kHz	Tumor (US)	15	0.1282	8.5467	8.50	8/1/2006	5.827	495	22499	0.34	1.07	5.897	523	24694	0.38	1.17
20 kHz	**K80 (30 min)** Tumor	15	1.6470	109.8000	110.00	8/1/2006	5.817	301	12514	0.19	0.60	5.781	367	15476	0.24	0.74
20 kHz	Tumor (US)	15	0.4540	30.2667	30.00	8/1/2006	5.753	408	18023	0.28	0.85	5.8	318	13491	0.21	0.64
20 kHz	**K84 (30 min)** Tumor	15	0.1785	11.9000	11.80	8/1/2006	5.879	523	11950	0.18	0.56	6.746	332	22499	0.34	1.06
20 kHz	Tumor (US)	15	0.191	12.7333	12.80	8/1/2006	5.950	563	15476	0.24	0.74	6.696	495	17810	0.27	0.85
500 kHz	**K60 (3 hr)** Tumor	15	0.7818	52.1200	34.65	7/31/2006	5.497	375	17150	0.26	0.54	5.464	353	15471	0.24	0.49
500 kHz	Tumor(US)	15	0.9320	62.1333	60.00	7/31/2006	5.517	355	16125	0.25	0.74	5.55	294	12995	0.20	0.60
500 kHz	**K75 (3 hr)** Tumor	15	0.4800	32.0000	32.00	8/1/2006	5.763	381	17661	0.27	0.84	5.794	346	13247	0.20	0.63
500 kHz	Tumor (US)	15	0.7773	51.8200	50.00	8/1/2006	5.710	380	13970	0.21	0.64	5.803	381	14770	0.23	0.68
20 kHz	**K64 (3 hr)** Tumor	15	0.3120	20.8000	20.00	7/31/2006	5.564	411	16710	0.26	0.77	5.633	395	17205	0.26	0.79
20 kHz	Tumor (US)	15	0.2275	15.1667	15.00	7/31/2006	5.614	341	15530	0.24	0.73	5.643	319	15160	0.23	0.71
20 kHz	**K74 (3 hr)** Tumor	15	0.2425	16.1667	16.20	8/1/2006	5.883	312	14000	0.21	0.67	5.878	334	11240	0.17	0.54
20 kHz	Tumor (US)		Completely Regressed													
500 kHz	**K66 (6 hr)** Tumor	15	0.0898	5.9867	6.00	7/28/2006	7.397	336	32320	0.50	1.54	7.1	266	18600	0.28	0.89
500 kHz	Tumor (US)	15	0.0717	4.7800	4.80	7/28/2006	7.097	380	25530	0.39	1.22	7.117	420	26450	0.41	1.27
500 kHz	**K79 (6 hr)** Tumor	15	0.1722	11.4800	11.50	8/1/2006	5.827	594	30048	0.46	1.43	5.846	648	27764	0.43	1.33
500 kHz	Tumor (US)	15	0.1030	6.8667	6.90	8/1/2006	5.817	590	27812	0.43	1.33	5.783	536	24211	0.37	1.16
20 kHz	**K67 (6 hr)** Tumor	15	0.6380	42.5333	43.00	7/28/2006	6.746	243	13370	0.20	0.64	6.667	282	17890	0.27	0.86
20 kHz	Tumor (US)	15	0.9900	66.0000	19.50	7/28/2006	6.696	393	23185	0.36	0.33	6.583	355	20475	0.31	0.29
20 kHz	**K77 (6 hr)** Tumor	15	0.1785	11.9000	11.80	8/1/2006	5.879	273	12900	0.20	0.61	5.836	267	11276	0.17	0.53
20 kHz	Tumor (US)	15	0.191	12.7333	12.80	8/1/2006	5.950	298	12865	0.20	0.62	5.696	285	12770	0.20	0.61
500 kHz	**K62 (12 hr)** Tumor	15	0.8830	58.8667	59.00	7/28/2006	6.689	282	15825	0.24	0.76	6.711	286	17310	0.27	0.83
500 kHz	Tumor (US)	15	1.2525	83.5000	83.00	7/28/2006	7.167	255	16760	0.26	0.79	7.046	258	15380	0.24	0.73
500 kHz	**K70 (12 hr)** Tumor	15	0.0860	5.7333	5.70	8/2/2006	5.885	774	20414	0.31	0.97	5.836	968	29130	0.45	1.38
500 kHz	Tumor (US)		Completely Regressed													
20 kHz	**K 61 (12hr)** Tumor	15	1.2450	83.0000	83.00	7/31/2006	5.826	513	19415	0.30	0.93	5.877	18760	18760	0.29	0.89
20 kHz	Tumor (US)	15	1.1534	76.8933	76.00	7/31/2006	5.850	319	17010	0.26	0.80	5.767	322	16490	0.25	0.78
20 kHz	Tumor (Metast)	15	0.3623	24.1533	21.00	7/31/2006	5.861	1292	69310	1.06	2.87	5.850	1067	58965	0.90	2.44
20 kHz	**K71 (12 hr)** Tumor	15	0.9216	61.4400	61.40	8/2/2006	5.633	465	13029	0.20	0.62	5.589	453	12876	0.20	0.61
20 kHz	Tumor (US)	15	0.8136	54.2400	54.20	8/2/2006	7.300	361	13706	0.21	0.65	7.256	369	14132	0.22	0.67

An experiment testing the effects of pH and temperature on the fluorescence of Doxorubicin: The four samples with the same concentration of Doxorubicin were subjected to different temperatures and pH levels before injection into the HPLC system. The results below show that the measured fluorescence of DOX is greatly dependent on both injection temperature and pH of the sample/system. **<u>Care should be taken to keep temperature and pH constant for each injection throughout the experiments.</u>**
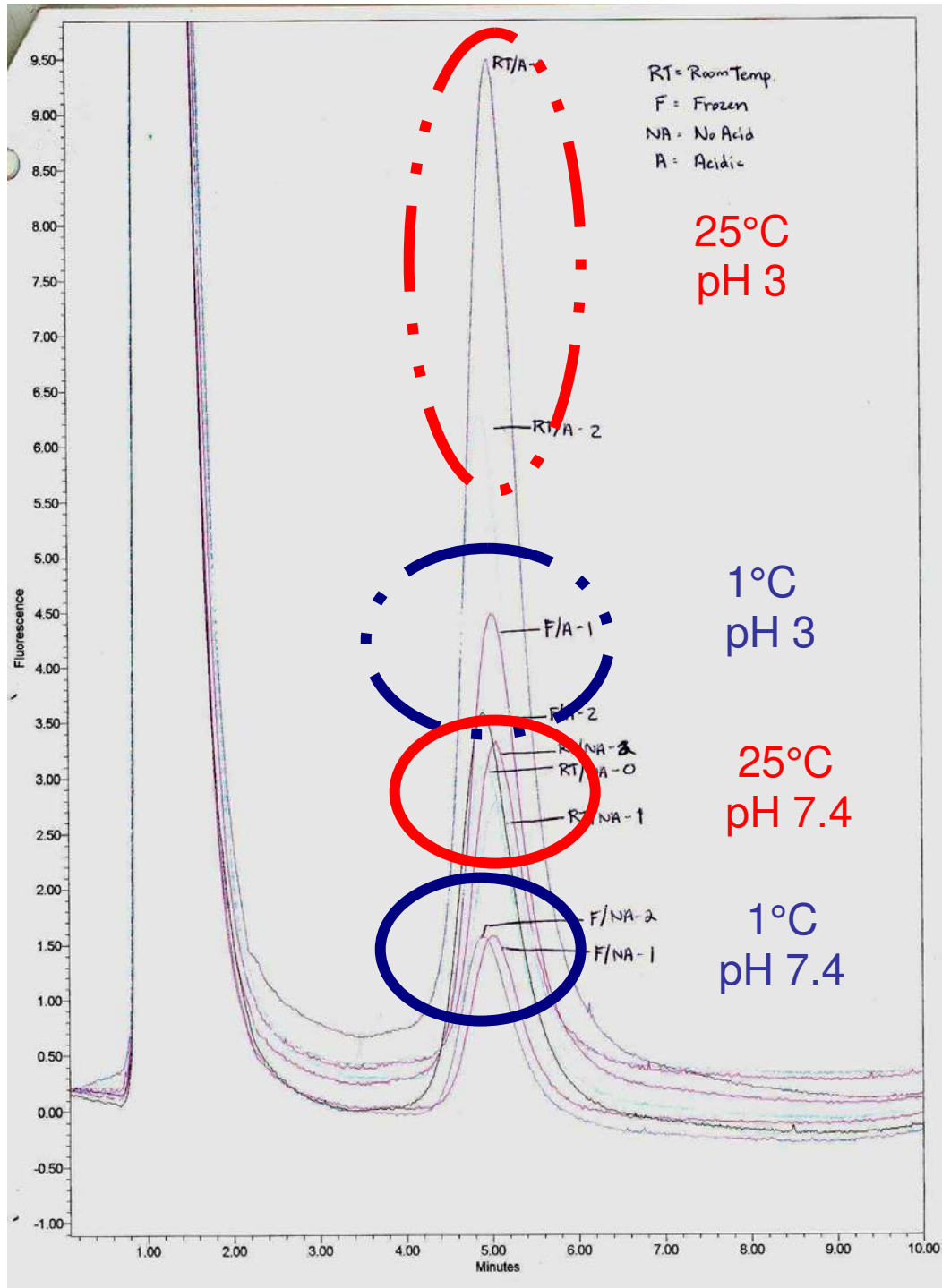
20 kHz Treatment – Tumor Growth Results

Rat K61 Tumor Data

Rat K63 Tumor Data

Rat K64 Tumor Data

Rat K67 Tumor Data

Rat K71 Tumor Data

Rat K72 Tumor Data

Rat K74 Tumor Data

Rat K77 Tumor Data

104

Rat K80 Tumor Data

Rat K82 Tumor Data

Rat K83 Tumor Data

Rat K84 Tumor Data

500 kHz Treatment – Tumor Growth Results

Rat K60 Tumor Data

Rat K62 Tumor Data

Rat K65 Tumor Data

Rat K66 Tumor Data

Rat K69 Tumor Data

Rat K70 Tumor Data

Rat K73 Tumor Data

Rat K75 Tumor Data

Rat K79 Tumor Data

Rat K81 Tumor Data

Rat K85 Tumor Data
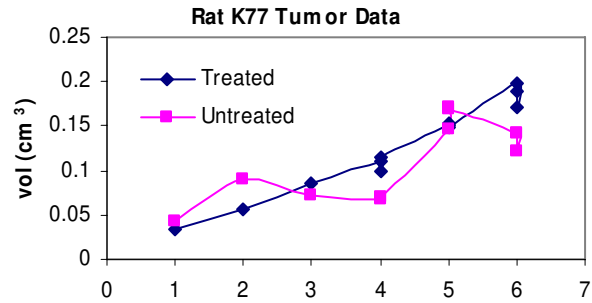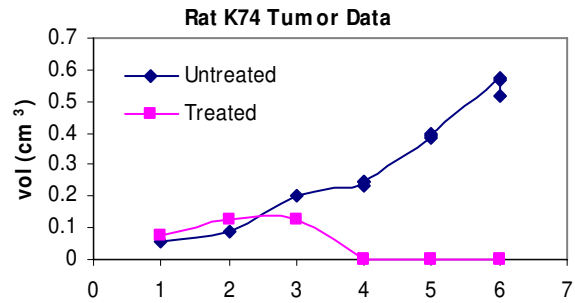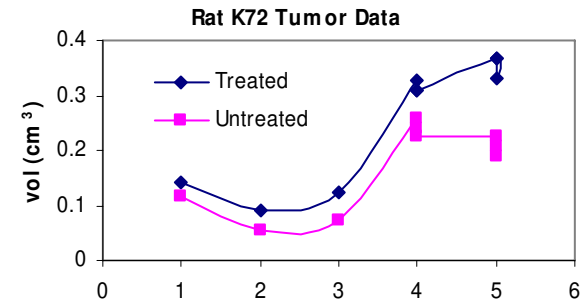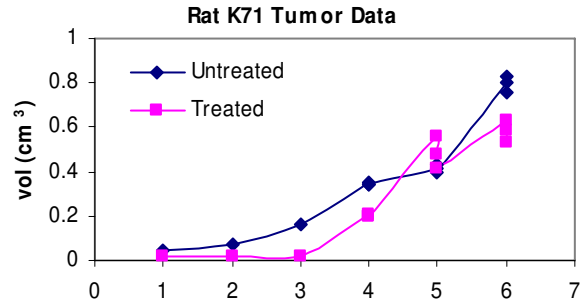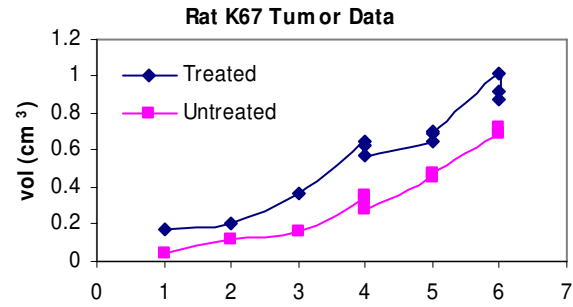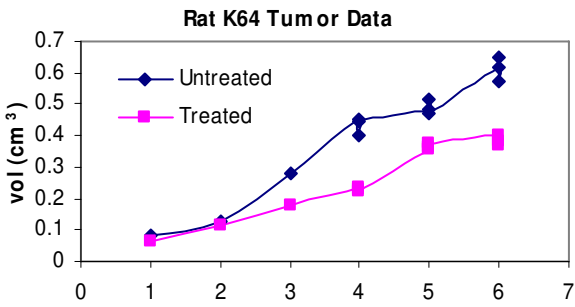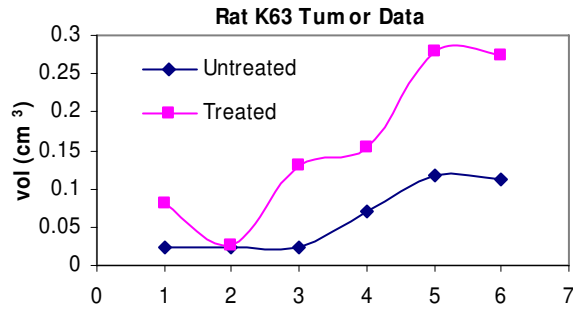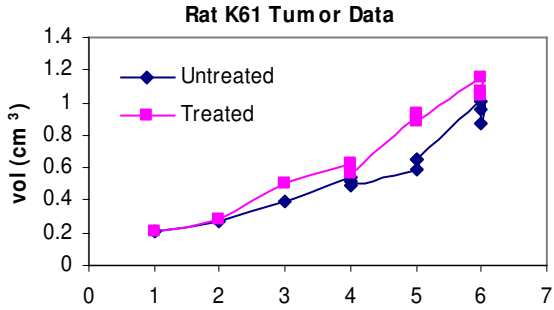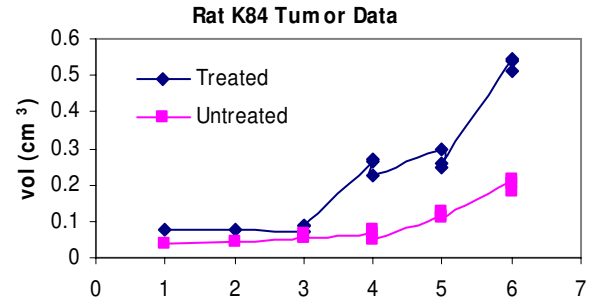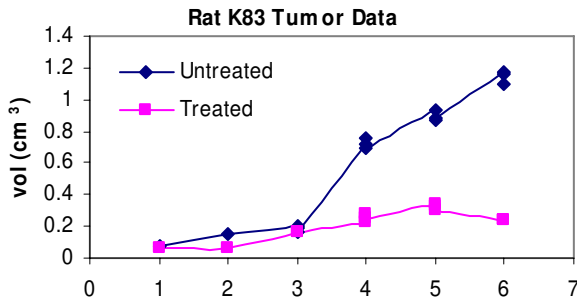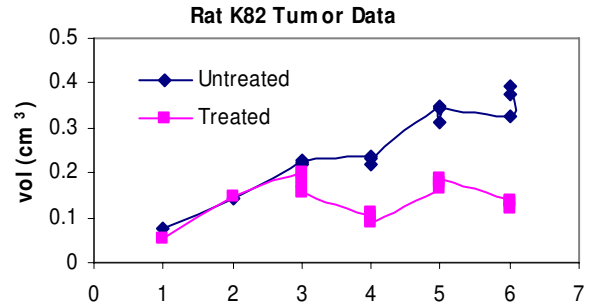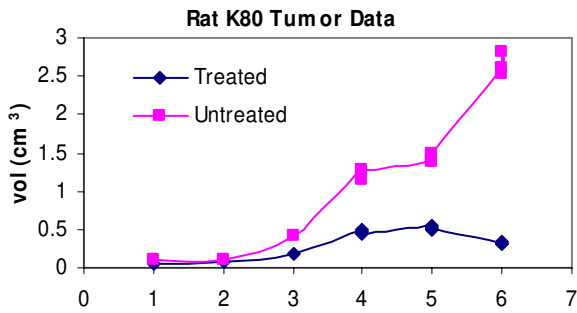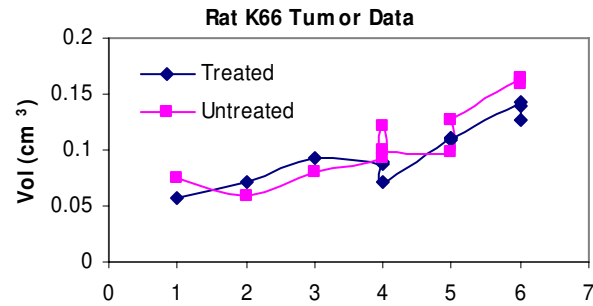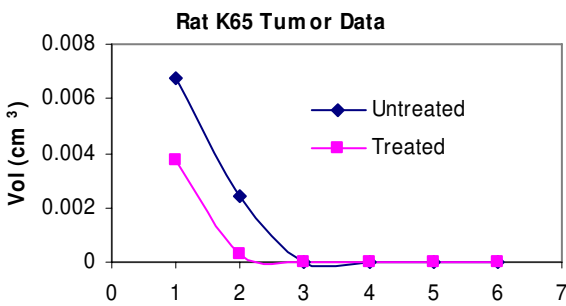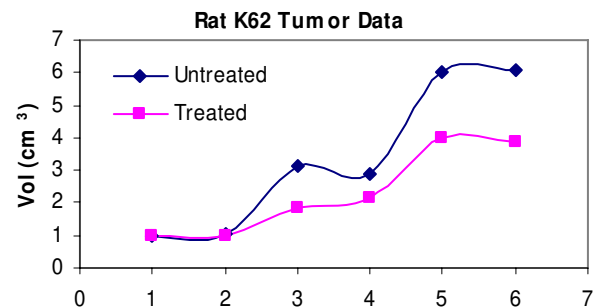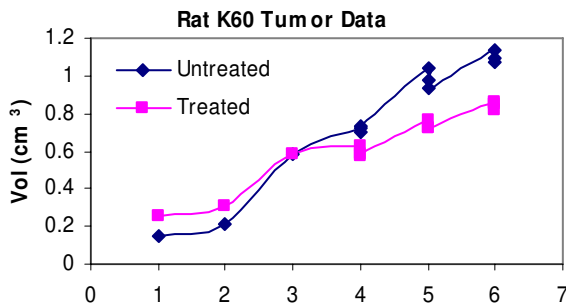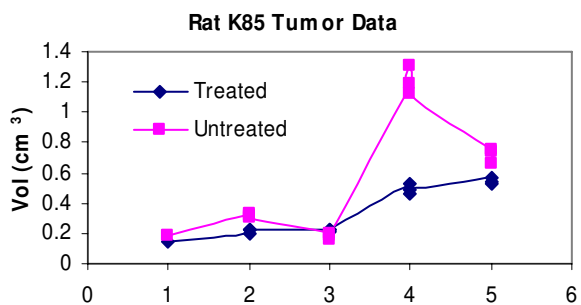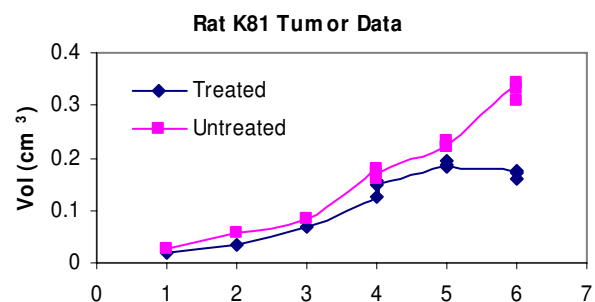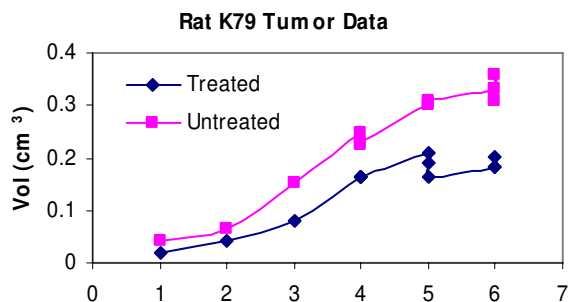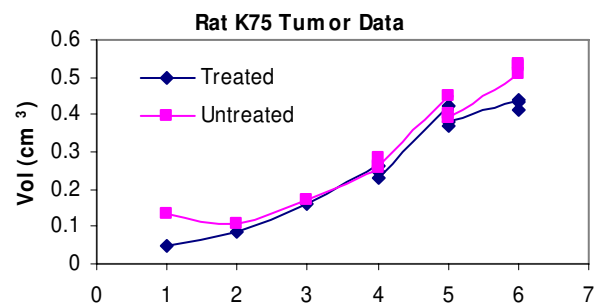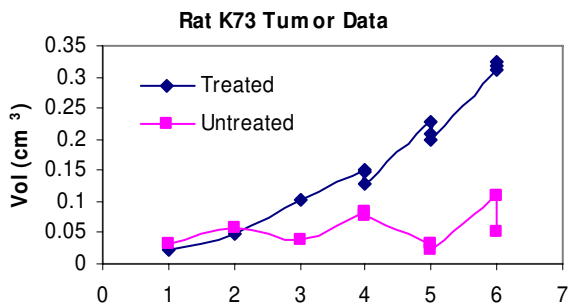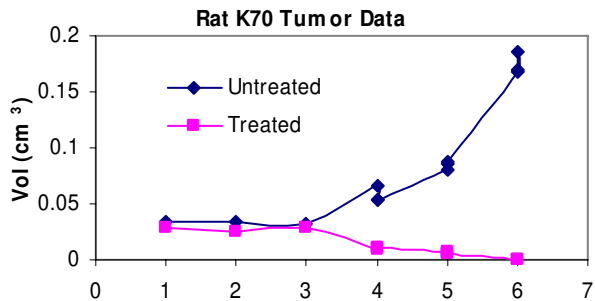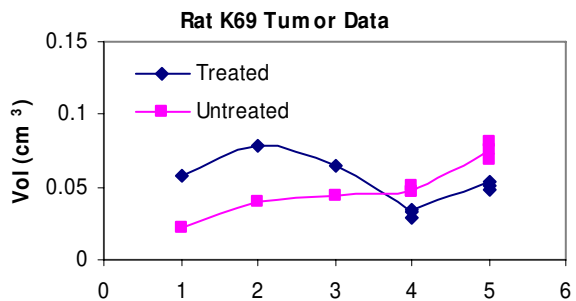
Appendix B

"HPLC for Newbies" Instruction Manual

Instruction manual which explains how to use the high performance liquid

chromatography system to analyze samples.

TABLE OF CONTENTS

INTRODUCTION

Purpose for this Manual

Although there are manuals for each piece of equipment, column, and software, they are very thick and detailed. This "HPLC for Dummies" manual was written to address the problems and issues confronted in a typical experiment. Using the operator's manuals provided with the equipment, it took me over a year to learn how to collect successful, reliable data. Hopefully, this manual will give the beginner the information and tools necessary to successfully collect reliable data the first time. If used correctly, HPLC can be a very valuable research tool.

This instruction manual will explain:
- the basic science behind HPLC and what it is used for
- what each piece of HPLC equipment is used for
- the different columns and how to choose the correct column and solvent for the system
- how to operate the pump, injector, detector, and data-collecting software in order collect simple information about a given chemical sample
- tips and cautions to prevent poor data collection and destruction of expensive columns and equipment

As a result of reading and following this manual, the reader should be able to successfully:
- understand the principles behind high-performance liquid chromatography
- select the correct column and solvent for the analysis
- safely operate the equipment without errors
- setup the system for injections
- correctly load and inject a sample into the system
- accurately collect and interpret data from the detector using the Millennium® software

Intended Audience

The audience for these instructions is college-level chemical engineering researchers who need to use the HPLC equipment for data analysis. These researchers need prior experience in a chemical laboratory, including training in chemical safety. They must be able to accurately measure volumes and weights using laboratory equipment and perform basic functions on a computer.

Prerequisites for Equipment Operation

In order to complete the tasks described in the instructions, the reader must:
- be in the laboratory (CB 173) with access to the equipment (pump, column, injector, detector, and computer)
- have the necessary chemicals (i.e. methanol, THF, water – depending on the experiment)
- have chemical waste containers,
- understand how to safely work in the lab with the chemicals to be used (i.e. read Material Safety Data Sheets)
- be wearing laboratory safety equipment (gloves, goggles, long-sleeved shirt, pants).

High Performance Liquid Chromatography (HPLC)

High Performance Liquid Chromatography (HPLC) is a chemistry based tool for quantifying and analyzing mixtures of chemical compounds. It's used to find the amount of a chemical compound within a mixture of other chemicals. An example would be to find out how much caffeine there is in the cup of cola.

Figure 1 depicts a typical setup for HPLC analysis, composed of the following components:

1. **Mobile Phase:** A non-reactive solvent used to carry the sample through the system.
2. **Pump:** This machine can pressurize the system to extremely high pressures, while maintaining a constant flow rate.
3. **Injector:** A known amount of sample is loaded into the injector and manually introduced into the system by turning its lever.
4. **Column:** The column separates the different chemicals in the sample, which then leave the column at different times. There are many variations of columns which separate chemicals using different methods (i.e. separate according to size, polarity, molecular weight, or hydrophobicity).
5. **Detector & Data System:** The compounds leaving the column are carried to a detector, which measures the amount of these compounds and sends this information to a computer for further data analysis.
6. **Waste:** The used mobile phase is collected as waste or saved for further analysis.
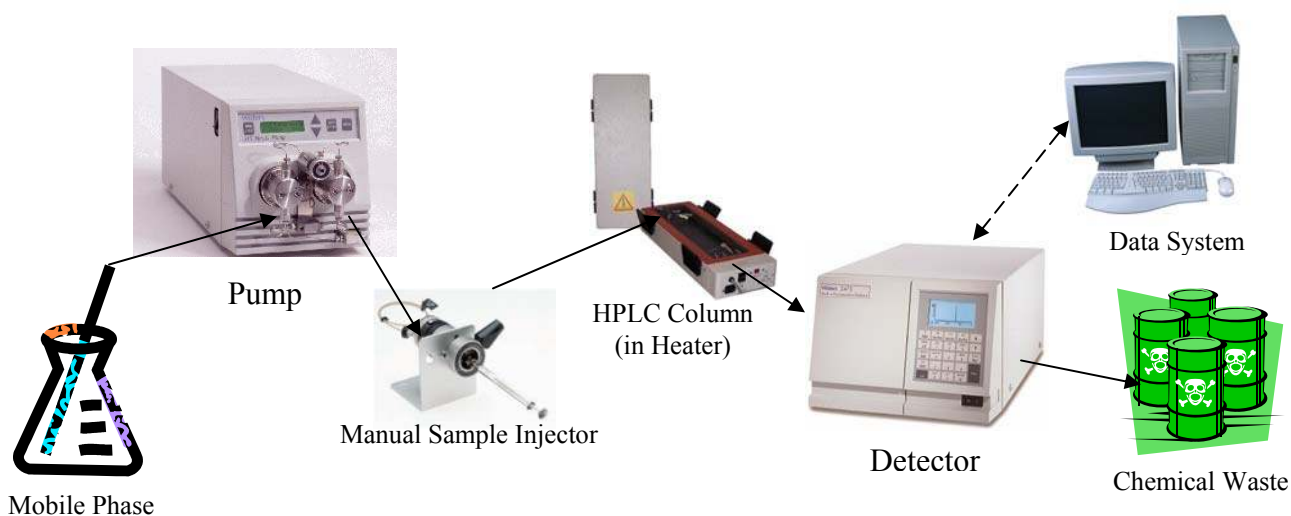
Figure 1. A typical high performance liquid chromatography system

The Waters 515 HPLC Pump

The Waters 515 Pump (Figure 2) increases the pressure and, thus, the flowrate of the mobile phase. This allows the sample to run through the highly-resistant column in a reasonable amount of time. Some notable items include:

Figure 2. The Waters 515 HPLC Pump

- Two pump heads which alternate, providing a constant flowrate without pulsation.
- One-way valves to prevent back-flow.
- Draw-off valve to remove air. Occasionally, air enters the chambers, which compromises the pump's effectiveness. (To remedy this problem, see "Priming the Pump" on page 3-13 in the Pump's Operator Guide.)
- LCD main display with four areas of information (Figure 3):
  - Menu Items Area: shows the operator-set flow rate
  - Flow Area: displays the actual flow rate
  - Status Area: tells the user if the pump is operational ("Run") or not ("Ready").
  - Pressure Area: displays the pressure in the solvent line going to the column.

Figure 3. LCD display of the Water 515 HPLC Pump.

4

Manual Sample Injector

The injector is where the prepared sample, dissolved in the same solvent as the mobile phase, is injected into the system. Then, with the injector in the LOAD position, the sample is injected into a small tube, called the sample loop. (Figure 4)

NOTE: In the current lab, the syringe holds 100µL and the sample loop holds 50µL.

Figure 5 diagrams the injector in the LOAD position. The mobile phase is pumped into position 2 and immediately leaves through position 3 towards the column. When injected, the sample follows the following path:

$$\text{Syringe} \rightarrow 5 \rightarrow 4 \rightarrow \text{Sample Loop} \rightarrow 1 \rightarrow 6 \rightarrow \text{Waste}$$

Since the syringe holds more sample than the sample loop, extra sample leaves the injector towards a waste vial. This ensures that every injection has the same volume of sample.

When the lever is pushed down, the injector changes to the INJECT position. This cuts position 5 off from position 4 and changes the flow of the mobile phase to include the sample loop. In other words, the mobile phase now follows the following path:

$$\text{Pump} \rightarrow 2 \rightarrow 1 \rightarrow \text{Sample Loop} \rightarrow 4 \rightarrow 3 \rightarrow \text{Column}$$

Thus, the sample is carried off into the column for separation.
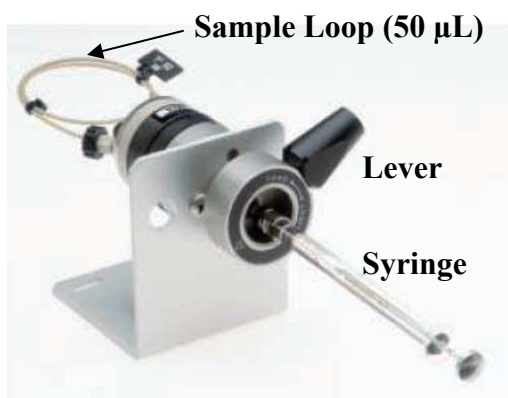
Figure 4. Picture of manual injector
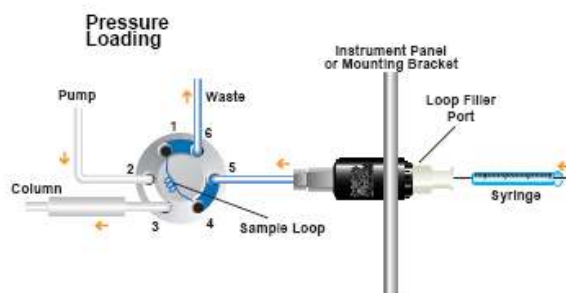
Figure 5. Diagram of sample loading into injector

HPLC Columns

The job of the HPLC column is to separate a mixture of compounds into its different components. This lab uses two types of HPLC columns: Analytical and Gel Permeation Columns (GPC).

Analytical Columns

- Compounds are separated according to polarity or hydrophobicity (the degree to which the compound is soluble in water)
- Contains an organic, hydrophobic stationary phase
- Compounds with larger hydrophobic contents (such as Compound B in Figure 6) will be slowed by like-like interactions in the column while more hydrophilic compounds (Compound A) travel faster through the column.
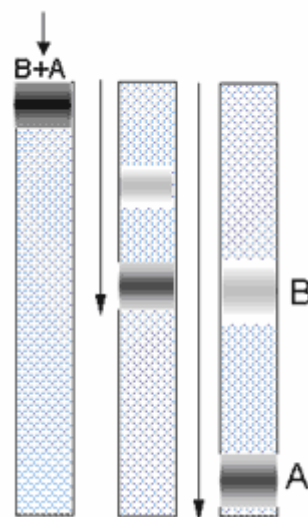
Figure 6. Separation of compounds in a reversed-phase HPLC column

Gel Permeation Columns (GPC)

- GPC columns separate compounds according to molecular weight.
- Contains particles with pores which selectively allow compounds smaller than the pore diameter to enter.
- Compounds with large molecular weights (Compound A in Figure 6) do not enter the pores and leave the column faster than smaller compounds (Compound B), which have to travel though the particle pores.

Waters 2475 Multi λ Fluorescence Detector

The fluorescence detector is a powerful HPLC tool. Its sensitivity is such that it can detect down to 3 picograms of material, making it one of the most sensitive detectors available. However, <u>it only detects fluorescent molecules</u>. Such molecules contain conjugated double bonds such as aromatic rings or dienes.
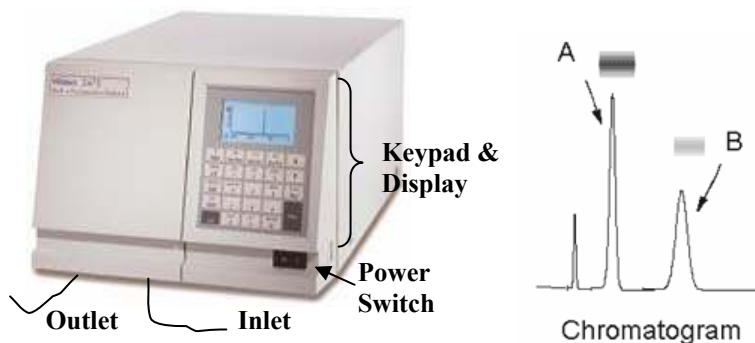
Figure 7. A labeled picture of a 2475 fluorescence detector and an example of the typical detector readout.

The detector converts chemical concentration into an electrical signal by the following steps:

1. The sample components, carried by the mobile phase, flow through the detector's flow cell, a transparent compartment inside the detector which gives its contents exposure to its lamp's light.
2. These components absorb specific wavelengths of light given off by a xenon lamp.
   - These wavelengths are selected for by reflecting, filtering, and focusing the lamp's light by mirrors, a filter wheel, and diffractive gratings (Figure 8).
3. Once the sample components absorb these specific wavelengths, they become fluorescent and then emit, or give off, their own wavelengths of light.
4. This light is reflected and focused again using a different set of mirrors and diffractive gratings onto a photomultiplier tube, which converts the light into an electrical signal (Figure 9); the brighter the fluorescence, the larger the electrical signal.

IMPORTANT: The xenon lamp is expensive and has a limited lifetime, so the fluorescence detector should only be on when samples are being analyzed. Once the injections are finished for the day, the detector <u>must</u> be turned off. Leaving the lamp on over the weekend is long enough to wear it out.
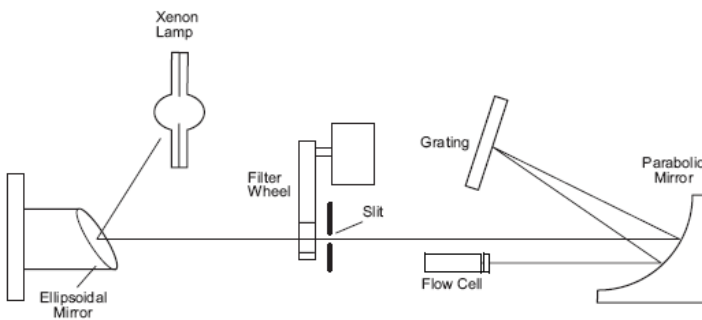
Figure 8. Setup for sample excitation
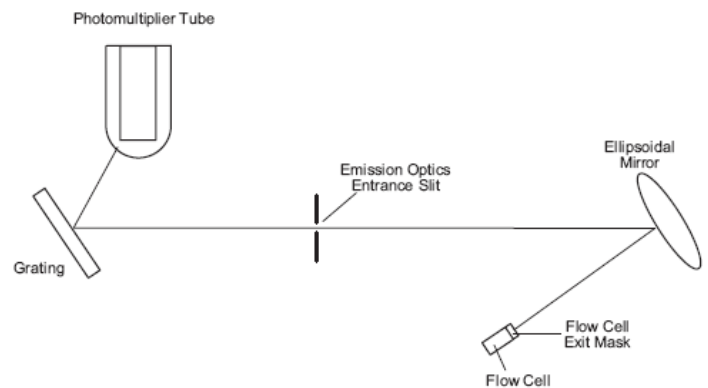
Figure 9. Setup for measuring sample emission

Waters 2410 Differential Refractometer

Since all compounds refract light, the differential refractometer (RI) is referred to as a "universal" detector. As a result it is the most widely used detector to monitor molecular weight distribution. The refractive index of polymers is constant above approximately 1000 MW. Therefore, the detector response is directly proportional to concentration. The RI detector (Figure 10) is sensitive down to about 4 micrograms.

Figure 10. Refractive Index Detector

Starting and Shutting Down the Detector

The RI detector takes 24 hours to warm up after being turned on. Therefore, it is best to always leave the machine on. The light source is a LED, so there isn't any worry of burning a lamp out (unlike the fluorescence detector).

NOTE: When the detector is not in use, keep a slow flow (0.100 ml/min) of non-buffered solvent (no salts). This minimizes the amount of time the 2410 refractometer needs for reequilibrium when you use it again.

IMPORTANT: Do not leave buffers in the system after use. Flush the lines with HPLC-grade methanol, then flush with HPLC-grade water (double distilled is adequate).

The Data System – Millennium[32]

The HPLC data system is a computer with special software that collects the electrical signals from the detector and performs a number of functions on that data. The software used in the lab is called Millennium[32]. A few of the operations this software can do include
- Identifying known peaks from user-recorded standards
- Integrating peaks to determine areas
- Curve fitting calibration data
- Taking the calibration data and calculating actual masses (i.e. mg) of components
- Determine molecular weight distribution plot of polymers

Columns, Solvents, and Sample Preparation

Which Column Should I Use?

There are three types of columns in our laboratory:

Analytical Columns

      Nova-Pak – This column separates compounds based on hydrophobicity/polarity. The more hydrophobic compounds are slowed by the carbon chains in the column. Only very-low molecular weight compounds should be used.

      Columns in stock: Nova-Pak C18

GPC Columns

      Styrogel – Designed particularly for low to medium molecular weight samples $(500 - 10^7)$, these columns are ideal for analysis of oligomers, epoxies, and polymer additives where high resolution is critical. This column is ideal for compounds such as polystyrene.

      Columns in stock: Styrogel HR 3
                                     Styrogel HR 4
                                     Styrogel HR 5E

      Ultrahydrogel – Packed with hydroxylated polymethacrylate-based gel, these columns are ideal for the analysis of aqueous-soluble samples, such as oligomers; oligosaccharides; polysaccharides; and cationic, anionic, and amphoteric polymers. They allow a wide pH range (2-12) and are compatible with up to 20% organic solvents. This column is ideal for compounds such as polyethylene-oxide.

      Columns in stock: Ultrahydrogel 250
                                       Ultrahydrogel 2000

The appendix contains charts for both Styrogel and Ultrahydrogel columns. From these diagrams and charts, you can determine which of the GPC columns will separate your samples. For example: suppose you had two polystyrene samples. One had a molecular weight of 25,000 and the other of 80,000. Looking at the GPC Column Selection Guide on page 27 or the calibration curves for Styrogel columns on page 26, two columns would provide separation of these two molecular weights: HR3 and HR 5E. The HR4 column would not be able to separate these molecular weights.

If you were analyzing a water soluble polymer, you would use the Ultrahydrogel calibration chart on page 29 to determine whether to use the 250 or 2000 model of the Ultrahydrogel columns.

Column Installation

After selecting the correct column, it is necessary to correctly install it with its guard column. The guard column is a smaller (and cheaper) version of the regular column. Its purpose is to save the column from particulates and any other compound that may foul its contents.

Figure 11 diagrams how the two columns should be installed. The arrows indicate the solvent flow direction.
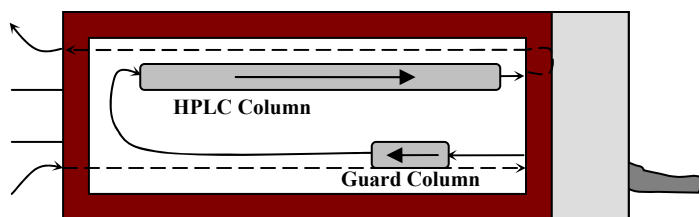
Figure 11. The direction of flow through the guard and chromatography columns.

Column Maintenance

For Nova-Pak Columns

❖ Protect the columns from contaminants by using a guard column upstream of the column. (See Figure 11.)
❖ Make sure your samples are completely soluble in the mobile phase.
❖ Make sure that solvents are miscible when changing mobile phases. This will prevent phase separation or precipitation.
❖ Always degas and filter mobile phases through a 0.22 μm membrane filter. Acrodisc® filters are recommended.
❖ Do not exceed an operating pressure of 40 MPa (400 atm or 6000 psi).
❖ A shift in retention may indicate contamination of the column. Flushing with a neat organic solvent is usually sufficient to remove the contaminant.
❖ If system backpressure increases with usage, replace the guard column.
❖ If flushing procedure does not solve the problem, wash the column with a sequence of progressively more nonpolar solvents. For example, water → tetrahydrofuran (THF) → methylene chloride → THF → water.

For Ultrahydrogel Columns

❖ The typical operating flow rates (ml/min) are 0.5-0.8 for the 250 Model and 0.3-0.6 for the 2000 Model. **Do not exceed 1.0 ml/min.**
❖ Use HPLC grade solvents, filtered through a 0.45 μm membrane filter.
❖ Protect the columns from contaminants by using a guard column upstream of the column. (See Figure 11.)
❖ Use the column only in the direction indicated by the arrow.
❖ Be careful not to introduce into the column during installation or removal.
❖ Slowly increase flow rates.
❖ These columns may be operated at a temperature range of 10°C to 80°C. High temperature analysis reduces viscosity, increases resolution and reduced adsorptivity.

For Styragel Columns

- ❖ Use HPLC grade solvents, filtered through a 0.45 μm membrane filter.
- ❖ Do not let the flow rate exceed 2.0 mL/min or the backpressure exceed 3.5 MPa (500 psi, 35 atm). Normal flow rate for these columns is 1 mL/min.
- ❖ Protect the columns from contaminants by using a guard column upstream of the column. (See Figure 11.)
- ❖ Minimize temperature cycling
- ❖ Protect the column from rapid changes in pressure
- ❖ When changing to a solvent with a different viscosity, it may be necessary to adjust the flow rate to stay from exceeding the maximum allowed backpressure

Storing the Column

Leaving the column unused for less than three days does not require special storage procedures; however <u>maintain a flow rate of 0.1 mL/min</u>. For longer storage, store the column in shipping solvent. If the mobile phase contains a buffer salt, first flush the column with 10 column volumes of highly purified water. For Ultrahydrogel columns, adding sodium azide (0.05%) to the storage water is recommended for storage over 72 hours or more. Make sure that the end plugs are firmly in place. **Never let the column dry out.**

Which Solvent Should I Use for the Mobile Phase?

The best rule of thumb when determining the mobile is this:

- ➢ <u>Choose the mobile phase that dissolves the sample and will not destroy the contents in the column.</u>

Common solvents used in the previously described columns are:

Nova Pak	**Styrogel**	**Ultrahydrogel**
Methanol/Water	Tetrahydrofuran (THF)	Water (HPLC grade)
Buffered water ($[NH_4]_2SO_4$)	Toluene	Buffered Water
Hexane	DMF	- Sodium sulfate
Acetonitrile/Water	Methylene Chloride	- Sodium acetate
Methylene chloride/CH_3OH	Chlorobenzenes	- Ammonium acetate
	Phenol	- Phosphate
		- Ammonium Formate

WARNING: **The pH range for the mobile phase is pH 2-8.** Any pH higher than 8 will ruin the column.

WARNING: The organic solvent conc. should not exceed 20%

Preparing the Sample

It is best to dissolve your sample in the same solvent as the mobile phase. This will lower the chance of reaction of precipitation after you inject it into the system. Sample concentration affects both viscosity and injection volume. While small sample amount produce narrower peaks, viscous samples may require larger, more dilute samples. Table 1 lists the recommended concentration of sample for optimal results.

Table 1. Recommended Sample Concentration

Molecular-weight Range	Sample Concentration
0 to 25,000	<0.25%
25,000 to 200,000	<0.1%
200,000 to 2,000,000	<0.05%
Above 2,000,000	<0.02%

OPERATING INSTRUCTIONS

Now that you have an adequate understanding of the system and of what each piece of equipment does, you are prepared to operate the equipment and run samples.

These instructions will guide you step-by-step in:
1. Starting the pump and increasing the flow rate to the desired amount.
2. Turning on the detector
3. Logging on to the data collecting software and preparing the computer for injections
4. Creating the appropriate data collection methods in the software program
5. Loading and injecting the samples
6. Using the software to view and analyze the results

Each of the tasks explained in this manual requires several steps. Hints and notes are provided with the instructions. Pictures and diagrams are provided to make it quick and easy to perform the directed tasks. *Important warnings and cautions should be read before continuing to the next step.*

Increasing the Flowrate/Pressure

STOP **NOTE:** Increasing the flowrate too quickly will cause a large pressure surge on the column, potentially destroying it.

NOTE: Keep in mind the maximum allowable pressure for the column being used. A safe maximum pressure for most columns is 3000 psi.

NOTE: If the pump is stopped for any reason, *start the pump again from 0.100 ml/min.* Starting the pump at a high flowrate without gradually ramping it up will cause damage to the column.

The default value for the flowrate is 1.000 ml/min. You must set the flowrate to 0.000 ml/min before starting the pump. To do this:

➢ Press the **EDIT ENTER** button once – a blinking square will appear over the left-most digit.

➢ Press the ▼ button once to set the flowrate to 0.000 ml/min.

➢ Press the **RUN STOP** button – the word "RUN" should appear on the top right corner of the display.

➢ Press the **EDIT ENTER** button again to make the blinking square appear.

➢ Press **EDIT ENTER** again to move the blinking square one digit to the right.

➢ Press the ▲ button once to increase the flowrate to 0.100 ml/min.

➢ Press **MENU** to implement the change. The flowrate and pressure should both increase.

Pressing **EDIT ENTER** twice, and then pressing ▲ once, followed by pressing **MENU** will increase the flowrate to 0.200 ml/min.

Continue to increase the flowrate in the same manner, <u>at a gradual pressure climb</u>, until you reach the desired flowrate. Sharp pressure increases could damage the column.
(The recommended flowrate for most applications is 1.000 ml/min, but typical flowrates range from 0.10 – 2.00 ml/min, depending on the column.)

Turning on the Fluorescence Detector (if using it)

➢ **NOTE:** Before turning the machine on, unplug the L-COM Data Cable from the back of the detector (see Figure 12). This is the cable connecting the detector to the computer.

If this does not happen, the detector will lock-up trying to finalize the setup process. Unplugging the cable solves the problem. The source of the problem is unknown, but service technicians estimated it would cost over $1000 to fix any potential source.

Disconnect Here
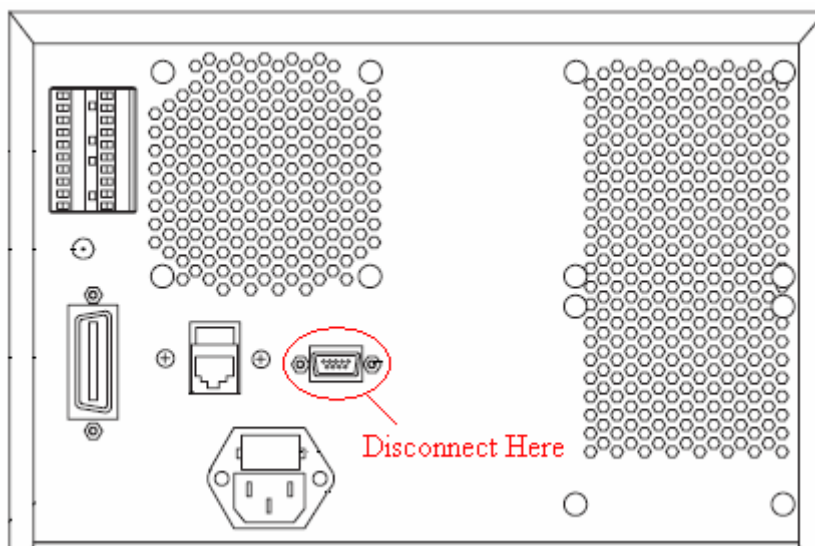
Figure 12. The back view of the Waters 2475 fluorescence detector

➢ Turn on the detector using the power switch on the lower right of the front of the machine.

Figure 13. Main screen of fluorescence detector.

It takes about 10 minutes to warm and set up. During the set-up process, the machine warms-up, performs self-diagnostic tests, calibrates, and restores previous settings.

After the set-up process, the main screen appears (Figure 13) on the detector.

➢ After the main screen appears, plug the L-COM Data Cable back into the detector at the same location where it was disconnected (see Figure 12).

Using the Millennium[32] Data Collecting Software

NOTE: Login to Millennium[32] only after the fluorescence detector has been successfully set-up and the L-COM Data cable is reconnected.

Logging into the computer
If you do not have a user account on the HPLC computer, you can access the program using the following information:

User Name: guest
Password: millennium

3. Setting Up for Injections

➢ Open the Millennium[32] software from the Start Menu by clicking:

Programs → Millennium[32] → Millennium[32] Login

➢ In the **Project:** field (see red rectangle in Figure 14), select "**General**"

➢ Double-click the "**Run Samples**" box (see red square in Figure 14).

➢ In the window that pops up, Select "**HPLC_Fluoro**" or "**HPLC_RI**" depending on your detector.

➢ Click **OK**

HINT: If an error occurs after clicking **OK**, it could be because the detector you selected is <u>off-line</u>. To bring your detector on-line, see "Changing Detectors" on page 25.

The **Run Samples** window (Figure 15) should appear after clicking **OK**.

NOTE: If you have not previously created an Instrument Method, go to page 21 (for the RI Detector) or page 22 (for the Fluorescence Detector) and follow the directions to create one.

➢ Choose your Instrument Method by clicking the white rectangle and selecting your method (see red box in Figure 15).
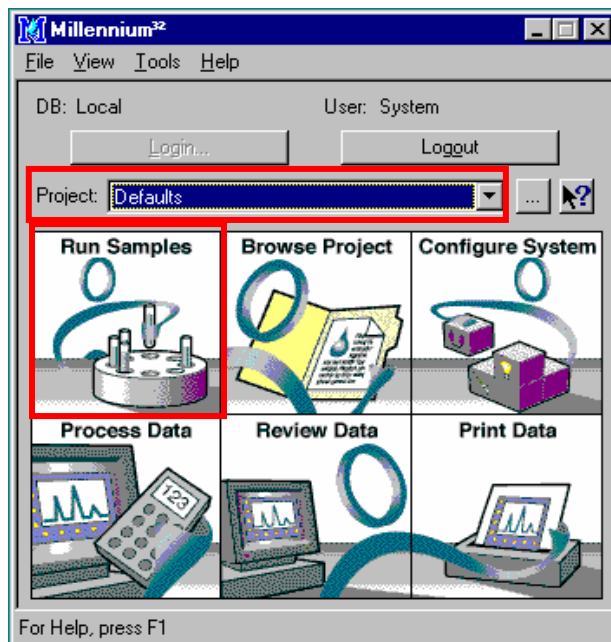
Figure 14. Main Menu of Millennium[32]

What is an Instrument Method?

An Instrument Method is a group of instrument settings programmed for a particular experiment or procedure. By creating an Instrument Method, you can save specific parameters such as:

➢ Excitation & Emission Wavelengths
➢ Gain
➢ Sampling Rate

15
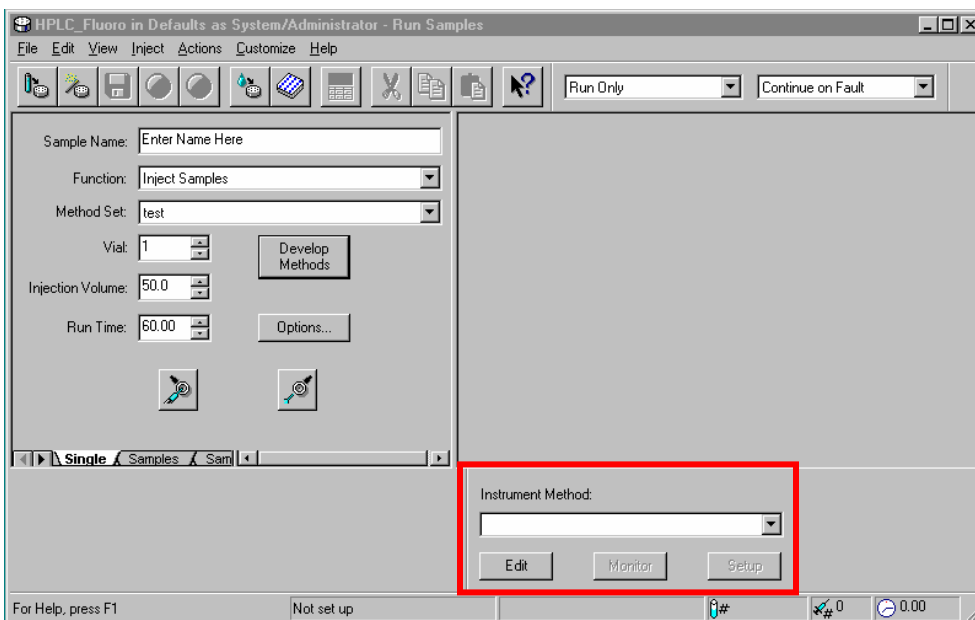
Figure 15. Run Samples Main Window

➢ Click the Monitor button in the Instrument Method Panel.

➢ Monitor the graph for a stable baseline. (See Figure 16)
   - if not initially stable, wait a little longer
   - if the baseline does not stabilize within one hour, see the Troubleshooting section in the fluorescence detector's User Manual

➢ Once baseline is stable, click the **Abort** button, , to stop monitoring.

➢ Enter Sample Name

➢ Keep Function as "Inject Samples"

➢ Choose your Method Set.

➢ Change Injection Volume to **50.0**. (The units are assumed to be µl.)
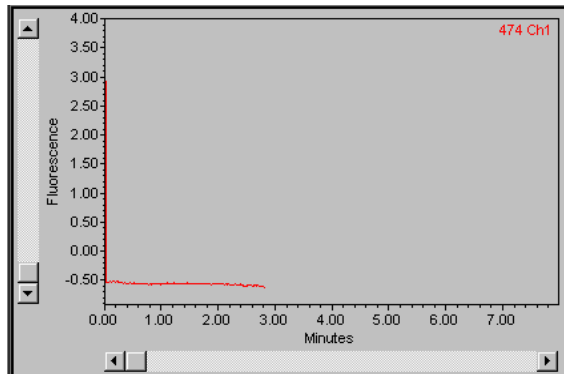
Figure 16. Run Samples Graph during Monitor Mode. Graph shows a stable baseline.

NOTE: It is a good idea to choose a run time larger than needed. You can always stop the data collecting during a run by pressing . However, if the run time selected is too short, the computer may stop collecting data before the run is complete. A good starting time is 60 minutes, though most run finish before 30 minutes.

➢ Change Run time to the desired amount.

16

4. Loading & Injecting Samples

NOTE: Make sure no air bubbles are injected into the system. This may distort the data, making it necessary to redo the run. You do not need to completely empty the syringe. If there is an air bubble at the end of the syringe plunger, stop the injection short to prevent injecting air.

➢ Lift injection lever to the LOAD position (Figure 17).

➢ Click the Prepare button on the Run Sample screen (on the computer).

➢ Completely fill the 100 μl glass syringe with the prepared sample.

IMPORTANT: After injecting the sample, leave the syringe in the injector. This prevents you from suctioning out any of the sample.

Figure 17. Diagram of the injector in the LOAD position

➢ Insert the syringe needle **completely** into the injection site and *slowly* inject all 100 μl of the sample.

> **NOTE**: Injecting slowly allows you to look and make sure no air bubbles enter the system. Injecting most or all of the 100 μl ensures that every injection is the same, because this fully loads the 50 μl sample loop in the injector (see "Manual Sample Injector, Page 3). If you were to only load 50 μl, you may sometimes inject just short of the 50 μl, causing error.

➢ Once the sample is completely injected and the words "Single Injection - waiting" appears in the middle-bottom of the computer screen, click the inject button *at the same time* as pushing the injection lever down to the INJECT position (Figure 18). This injects the sample into the system.

Figure 18. Diagram of the injector in the INJECT position

If Using the Fluorescence Detector

➢ Then, 3-4 seconds after injecting the sample, press the button on the top-middle of the fluorescence detector's front panel (if necessary).

> **NOTE**: Sometimes, the detector's beginning fluorescence value is different than "0.00," especially for the first injection after turning the machine on. After the initial zeroing, the detector *usually* returns to zero for subsequent injections.

➢ One minute after injection, it is safe to return the injector lever to the LOAD position and remove the syringe.

5. Analyzing the Data

➢ Select (double-click) "**Browse Project**" from the Millennium[32] Main Menu screen (see red box in Figure 19).

➢ Select your project from the list.

➢ (Select the project under which the samples were run. Choose **General** if you followed the instructions under "Setting up for Injections".)

➢ Click **OK**.

➢ Click on the "**Injections**" tab (see red box in Figure 20). This shows all of the injections performed under this project.
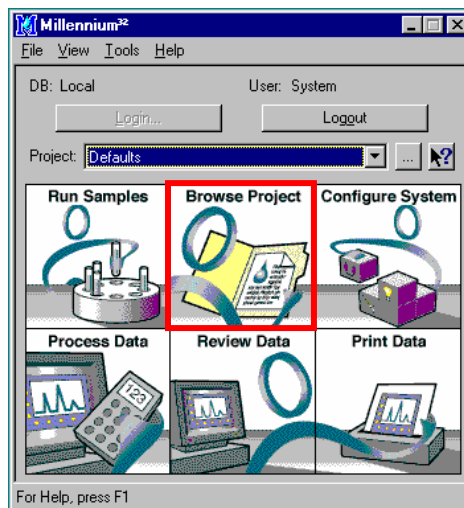
➢ Click the ⬚Update button at the middle top of the window (see red box in Figure 20). This updates the list to include the most current injections.

STOP If this is the first time to analyze these peaks, you must first setup a Processing Method. To do this, see "Creating a Processing Method" on page 23.

➢ Click on the injection(s) you want to analyze.

➢ Click the Process button 🔲 at the top-left of the window.

➢ On the pop-up window, select the option: **Use specified processing method** and choose the processing method setup for your particular sample.

➢ Click **OK**.

➢ Select the "Results" tab in the Browse Project window (see red box in Figure 21).

➢ Then click the ⬚Update button.

➢ Double-click the injection you want to view.

Figure 19. Main Menu of Millennium[32]

Figure 20. Browse Project Main Screen – Injection tab selected

Figure 21. Browse Project Main Screen – Results tab selected

18

A screen with two areas will appear. The top area will display the detector's readout with red lines drawn under the individual peaks (see Figure 22). The bottom area displays a chart with the results from integrating the area under each peak.
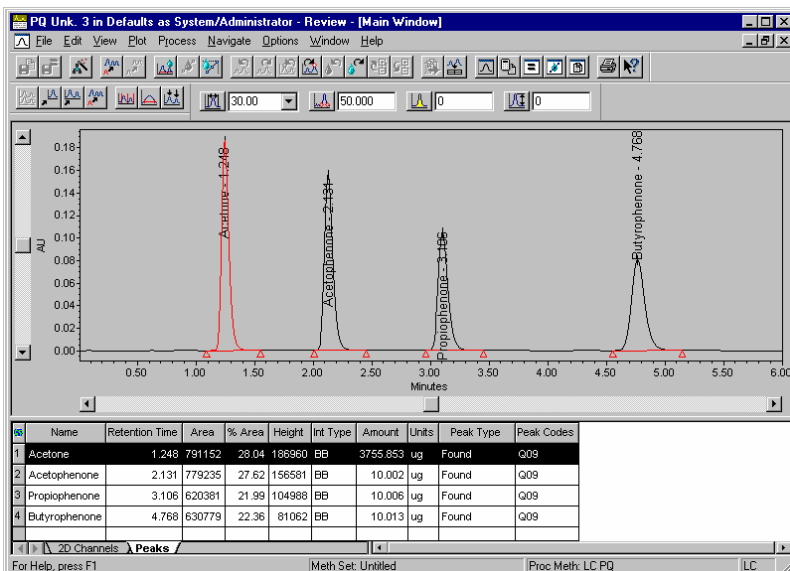

Figure 22. Review Mode Window – Data has been processed (integrated)

For HPLC, the chart shows the following:

Name	The name of the most-likely compound creating that peak. The name was assigned during the creation of the processing method. Unknown peaks will not have a name.
Retention Time	The time, in minutes, after injection in which the compound passed through the injector.
Area	The area under the peak. This is in arbitrary units. A calibration with known standards is necessary for the area to have significance.
% Area	The percent of the area of that particular peak compared to the total area off all the peaks found.
Height	The height of the peak, in units of fluorescence.

NOTE: The GPC Review Screen may look slightly different than Figure 22.

Ignore the rest of the columns. To learn about the information they provide, see the Millennium[32] Users Manual.

Conclusion

Congratulations, you have successfully analyzed your sample! Hopefully, everything ran smoothly and you received reliable results. As you may have recognized, these instructions are only sufficient to make simple injections and perform basic data analysis. There is much more that an HPLC system can do. However, these items are beyond the scope and purpose of this manual. To learn more about the system's capabilities, you are encouraged to read the various manuals that accompany the equipment.

For example, to learn how to set up a calibration curve in order to determine the molecular weights of your samples, look it up in the GPC Manual.

In the lab you'll find manuals for the Pump, the RI and Fluorescence Detectors, each type of column, and various Millennium[32] software manuals (including a manual specifically for GPC).

If you encounter problems that cannot be solved by using the manuals and guides, call Waters technical support at 1-800-252-4752, or the regional technical specialist, O. Lee Stone, at extension 6768.
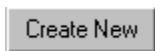
Good Luck.

APPENDIX

Creating an Instrument Method (Refractive Index Detector)

Click the [Develop Methods] button. This opens the New Method Set wizard. (Figure 23)

Then click [Create New]. This opens the Instrument Method Editor.

Right-click on the PCM button at the top of the window and select "**Delete Instrument**" (see Figure 24)

Click the "**Temperature**" tab.

Then check the box next to "**Internal Temp Enable**". (See red box in Figure 25)

Type in **30.0** in the white box. (See red box in Figure 25)

Click the save button at the top left of the window.

Name the Instrument Method.

Click **Save**.

Close the Instrument Method Editor. You should return to the "New Methods Set" window.

Click [Next >]. The Select Default Methods window will appear. (See Figure 26)

For now, just click [Next >].

> However, once a processing method has been created for your particular experiment (see "Creating a Processing Method" on page 23.), you can return to this window and select that particular processing method. This will allow for automatic data processing immediately after each injection is complete.
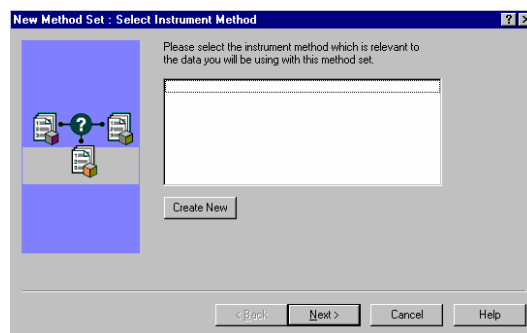
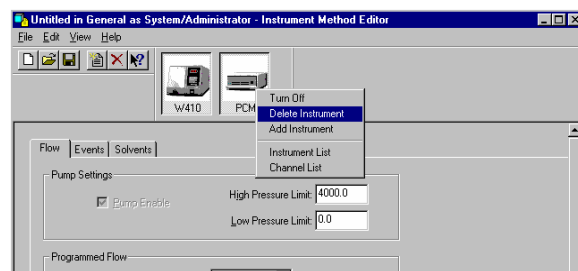Name your Method and click [Finish].
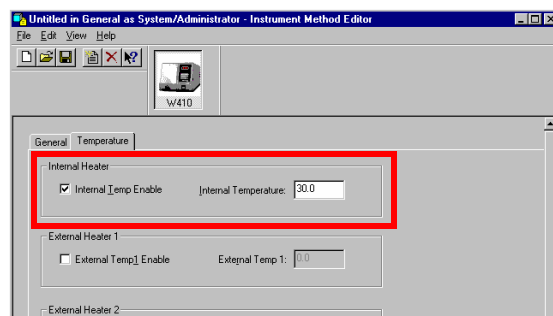

Figure 23. New Method Set window

Figure 24. Deleting the PCM

Figure 25. Setting the Internal Temperature
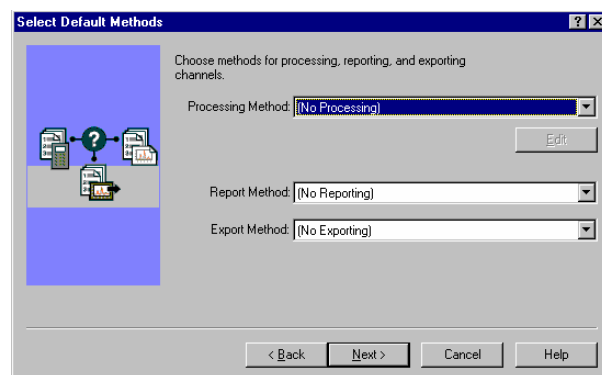
Figure 26. Select Default Methods window

21

Creating an Instrument Method (Fluorescence Detector)

➢ Click the [Develop Methods] button. This opens the New Method Set wizard. (Figure 27)

➢ Then click [Create New]. This opens the Instrument Method Editor (Figure 28).

➢ Enter the Excitation Wavelength (in nm) & Emission Wavelength (in nm) into the indicated areas. (See left red box in Figure 28)

➢ Set the Gain[1]. (See right red box in Figure 28)

➢ Click the save button at the top left of the window.

➢ Name the Instrument Method

➢ Click Save

➢ Close the Instrument Method Editor. You should return to the "New Methods Set" window.

➢ Click [Next >]. The Select Default Methods window will appear. (Figure 29)

➢ For now, just click [Next >]. However, once a processing method has been created for your particular experiment (see "Creating a Processing Method" on the next page), you can return to this window and select that particular processing method. This will allow for automatic data processing immediately after the each injection is complete.
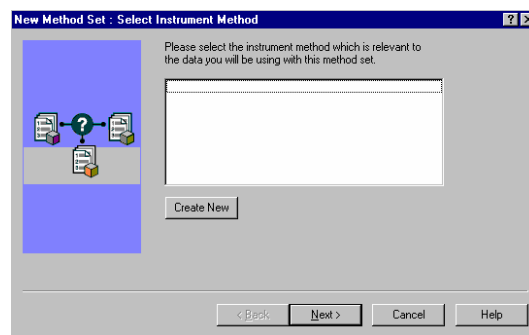
➢ Name your Method and click [Finish].
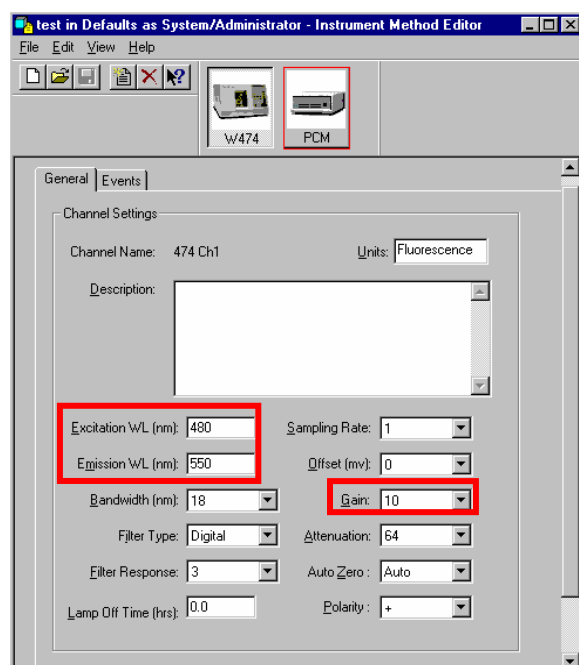
Figure 27. New Method Set window

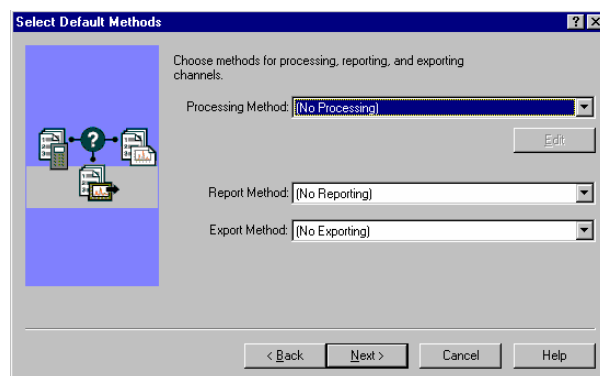**Figure 28. Instrument Method Editor for the fluorescence detector.**

Figure 29. Select Default Methods window

Creating a Processing Method

What is a processing method?

By creating a processing method, you setup how you want to integrate your samples. This method can then be used on all the similar samples you want to analyze. For example, suppose you were using HPLC to analyze the amount of Doxorubicin, a drug, in various tissue samples (tumor, heart, liver, ect.). You may perform 50 injections over the course of the experiment. By setting up a processing method for the detection of doxorubicin and using that method to find and integrate the Doxorubicin peak, you can analyze those 50 peaks (and any other peaks from other compounds) quickly and with consistency. Otherwise, you would have to manually integrate each peak, which takes lots of time and introduces human error.

Also, in GPC, a processing method can be used to calculate the molecular weight from a calibration curve create by injecting standards with known molecular weights.

To create a processing method (For Analytical HPLC Analysis):

➢ From the "Injections" screen in the "Browse Projects" window (see Figure 20), click on the injection that you want to use to setup the method.

➢ Then click on the Review button ⊞ at the top left of the window. The review window will appear which displays the detector's readout for that particular run (Figure 30)

➢ The easiest way to create a Processing Method is to use the Processing Method Wizard by clicking on the 🔧 button at the top-left of the window.

➢ Select "**Create a New Processing Method**" and click **OK**.

➢ Select **LC** for the Processing Type

➢ Click **OK**

➢ Follow instructions given in the wizard, using the following guidelines:

- On the "Calibration-General" and "Calibration-Default Amount" screens, just click the [Next >] button.

Figure 30. Review Mode Window – Data has not yet been processed (integrated)

- When asked, select the "**External Standard Calibration**" option.

- When asked to name the peaks, name the peaks that you know. There may be unknown peaks – that is OK.

- If you do not approve of the final integration results, redo the processing method until it is satisfactory.

To create a processing method (For GPC / Molecular Weight Analysis):

➤ From the "Injections" screen/table in the "Browse Projects" window (see Figure 20), click on the injection that you want to use to setup the method.

➤ Then click on the Review button ▦ at the top left of the window. The review window will appear which displays the detector's readout for that particular run (Figure 31)

➤ The easiest way to create a Processing Method is to use the Processing Method Wizard by clicking on the ▧ button at the top-left of the window.

➤ Select "**Create a New Processing Method**" and click **OK**.

➤ Select **GPC** for the Processing Type

➤ Click **OK**

➤ Follow instructions given in the wizard, using the following guidelines:

- The first four screens allow you to setup how the computer will integrate your peaks – follow the directions appearing at the top.
- On the GPC Calibration screen (Figure 32):
  o Select the type of calibration you wish to perform:
    ▪ Relative:
    ▪ Universal:
  o Select the type of calibration fit the computer should use to create the calibration curve.
  o Select the variable to be used in the calibration
    ▪ Time: the time for the component's peak to appear
    ▪ Volume: the mobile phase volume required to flush the component out
- On the GPC – Column Set screen (Figure 33):
  o Exclusion or Total Void Volume Time (V_o) – For the typical GPC column (300mm x 7.8mm), this is 5.5-6.0. You may take an educated guess or call Waters support.
  o Total Retention Volume Time (V_t) – the retention time of the last peak (at a flow rate of 1 mL/min). You'll have to run a sample at 1 mL/min to determine this.

Figure 31. Review Mode Window – Data has not yet been processed (integrated)
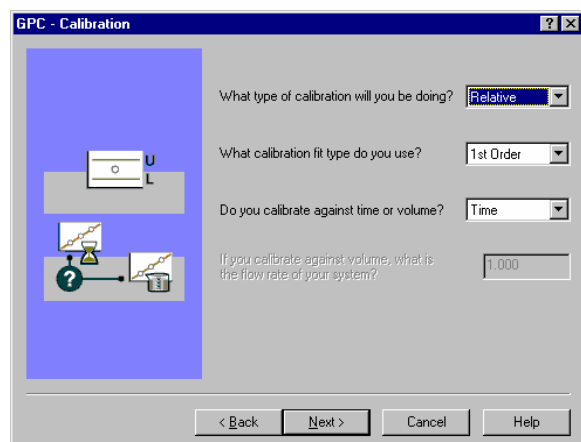
Figure 32. The GPC – Calibration window from the Processing Method Wizard.
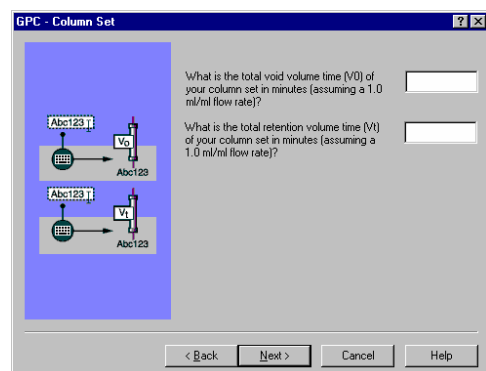
Figure 33. The GPC – Column Set window from the Processing Method Wizard.

24
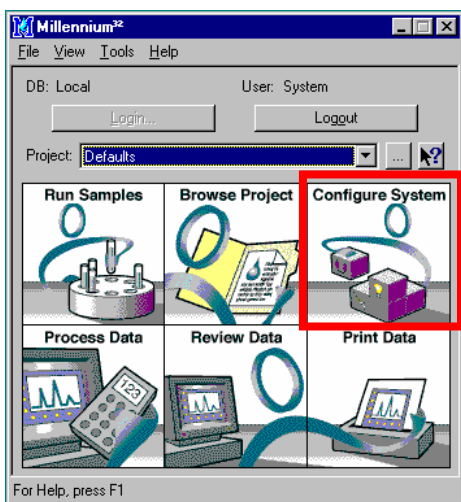
Figure 34. Main menu of Millennium³²

Figure 35. Configure System Window

Changing Detectors

The software only allows one detector to be online at a time. If the detector you wish to use is not online, you must first take the other detector offline and then bring the desired detector online. To do this:

➢ Double click the **Configure System** box in the main menu (see red box in Figure 34).

➢ Select **Acquisition** and click **OK.** (see Figure 35)

➢ In the "Configuration Manager" Window that appears (Figure 36), Click the + box next to **Acquisition Servers**, and click the + box next to **Cb173-01**. The two detectors, **HPLC_Fluoro** and **HPLC_RI** (the refractive index detector) should appear.

➢ Right click on the detector you wish to take offline.

➢ On the menu that appears, click on **Take Offline.**

➢ Right click on the detector you wish to take online.

➢ On the menu that appears, click on **Bring Online.** Figure 36 shows how to bring the RI detector online.

➢ Close the Configuration Manager and return to the main menu to setup the injections.

Figure 36. Configuration Manager - bringing the RI detector online.

25

Column Information

Nova-Pak® Packings

The 4 µm small particle size of Nova-Pak® bonded phases offers high resolution as well as more efficient and faster chromatography. This is accomplished by using shorter columns, thereby reducing solvent consumption or by using longer columns to resolve even the most complex mixture. Analytical columns with 4 micron particle size packings are available in 75, 150 and 300 mm length steel columns. New steel cartridge columns with reusable endfittings are available in 50, 100, 150 and 250 mm lengths. Semi-preparative columns with 6 micron particle size packings give you an unparalleled range of separation possibilities. Stringent QC procedures in our cGMP manufacturing facility ensure batch-to-batch reproducibility.

Physical Characteristics

Packing	Chemistry	Particle Size	Particle Shape	Pore Size	Carbon Load	End-capped
Nova-Pak®	C_{18}	4 µm	Spherical	60Å	7%	Yes
	C_8	4 µm	Spherical	60Å	4%	Yes
	Phenyl	4 µm	Spherical	60Å	5%	Yes
	CN HP	4 µm	Spherical	60Å	2%	Yes
	Silica	4 µm	Spherical	60Å	N/A	N/A
Prep Nova-Pak® HR	C_{18}	6 µm	Spherical	60Å	7%	Yes
	Silica	6 µm	Spherical	60Å	N/A	N/A

Styragel® HR High-Resolution Columns

Designed particularly for low molecular weight samples, the Waters Styragel® HR columns are ideal for the analysis of oligomers, epoxies, and polymer additives where high resolution is critical. Packed with rigid 5 µm particles, with a typical plate count greater than 16,000 plates per column, these columns deliver unrivaled resolution and efficiency in the low-to-mid molecular weight region.

Calibration Curves for the Waters Styragel® HR Series of High-Resolution Columns

GPC Column Selection Guide

Effective Molecular Weight Range	10^1	10^2	10^3	10^4	10^5	10^6	10^7	10^8

Ultra-High Molecular Weight Analysis
Waters Styragel® HMW Series
20 micron particle size
Ambient to 150 °C

Applications:
UHDPE
UH-Polystyrene
UH-Isoprene
UH-PMMA

Styragel® HMW 20M
Styragel® HMW 6E
Styragel® HMW 2

Mid-Range Molecular Weight
Waters Styragel® HT Series
10 micron particle size
Ambient to 150 °C

Applications:
ABS
Acetyl
Acrylics
EVA
Nylon
PEEK
PET/PBT

Styragel® HT 6E
Styragel® HT 6
Styragel® HT 5
Styragel® HT 4
Styragel® HT 3
Styragel® HT 2

Low Molecular Weight Analysis
Waters Styragel® HR Series
5 micron particle size
Ambient to 80 °C

Applications:
Additives
Epoxy
Oligomers
Phenolics
Unsaturated Polyester
Urea/Formaldehyde
Polyethylene Glycol
Ethanolamines
Melamine Resin

Styragel® HR 5E
Styragel® HR 4E
Styragel® HR 6
Styragel® HR 5
Styragel® HR 4
Styragel® HR 3
Styragel® HR 2
Styragel® HR 1
Styragel® HR 0.5

Effective Molecular Weight Range	10^1	10^2	10^3	10^4	10^5	10^6	10^7	10^8

GPC Solvent Selection Guide

Polymer	GPC Solvent	Shipping Solvent
Polyisobutylene	Toluene	
Polybutylene Chlorinated Rubber Polybutadiene Polyisoprene Polydimethylsiloxane	Toluene/75%	
Chlorinated Polyethylene Polyethylene – Ethylacrylate Polyethylene – Vinylacetone Polyethylene – Methacrylic acid Polyphenyleneoxide Poly-4-methylpentene(1) Polyethylene	TCB/135 - 160 °C	Waters Styragel® Columns shipped in *Toluene*
Ultra-high Molecular Weight Polyethylene Polypropylene	TCB/135 - 160 °C	
Polyetheretherketone Polyetherketone	Phenol/TCB 1:1/145 °C	
Polycarbonate	Methyl Chloride	
Polyglycolic acid	gamma-Butyl lactone	
Acrylonitrile – Methylmethacrylate Cellulose Acetate Cellulose Acetate – Butyrate Cellulose Acetate – Proprionate Cellulose Nitrate Cellulose Proprionate Cellulose Triacetate Diallyl Phthalate Ethyl Cellulose Epoxy Polyester Alkyd Polybutene(1) Polybutadiene – Styrene Phenol – Formaldehyde Phenol – Furfural Polymethylmethacrylate Polypropyleneglycol Polystyrene Polysulfone Polyvinylacetate Polyvinylbutyral Polyvinylchloride Polyvinylchloride – Acetate Polyvinyldienechloride Polyvinylformal Polystyrene Acrylonitrile Polystyrene – Alphamethylstyrene Polyester Thermoset Phenolics Rosin Acids Polyglycolic Acid	THF/40 °C	Waters Styragel® Columns shipped in *THF*
Melamine – Formaldehyde Nylon (All types) Polybutylene – Terphthalate Polyethylene – Terphthalate	Hexafluoroisopropanol + 0.075 M Sodium Trifluoroacetate/55 °C or m-Cresol + 0.05 m LiBr/100 °C	
Poly Acrylonitrile ABS (Acrylnitrile – Butadiene – Styrene) ASA (Acrylic – Styrene – Acrylonitrile) ABA (Acrylonitrile – Butdiene – Acrylate) Carboxymethyl Cellulose ABS/Polycarbonate Polybutadiene – Acrylonitrile Polyurethane	DMF + 0.05 m LiBr/85 °C	
Polyacetal Polyoxymethylene	DMF + 0.05 m LiBr/145 °C	Waters Styragel® Columns shipped in *DMF*
Polyimide Polyamide – imide Polyetherimide Polyethersulfone Polyvinyldienefluoride	N-Methyl Pyrrolidone + 0.05 m LiBr/100 °C	
Polyfuran – Formaldehyde	Dimethylacetamide/60 °C	

Ultrahydrogel™ Columns Calibration Curves

Column dimensions: 7.8 mm I.D. x 300 mm
Sample: PEG and PEO standards
Mobile phase: Distilled water
Flow rate: 1 mL/min

A Ultrahydrogel 120
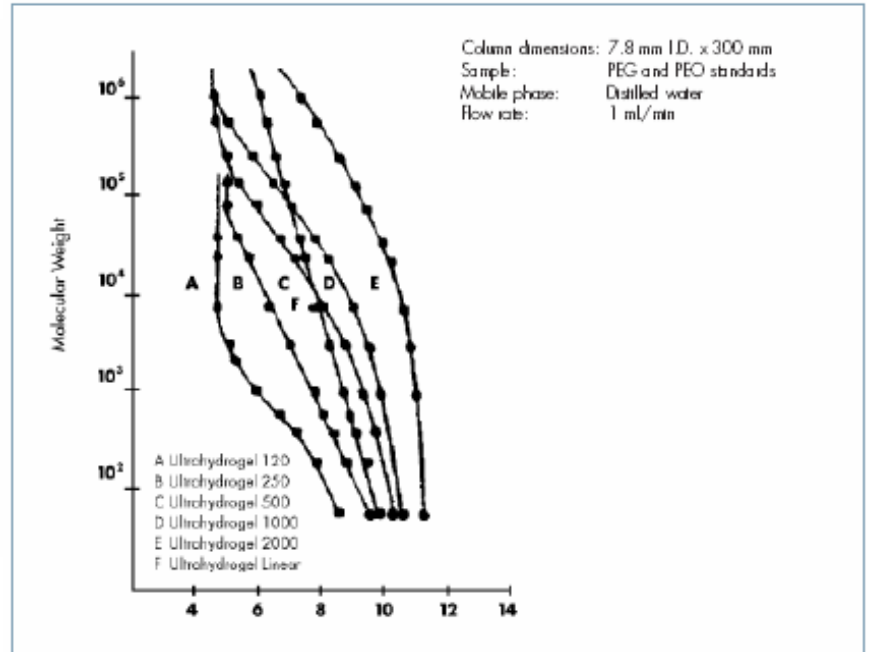B Ultrahydrogel 250
C Ultrahydrogel 500
D Ultrahydrogel 1000
E Ultrahydrogel 2000
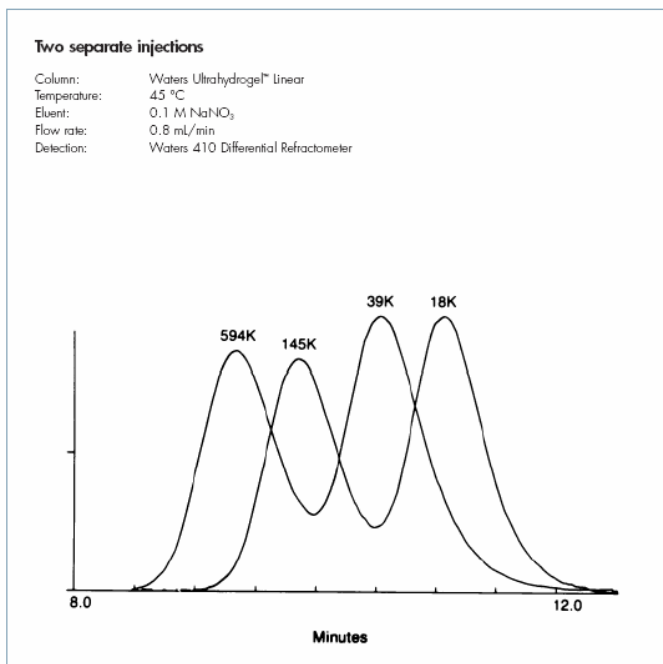F Ultrahydrogel Linear

Ultrahydrogel™ Columns

Packed with hydroxylated polymethacrylate-based gel, Waters Ultrahydrogel™ SEC columns are ideal for the analysis of aqueous-soluble samples, such as oligomers; oligosaccharides; polysaccharides; and cationic, anionic, and amphoteric polymers. Measuring 7.8 x 300 mm, these high-resolution columns offer many advantages over conventional aqueous SEC columns, such as:
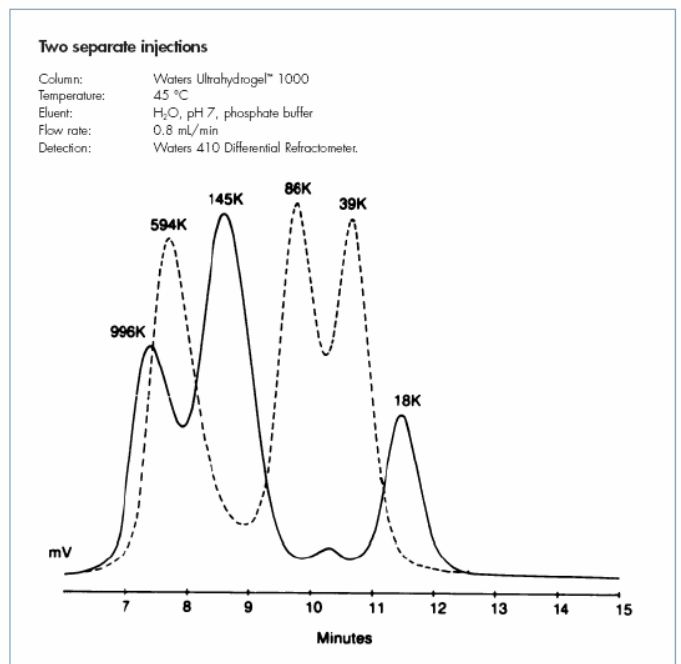
- A wide pH range (2–12)
- Compatibility with high concentrations of organic solvents (up to 20% organic, 50% organic if the mobile phase is introduced by gradient)
- Greater flexibility for the mobile phase
- Minimal non-size exclusion effects

Overlay of Two Poly(Ethylene Oxide) Samples

Two separate injections

Column: Waters Ultrahydrogel™ Linear
Temperature: 45 °C
Eluent: 0.1 M NaNO₃
Flow rate: 0.8 mL/min
Detection: Waters 410 Differential Refractometer

Poly(Ethylene Oxide) Standards

Two separate injections

Column: Waters Ultrahydrogel™ 1000
Temperature: 45 °C
Eluent: H₂O, pH 7, phosphate buffer
Flow rate: 0.8 mL/min
Detection: Waters 410 Differential Refractometer.

29

[1] The smaller the gain, the less sensitive the readings - but it allows a larger range of peak sizes. For example, larger gains allow better precision for small amounts of material being analyzed, but if a substance passes through the detector and it fluoresces a lot, the sensor in the detector overloads and it is temporally turned off in the middle of data collection (see figure on right):